NEW AND IMPROVED THERMOSETS BASED ON EPOXY RESINS AND DENDRITIC POLYESTERS

Adrian Marius Tomuta

Dipòsit Legal: T.191-2014

Adrian Marius Tomuta

New and improved thermosets based on epoxy resins and dendritic polyesters

PhD THESIS

Supervised by Dra. Àngels Serra i Albet and
Dr. Xavier Ramis Juan

Departament de Química Analítica i Química Orgànica

UNIVERSITAT ROVIRA I VIRGILI

Tarragona 2013

UNIVERSITAT ROVIRA I VIRGILI

DEPARTAMENT DE QUIMICA ANALITICA
I QUIMICA ORGANICA

C/ Marcel.lí Domingo s/n
Campus Sescelades
43007 Tarragona (Spain)
Tel. 34 977 55 97 69
Fax 34 977 55 84 46
e-mail: secqaqo@urv.net

Angels Serra Albet, Professor of the Analytical and Organic Chemistry Department of Rovira i Virgili University, and Xavier Ramis Juan, Professor of the Heat Engines Department of the Polytechnic University of Catalonia,

WE AGREE that the present work, entitled "New and improved thermosets based on epoxy resins and dendrític polyesters" presented by Tomuta Adrian Marius to obtain the title of Doctor, has been carried out under our direction and meets the requirements to qualify for the European Mention.

Tarragona, 24 september 2013

Dra. Àngels Serra i Albet

Dr. Xavier Ramis Juan

Acknowledgements

I would like to acknowledge those individuals who have contributed their time and talents in assisting me to complete this work.

I would like to acknowledge and extend my heartfelt gratitude to Prof Dr. Angels Serra my supervisor for opportunity of being one of her PhD students for her constructive discussions about polymer chemistry for her guidance, patience, encouragement and support throughout my PhD thesis, also I would like to give my appreciations to Prof Dr. Xavier Ramis my co-supervisor for his help and support during all this years.

I would also like to thank Dr. Xavier Fernández-Francos for his help in rheology and thermomechanical characterization and to Dr. Francesc Ferrando and Dr. Silvia de la Flor from Mechanical Engineering department of URV for all their help in mechanical testing of epoxy thermosetting samples.

I would like to express my appreciation for other people that were present in our laboratory and helped me during my PhD years, special thanks to Silvana Sauca, for helping me, especially during my arrival and accommodation days in the 330 laboratory.

I want also to mention my dear colleagues from our lab: David, Mireia, Marjorie, Cristina Acebo, Cristina Mas, Dailyn, Xavier, Asta, Karolina, Ana, Surya with Komal and Aaryan. I want to thank them for being my friends all these years. There are also some dear phD students from other laboratories that I want to acknowledge like: Mariluz, Cristina, Alev, Zeynep, Quique, Mercè, Rodolfo, Camilo, Marc, Sebastian, Miriam, Xavi, Emma, Isidro, Isma, Araceli and many others, remembering them will be my pleasure.

I would like to thank Prof. Brigitte Voit, for giving me the opportunity to work for three months in her group in Dresden, as well as to Dr. Albena Lederer for her help. Also, I would like to thank the colleagues I met there (Tobias and Michael) for the good times I had in and outside laboratory.

I would also like to thank both the technicians of the department (Juan Luis, Tere and Thaís), Research Service Resources (Ramón, Mercè, Rita, Mariana, etc..) and Mechanical Engineering laboratory (Josep) because without their help, thesis work would not have been possible. Thanks also to Avelina, Eulàlia, Olga and Dunnia to make me easier all the bureaucracy over the years.

Lastly I want to give my appreciations and dedicate this thesis to my parents, my brothers and my sister.

Thanks to all, Adrian

To raise new questions, new possibilities, to regard old problems from a new angle, requires creative imagination and marks real advance in science.

Albert Einstein

Table of Contents

Chapter 1

General Introduction

Polymers play an important role in our daily lives. They are one of the most useful materials ever created. Polymers can be rubbery or rigid and can be shaped into an endless variety of objects, ranging from car bumpers to squeezable bottles and soft fabrics. Polymer products, especially those used by industries, often have a useful life of many years. According to their structure and behaviour, polymers can be classified as thermoplastics and thermosetting or thermosets.[1]

Thermoplastics soften or melt on heating and can be converted into any shape before they cool down to a solid. Melting and solidification of these polymers are reversible and they can be reshaped by the application of heat and pressure, each cycle causing some deterioration in properties. Their polymer chains consist of linear or branched chain molecules having strong intramolecular bonds but weak intermolecular interactions. Important commercial examples include polyethylene, polyvinyl chloride, polystyrene, polypropylene, polyamides, polycarbonate and polyesters.[2]

Thermosetting resins change irreversibly under the influence of heat into an infusible and insoluble material by the formation of covalently cross-linked stable networks in the presence of a curing agent. Such polymers are prepared through the formation of long or branched chain molecules, which are capable of further reaction with each other by the application of heat. Sometimes irradiation is employed to achieve cross-linking.[3] Important thermosetting resins are epoxy resins, unsaturated polyesters, alkyds, vinyl esters, allyl resins and phenolics, among others.[4]

Thermosetting polymers have cross-linked or network structures with covalent bonds between molecules. Once solidified by the cross-linking process, they cannot be remelted or reshaped. Since thermosets cannot be remelted, engineers use them in applications that require high resistance to heat, as coatings, adhesives, electronic and electrical materials, etc.[5]

1.1. Epoxy resins

Epoxy resins constitute a class of thermosets which contains more than one epoxide group per molecule, which are very reactive to many curing agents.[6] They are used as reinforced composites, adhesives, high performance coatings and encapsulating materials. Epoxy thermosets have excellent electrical and mechanical properties, good adhesion to many metals and resistance to moisture and thermal and environment exposure. The widespread use of epoxies is due to the easy processing before curing, excellent wetting properties with reinforcements, good weathering resistance, excellent dimensional stability and high chemical and corrosion resistance.[6]

Epoxy resins are characterised by the presence of more than one epoxy group per molecule. Epoxide groups may lie within the body of the molecule but are usually terminal. The three membered epoxy ring is highly strained and is reactive to many substances, that can act as curing agents.[5]

In 1936, De Trey Freres produced a low melting bisphenol A based epoxy resin which gave a thermoset composition with phthalic anhydride. In 1939, a high molecular weight resin was produced in the US from bisphenol A and epichlorohydrin and esterification with unsaturated fatty acids provided an air dried coating. The commercial interest in epoxy resins became apparent with the publication of a patent in 1940 which described liquid polyepoxides.[7]

The first and still the most important class of commercial epoxy resins is the reaction product of bisphenol A (BPA) and epichlorohydrin in the presence of sodium hydroxide. It is called diglycidyl ether of bisphenol A (DGEBA). It has the general structure shown in **Figure 1**. High molecular weight resins are prepared by reducing the excess of epichlorohydrin and reacting under strongly alkaline conditions.

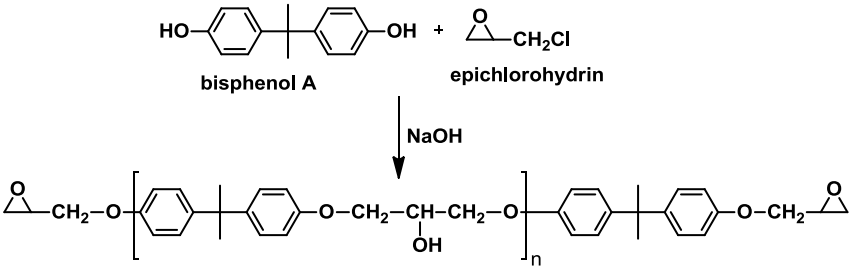

Figure 1. Synthesis of DGEBA from bisphenol A and epichlorohydrin

There are other types of resins with different structure that leads to materials with different characteristics (**Figure 2**). Some of the most typical resins are collected in the following figure. The non-epoxy part of the molecule can have an aliphatic, cycloaliphatic or aromatic structure.[8]

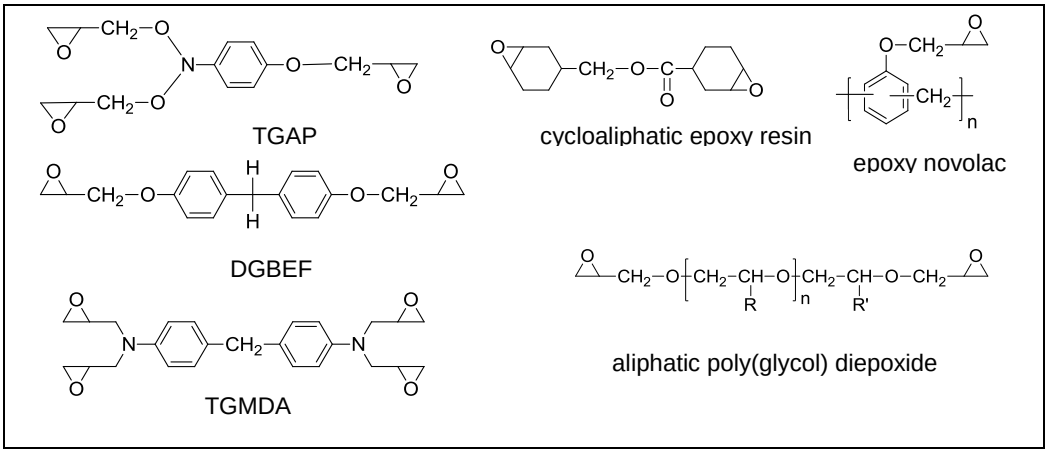

Figure 2. Structure of several epoxy resins

One of the main characteristics of epoxy resins, which are necessary to adjust the formulation composition to cure, is the epoxy content. It is expressed in epoxide equivalent which is defined as the weight of the resin per mol (or equivalent) of epoxide group. For pure diglycidyl ether with two epoxy groups per molecule, the epoxide equivalent will be the half of the molecular weight.

1.2. Cross-linking process

The epoxy resin should be mixed with a curing agent or hardener to obtain the thermoset and then heat or stimulate by an external irradiation. The choice of this agent depends upon the processing methods, conditions, structure of the resin and the properties required. Two types of curing agents are widely used: catalytic and stoichiometric agents. [9] In addition, some agents may involve both catalytic and stoichiometric systems.

A catalytic curing agent acts as an initiator for the resin homopolymerization process whereas a stoichiometric curing agent reacts as a co-monomer in the polymerization reaction.

1.2.1. Catalytic cure

Lewis bases contain unshared electron pairs which can attack as nucleophiles sites of low electron density. Among them, tertiary amines are used for anionic homopolymerization of epoxies and the reaction involves a zwitterion, which consist in an ammonium and an alkoxide group. This alkoxide opens up a new epoxy group generating another ion which in turn reacts with a further epoxy group. In the case of glycidyl ether resins this reaction occurs at both ends of the molecule resulting in a cross-linked structure. Cycloaliphatic epoxy resins cannot be cured by anionic initiators.

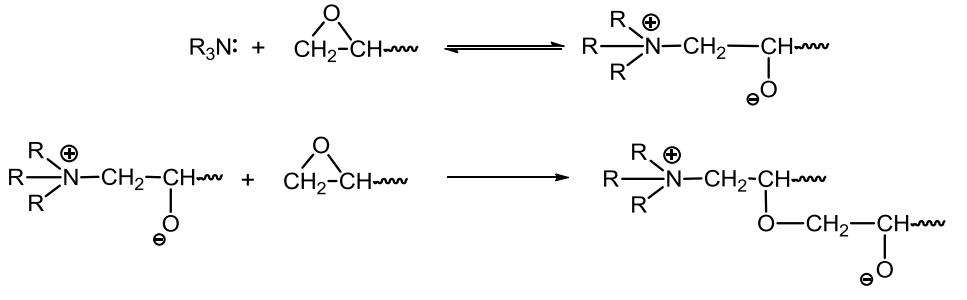

Figure 3. Reaction mechanism of curing of epoxy resins with tertiary amines

As anionic curing agents, imidazoles, substituted pyridine and other tertiary amines, which are represented in **Figure 4**, are usually applied.[5]

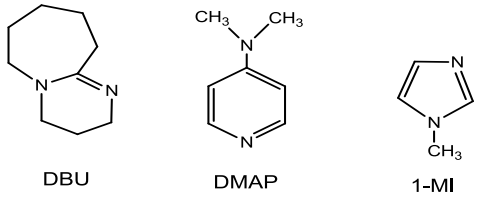

Figure 4. Structure of anionic initiators used in the crosslinking of epoxy resins

To get crosslinked networks a functionality of four is required. In case of catalytic cure, the functionality of epoxide group is two, because each epoxide group can form two new covalent bonds, and therefore the global functionality of a diepoxy resin is four.

Lewis acids such as BF_3 are electron deficient and hence they attack sites of high electron density, such as the oxygen in the oxirane ring. BF_3 reacts with epoxy resins causing gelation within few minutes. Complexing boron trihalides with amines is found to enhance the reaction.[10]

Reasonable pot lives using these complexes can be achieved because elevated temperatures are required to break the complex. Reactivity is controlled by the choices of the halide and the amine. The amine choice also affects other properties such as solubility in resin and moisture-sensitivity. The most used complex is the one with monoethylamine ($BF_3 \cdot NH_2C_2H_5$), a crystalline material which, cures epoxy resins at 80–100ºC.[11] The reaction mechanism is collected in **Figure 5**.

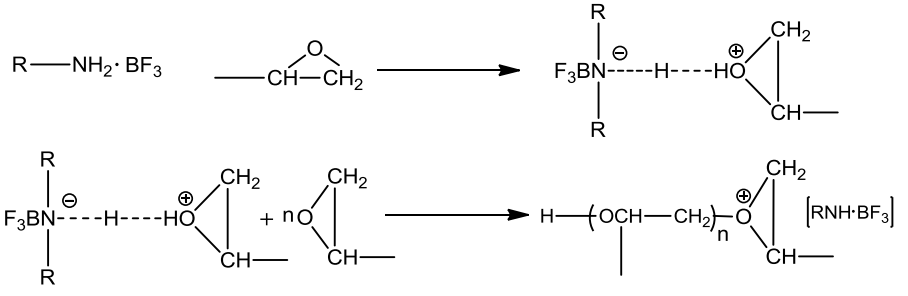

Figure 5. Reaction mechanism of curing of epoxy resin with BF_3 amine complexes

Our research group have proposed the use of a series of lanthanide triflates as cationic epoxy initiators, such as $Sm(OTf)_3$, $Yb(OTf)_3$ or $La(OTf)_3$.[12] Lanthanide triflates are stable in water and air atmosphere. They are also thermally stable and have low toxicity. They have a strong Lewis acidity enhanced by the electron-withdrawing trifluoromethanesufonyl group.

It is worth mentioning that $Yb(OTf)_3$ is the one that accelerates more the curing process thus allowing to perform isothermal curing at lower temperatures. This can be attributed to the higher Lewis acidity and Pearson hardness of Yb^{3+} in comparison with the other lanthanide cations.[13] In addition, the materials obtained using the $Yb(OTf)_3$ presented higher values for T_g than those obtained using $La(OTf)_3$ and also higher thermal degradability.[14]

Other thermal cationic initiators are benzyl sulfonium, benzyl ammonium and benzyl phosphonium salts, which have latent characteristics. That is, they show no activity under normal conditions but they are triggered by an external stimulation like heating at a definite temperature producing a fast curing of the epoxy resin.[15]

Photoinitiated cationic curing of epoxies is a fast developing technique. Photoinitiators include aryl diazonium salts, diaryl iodonium salts and sulfonium salts. These photoinitiators, under UV irradiation, generate protons capable to initiate the homopolymerization reaction.[16]

In cationic initiated homopolymerization of epoxides the competition between the activated chain end mechanism (ACE) and the activated monomer mechanism (AM) has been reported.[17] Both mechanisms are depicted in **Figure 6**.

Hydroxyl groups or the presence of traces of water favors the AM mechanism[18] which leads to chain transfer process, finally affecting the characteristics of the materials. AM mechanism allows the chemical incorporation of hydroxylic structures to the polymeric network.

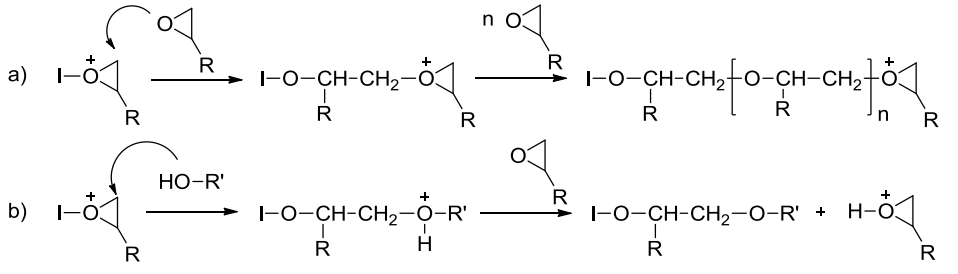

Figure 6. Mechanisms in the cationic curing of epoxy resin: activated chain end (a) and activated monomer (b)

Cycloaliphatic epoxy resins are more reactive than glycidylic towards cationic curing because of the more strained ring of the formers.[19]

1.2.2. Stoichiometric cure

Primary and secondary diamines are widely used as curing agents for epoxy resins. The reactions taking place during curing are represented in **Figure 7**.

The reaction of an epoxy group with a primary diamine initially produces a secondary alcohol and a secondary diamine. The secondary diamine in turn reacts with epoxy group to give a tertiary diamine and two secondary hydroxyl groups.

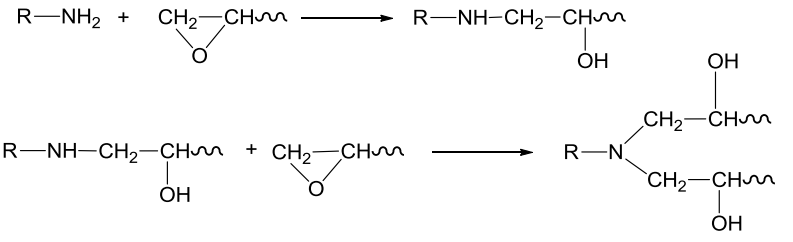

Figure 7. Reaction mechanism of curing of epoxy resin with primary amines

The hydroxyl compounds accelerate the rate of amine curing.[20] During this process, the hydrogen atom of hydroxyl group partially protonates the oxygen atom of epoxy group, making the methylene group more susceptible to nucleophilic attack by the amine. Some commercial amine curing agents are represented in **Figure 8**.

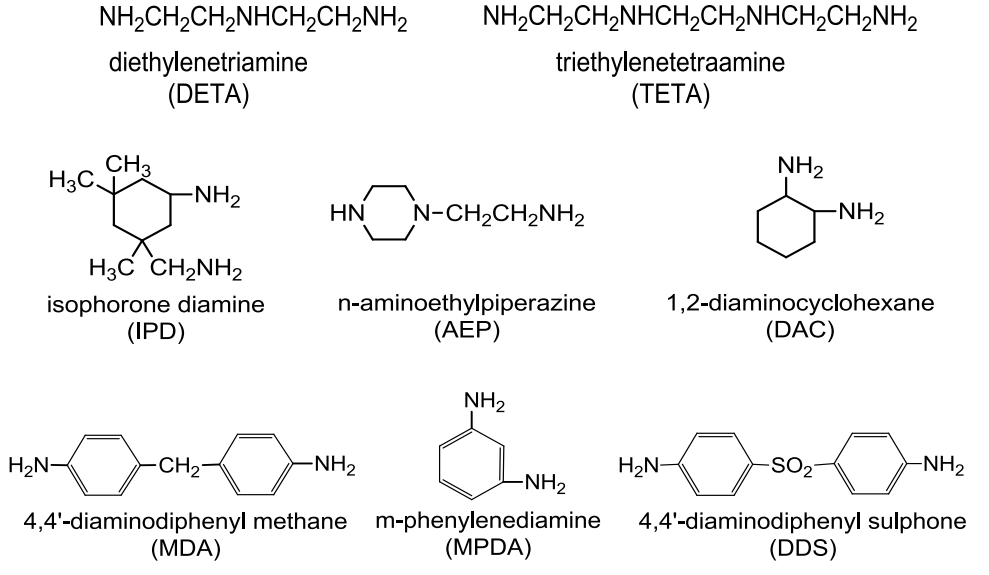

Figure 8. Structure of the most used primary amines in the curing of epoxy resins

Aliphatic amines have higher reactivities than the aromatic counterparts and then they are able to cure at room temperature. Aromatic amines have been developed to achieve greater heat and chemical resistance than those of aliphatic amines, but heating is needed to reach the complete curing.

The stoichiometry of these curing agents is based in the fact that every labile H (linked to nitrogen) reacts with an epoxy group. Thus, 2 mol of DGEBA are needed for 1 mol of a primary diamine. In this case, epoxy groups have a functionality of one and amines have a functionality of one for each active hydrogen.

Therefore, to cure a diepoxy resin a primary diamine is required to reach crosslinked networks. Sometimes, under-stoichiometric formulations are used to improve adhesion or mechanical characteristics.

Cycloaliphatic epoxy resins cannot be cured by amines because of the steric hindrance produced by the protons of the cycloaliphatic ring on the epoxide towards nucleophylic attack but they are the most common curing agents for diglycidylic resins.

Acid anhydrides are also one of the most important classes of epoxy curing agents, especially in composite and electronic applications.[6] The most common types of anhydrides are represented in **Figure 9**.

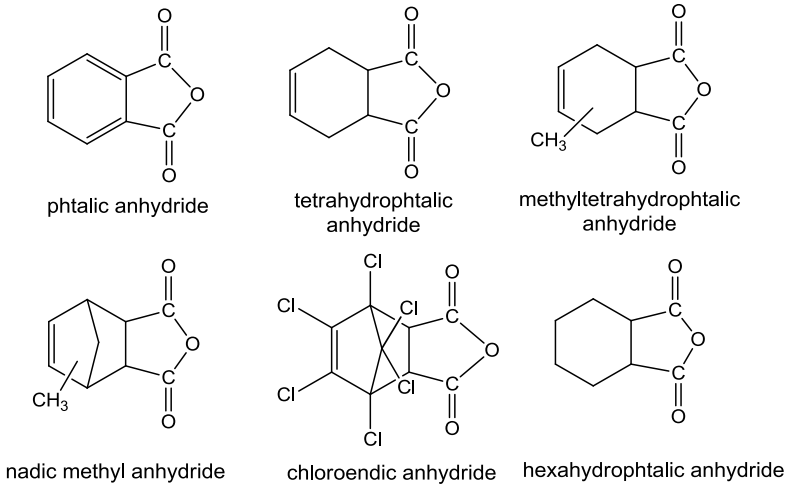

Figure 9. Structure of the most used anhydrides in the curing of epoxy resins

Anhydrides are usually used at ratios of 0.85:1.1 mol of anhydride per epoxy equivalent, although the stoichiometric proportion is 1:1. Epoxy anhydride systems show long pot life, low exotherms and little shrinkage when cured at elevated temperatures. They exhibit good mechanical and electrical properties. Tertiary amine, metallic salts, and imidazoles often act as accelerators for anhydride cured epoxy systems.[5]

The reaction of anhydrides with epoxy groups is complex, with several competing reactions. Different reactive processes can occur in catalysed and non-catalysed epoxy/anhydride curing. The most significant reaction mechanisms in non-catalysed systems are represented in **Figure 10**.

In this case, the reaction begins by the presence of hydroxyl groups or water in the reactive mixture. Etherification and homopolymerization reaction, catalysed by acid can also compete, depending on the cure temperature.

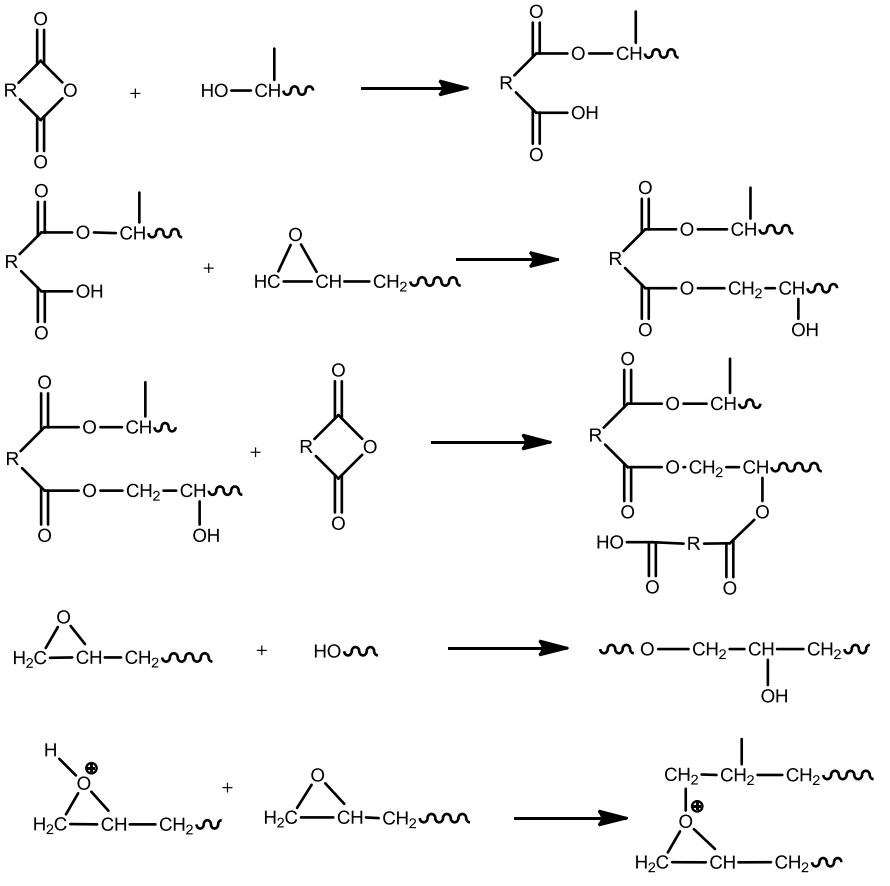

Figure 10. Reaction mechanism occurring in the non-catalysed curing of epoxy resins with anhydrides

As previously said, the reactivity of the epoxy/anhydride system is low. For this reason the addition of some catalyst in the proportion of 0.5 to 3% to help to reduce the curing time and also to prevent the degradation of the thermoset is usually done.[6] Tertiary amine catalyzed mechanism is shown in **Figure 11**.

Firstly, the tertiary amine is reacting with one oxirane ring and in this way forming a zwitterionic intermediate containing an ammonium and an alkoxide anion (A). This reacts fast with an anhydride molecule generating a carboxylate group (B). The propagation occurs between the reaction of the formed carboxylate group and another epoxy group

forming a new alkoxide group (C). This species can give the alternate copolymerization reaction (D). They are no clear evidences in reference to the termination step of polymerization and if the tertiary amine is getting bonded to the matrix during the reaction. Some authors are describing it permanently bonded [21] and some are contradicting this fact.[22]

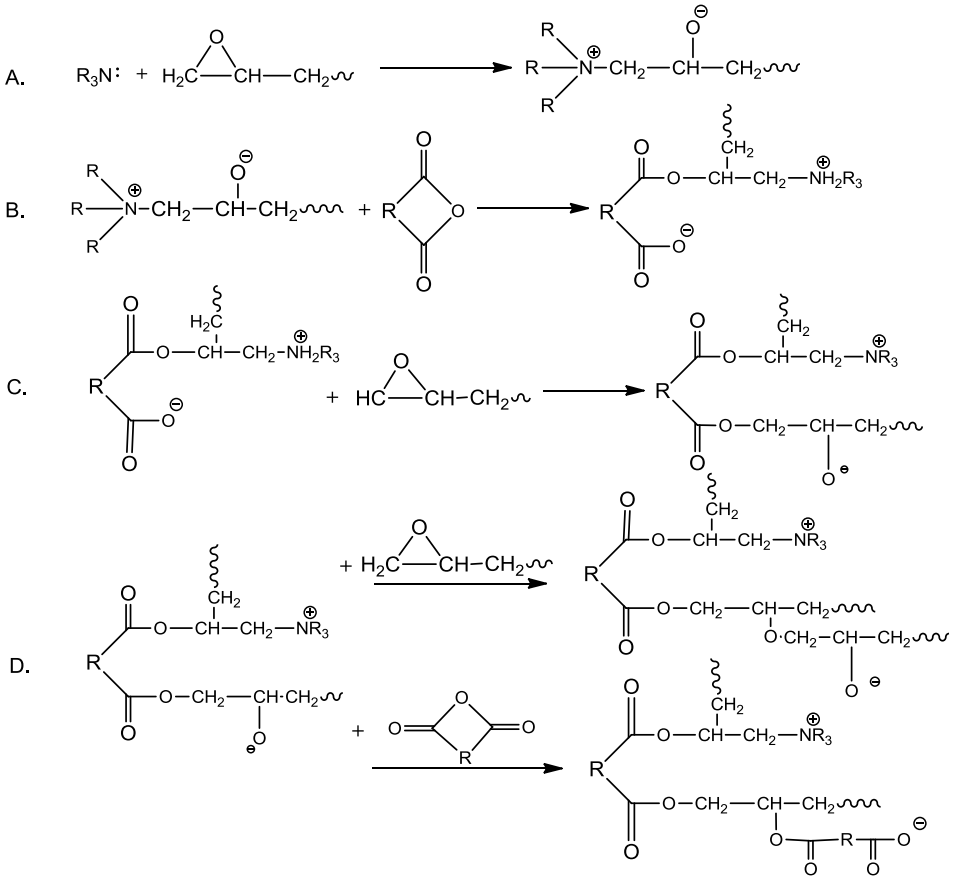

Figure 11. Reaction mechanism occurring in the amine-catalysed curing of epoxy resins with anhydrides

Whereas the non-catalyzed reaction of anhydrides and epoxides follows a polycondensation kinetics, the catalyzed process follows a ring-opening mechanism consisting in an alternating copolymerization. In this catalyzed system the stoichiometric ratio is one epoxy group per anhydride.

Dihydrazides were first described in 1958, by Wear [23] as useful curing agents for epoxy resins. Depending on their structure T_g's over 150°C and pot life over 6 months as

cure time can be obtained. They can be considered as latent curing agents, which can be triggered at high temperatures. Among the most commercially available dihydrazides those represented in **Figure 12** can be considered.

In epoxy resins, dihydrazides are typically formulated as one mol of NH active hydrogen of dihydrazide per epoxy equivalent. That is, all four of the primary hydrogens will react, each with one epoxy group, but formulations, 0.7-1.2 have been used with little to no reduction in properties. Cure temperature of the epoxy is related to the melt temperature of the dihydrazide. However, curing with dihydrazides can be accelerated with various electron donating compounds, such as ureas, imidazoles and imidazole adducts, as well as inorganic compounds like lead octoate and stannous octoate.

The advantages of the dihydrazide-epoxy curing are that they are B-stageable, allowing for use in prepregs, adhesive films, moulded parts etc.

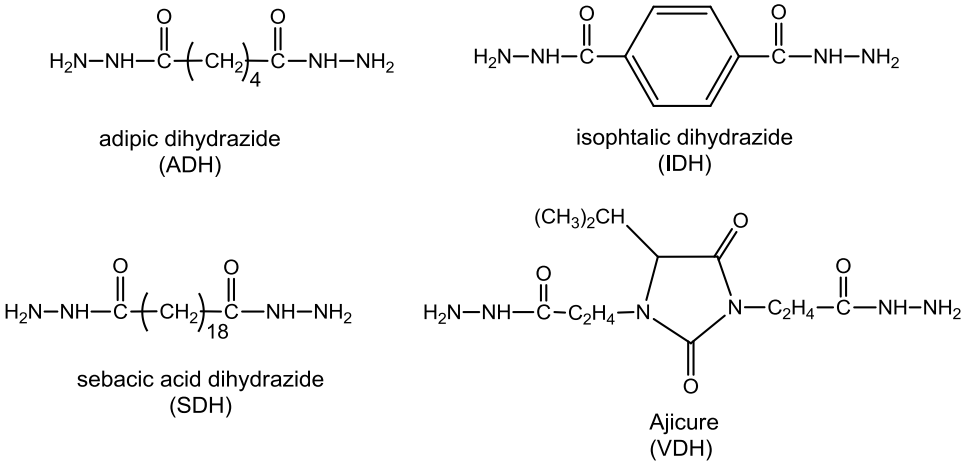

Figure 12. Chemical structures of commonly used dihydrazides

1.3. Network structure

The ratio of resin to hardener has a strong effect on the structure of the cured resin and its properties. Similarly, the type of curing agent and resin affect the material characteristics. For this reason it can be said that epoxy materials are extremely versatile thermosets.

The extent of cross-linking is a measure of the degree of cure. The most important properties are obtained at maximum cross-linking. The curing temperature largely influences the ultimate cross-link density achieved. Heating increases molecular mobility resulting in higher cross-link density which in turn affects the chemical resistance of the cured matrix positively.

The reactivity of epoxy resin-hardener systems are usually determined by DSC, which allows measuring the heat evolved, the existence of unreacted structures or the T_g

achieved after curing. DSC has also been used to study the kinetics of the curing which allows the prediction of the curing schedule, which is of great importance in the technological application. The disappearance of epoxy groups during cure can be followed by IR spectroscopy and gives direct information on the reaction mechanisms that completes the information extracted by DSC. In **Figure 13** a representation of the formation of the network is depicted.

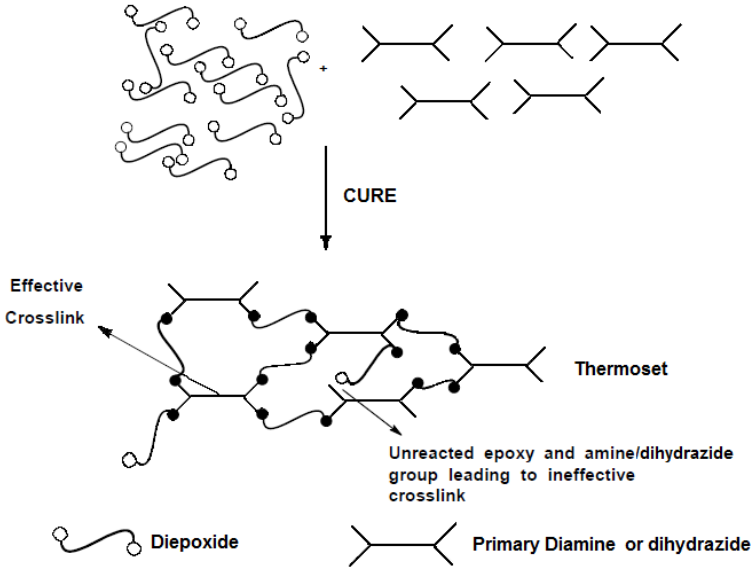

Figure 13. Formation of resin-hardener networks

1.4. Epoxy curing process

The synthesis of a thermosetting polymer starts from monomers which react between them or with the corresponding curing agent to form branched structures with the subsequent increase in the viscosity (sol stage). At a particular conversion of functional groups, gelation takes place, meaning that a giant macromolecule is formed. This sol–gel critical transition is a typical feature of thermoset preparation.

At gelation, viscosity increases to infinite and after gelation an insoluble fraction (the gel fraction) is formed in the system.[1] Eventually at full conversion of functional groups, in stoichiometric formulations, the sol fraction disappears and the final thermosetting polymer is composed of one macromolecule of a gel. In thermosetting polymers, gelation is an irreversible process. The only way to destroy the gel is by breaking the covalent bonds generated by the chemical reaction. Practical ways to determine gelation are frequently related to the fact that the viscosity of the reaction mass becomes infinite at the gel conversion. When vitrification takes place, the system is transformed from a gel into a glass. At this point there is a reduction of the system's mobility through the

formation of covalent bonds, up to a point where the cooperative movements of large portions of the polymer, which are characteristic of rubbery and liquid states, are no longer possible. Thus, the reaction stops and only an increase in the cure temperature can restart the polymerization reaction. **Figure 14** represent the gelation and vitrification processes.

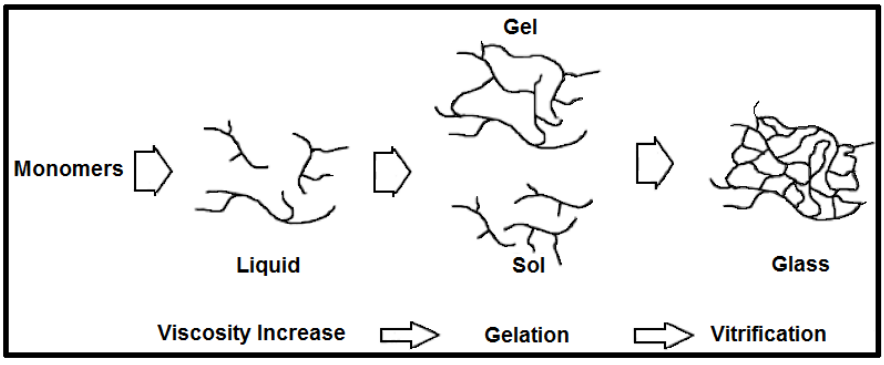

Figure 14. Phenomenological evolution of the curing process

The epoxy polymerization represents a fundamental stage of the overall manufacturing process which indeed will affect the final performances of the cured material system. For this reason, it become imperative to analyse and to understand the different curing and kinetics evolution steps in order to achieve an optimal level of performance in the final composite. The curing of a thermoset epoxy resin can be expressed in terms of a time–temperature-transformation (TTT) diagram (**Figure 15**). In the TTT diagram, the time to gelation and vitrification is plotted as a function of isothermal cure temperature.

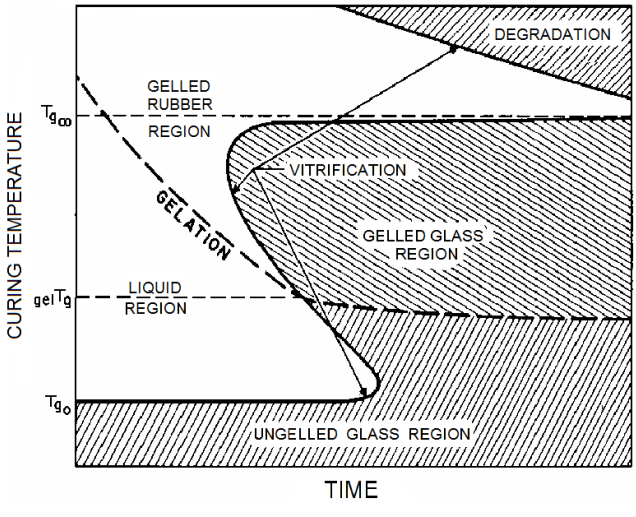

Figure 15. Time-temperature-transformation diagram (TTT)

The main features of TTT diagram are: gel point and onset of vitrification. The gel point is defined as the onset of the formation of insoluble, cross-linked polymer (gel fraction) in the reaction mixture. However, a portion of the sample may still be soluble (sol fraction). The onset of vitrification is when the glass-transition temperature (T_g) of the curing sample overcomes the curing temperature T_c. Ideally, a useful thermosetting system suitable for structural applications would cure until all monomers are built into the network, resulting in no soluble fraction. The S-shaped vitrification curve and the gelation curve divide the time-temperature plot into four distinct states of the thermosetting-cure process: liquid, gelled rubber, ungelled glass and gelled glass.

The most significant temperatures in the plot are: T_{g0} which is the glass-transition temperature of the unreacted resin mixture; $T_{g\infty}$ the glass-transition temperature of the fully cured resin; and ${}_{gel}T_g$ which represents the point where the vitrification and gelation curves intersect.

In the early stages of cure before gelation or vitrification, the epoxy curing reactions are kinetically controlled. When vitrification occurs the reaction becomes diffusion controlled, and the reaction rate is reduced. With further cross-linking of the glass, the reaction rate continues to decrease and it is eventually stopped.

In the region between gelation and vitrification (rubber region) the reaction can range from kinetic to diffusion control. This competition causes the minimum in vitrification temperature reported in the TTT diagram between ${}_{gel}T_g$ and $T_{g\infty}$. As the cure temperature is raised, the reaction rate increases and the time to vitrification decreases until the decrease in diffusion begins to overcome the increased kinetic reaction rate.

Below $T_{g\infty}$, the reaction does not go to completion. As curing proceeds, the viscosity of the system increases as a result of increasing molecular weight, and the reaction becomes diffusion-controlled and eventually is quenched as the material vitrifies. After quenching, the cure conversion can be increased by raising the temperature. This is often practiced as post-cure for certain epoxy systems to achieve maximum cure and performance. Post-cure is only effective at temperatures higher than $T_{g\infty}$. However, it must be noted that at temperatures sufficiently above $T_{g\infty}$, onset of network degradation can also be seen if enough time is maintained.

The TTT diagram is useful in understanding the cure kinetics, conversion, gelation, and vitrification of the curing thermoset. Gelation and vitrification times can be determined from the intersections of the storage and loss moduli and the maxima in the loss modulus of an isothermal dynamic mechanical spectrum, respectively. Some other techniques have been developed using rheological and dynamic mechanical analysis instruments to determine the gel point and vitrification.

Understanding the gelation and vitrification characteristics of an epoxy/curing agent system is critical in developing the proper cure schedule/process to achieve optimum performance. One important application is the management of cure temperatures (T_c) and heating rate: if T_c is too low, vitrification may occur before gelation and further reactions may not be completed, resulting in an incomplete network structure and poor performance. Furthermore, attention must be paid to the relationship between mixing of reactants and gel point. Epoxy resins and curing agents must be carefully mixed prior to

the gel point since the rapid viscosity build-up at gel point inhibits homogeneous mixing of reactants, resulting in potential network and morphological inhomogeneities and defects.

1.5. Epoxy thermosets properties

The properties of cured epoxy resins vary in importance depending on the use of the cured material. The main properties of interest from an application point of view are mechanical properties, chemical and thermal resistance, electrical properties and flame and weathering resistance. Epoxies have excellent mechanical properties compared to other thermosets. They show a good combination of tensile strength, modulus, flexural and impact strength.

1.5.1. Chemical resistance

Epoxy thermosets are versatile from the view point of chemical resistance. Three dimensional cross-link networks are stable in front of the attack by corrosive chemicals, including weak alkalis, strong acids, and organic solvents. They are attacked by some strong acids, but are resistant to strong alkalis. The chemical resistance of a completely cured resin is a function of its structure and chemical composition, molecular weight and the degree of cross-linking.

1.5.2. Thermal resistance

Heat resistance is directly related to resin composition. Molecular weight between crosslinks, crosslinking degree and chemical structure of the network have direct effects on strength and rigidity at elevated temperatures. The crosslinked nature enhances the resistance to softening and deformation at high temperature. The structural transitions of these cross-linked networks are characterized by DSC, DMTA or measuring heat distortion temperature (HDT). These studies give the transition temperature at which amorphous boundaries transform to a rubbery state. The HDT is a measure of the heat resistance of the resin.

1.5.3. Mechanical properties

Unmodified epoxy resins exhibit brittleness and low elongation after cure. These polymers usually craze on their free surface and the crazed areas are converted into cracks, which propagate with brittle energy absorption resulting in fracture. The high glass transition temperatures of epoxy thermosets are the result of cross-linked structures and this is achieved at the expense of reduced toughness and damage tolerance.

1.6. Improvement of the reworkability in epoxy thermosets

Traditional thermosetting materials display poor tractability which limits their use in applications where degradability or reworkability is advantageous.[24] The concept of reworkability in thermosets is related to the ability of a material to break-down under controlled conditions in order to be removed from a given substrate (**Figure 16**), but it does not mean that the polymeric material can be reused or recycled.

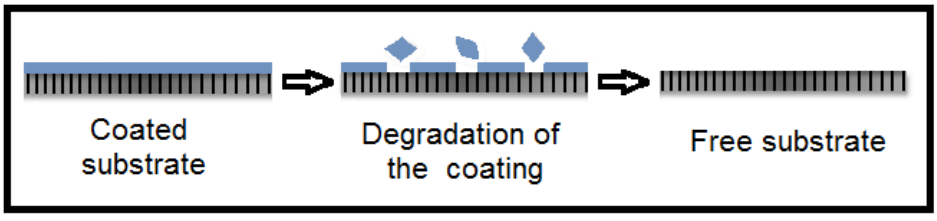

Figure 16. Reworkability in thermosets

Ober et al.[25,26] went further in this approach and prepared cycloaliphatic epoxy resins with ester groups highly substituted in β position. On that way the pyrolytic elimination of esters is favoured and allows the elimination of the coating at temperatures between 200 and 250 ºC.

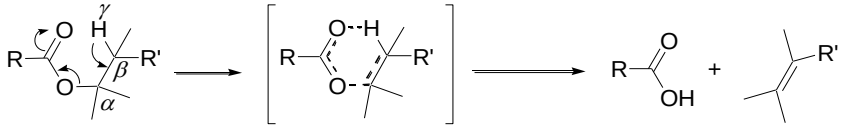

Figure 17. Mechanism of pyrolytic degradation of esters (β-elimination)

1.7. Improvement in toughness in epoxy thermosets

Toughening generally refers to improvement in mechanical and thermal stress resistance and does not affect other properties like thermal stability, strength and hardness. Toughness of a specimen refers to the total energy required to cause failure, i.e., the total area under the stress-strain curve or the energy absorbed in an impact test. Toughening of the resin by the addition of suitable toughening agents or chemical modifiers means to improve the amount energy absorption capacity. This results in enhancement of impact resistance, elongation and resistance to crack propagation.

There are several classical approaches to enhance the toughness of epoxy resins which include:

- Chemical modification of the network backbone to make it more flexible;

- Increasing the molecular weight of the epoxy resin to improve the molecular weight between crosslinks;
- Lowering the crosslink density of the matrix by adjusting the ratio epoxy resin/crosslinking agent or by adding reactive diluents;
- Incorporation of toughness modifiers in the formulation;
- Incorporation of inorganic fillers/reinforcements into the neat resin.

Unmodified DGEBA resins exhibit brittleness and low elongation after cure. Aliphatic diepoxides enhance the flexibility providing chain segments with greater free rotation between crosslinks. Also, the selection of flexible curing agents can help to increase impact resistance.

Diluents reduce the resin viscosity and simplify handling. Dibutyl phthalate can be used as non-reactive diluents whereas phenyl glycidyl ether, butyl glycidyl ether and octylene oxide are used as reactive diluents in epoxy resins.[27] Since diluents affect the physical properties of the resin and retard cure, they are used in small proportions (less than 10 phr).

Flexibilizers and plasticizers are added to improve the flexibility and as a result, the toughness of the resin. Low molecular weight polyamides from dimer acids, low molecular weight polysulphides, polyamines and polyglycol diepoxides have been used as flexibilizers in epoxy resins. Oligomeric aliphatic polyesters containing carboxyl end groups are used to incorporate flexible chain segments in epoxy resins. Flexibilization is accompanied by reduction of T_g, elastic modulus and hardness properties.

Among the various types of elastomeric materials which have been studied, it can be considered poly(siloxanes),[28] fluoro elastomers,[29] acrylated elastomers,[30] reactive butadiene-acrylonitrile solid [31] and liquid rubbers.[32]

Thermoplastic toughening of epoxy resins, studied since the early 1980s, showed a considerable progress in toughness enhancement. The main advantage in using thermoplastics to toughen epoxies is that their inclusion needs not result in any significant decrease in desirable properties such as modulus and yield strength as is the case with rubber toughening. Polysulphones, polyether sulphones, poly ether-ketones and poly ether-ether ketones are the major thermoplastics employed in epoxy toughening. The first two toughening studies with thermoplastic additives were carried out by Bucknall and Partridge in 1983.[33] In comparison, with rubber modification the level of toughness improvement achieved by thermoplastic modification is generally poor especially with relatively low T_g systems based on difunctional resins.

In rubber modification the rubber is initially miscible with the resin and the hardener. When the reaction starts, the rubber first forms a copolymer with the resin, then phase-separates. Thus, the cured thermoset possesses a dispersed rubbery phase.

The factors likely to influence morphology include elastomer concentration, molecular weight, type and extent of hardener used and curing conditions. The morphological factors considered important for optimum toughening in rubber modified epoxies are the rubber volume fraction, particle size and particle size distribution.

The main toughening mechanisms initiated by the presence of rubber particles are localized shear deformation in the form of shear bands running between rubber particles[34] and internal cavitation or debonding of rubber particles[35] with subsequent plastic growth of voids in the epoxy matrix.

The effect of the rubber particle size on deformation mechanism in epoxy system was studied by Sultan and McGarry.[32] Shear mechanism is enhanced by the presence of small rubber particles while crazing appears as the main reason for toughness improvement with large rubber particles and the fracture energy of such a material is five times more than that with smaller rubber particles.

Fillers are used for tooling and casting applications.[36] They reduce the cost of the resin at the same time reducing the cure shrinkage. Powdered metal oxides reduce the ultimate tensile and compressive strength of the resin, but have little effect on impact strength. Reinforcement of the resin matrix with fibres will improve toughness considerably. However, many applications do not allow the use of reinforcement fibres and yet require improved toughness and impact resistance.

Polymer nanocomposites have attracted great interest, both in industry and in academics, because they exhibit remarkable improvement in material properties compared with virgin polymer or conventional micro and macro composites.[37,38,39] Conventional composites usually require a high content (>10%) of the inorganic fillers to impart the desired mechanical properties. Such high filler levels increase their density of the product and can cause the deterioration in properties through interfacial incompatibility between the filler and the organic material. Besides, processability worsens as filler content increases. In contrast, nanocomposites show enhanced thermo mechanical properties even with a small amount of layered silicate (≤5%).

Polymer nanocomposites are generally defined as the combination of polymer matrix and fillers that have at least one dimension in nanometer range. The nanofillers can be one-dimensional (layered minerals such as clay),[40,41] two-dimensional (like carbon nanotube, nanowires, nanofibers, cellulose whiskers, etc.),[42] and three-dimensional (spherical particles include silica nanoparticles, nanowhiskers, etc.).

Polymer nanocomposites are known for its outstanding mechanical properties like high elastic modulus[43,44] increased strength[45,46] barrier resistance[47,48] flame retardancy,[49] etc., with very small addition (less than 5 wt.%) of nano particles. This is due to the very large surface area of interaction between polymer matrix and nano filler.

Epoxy nanocomposites are highly versatile polymer systems for the new era of making lighter structural composites for various aerospace and automobile applications. The final morphology, physical, chemical and barrier properties of the nanocomposites were influenced by processing method, clay modifier and curing agents. Epoxy clay nanocomposites showed remarkable improvement in tensile, flexural and fracture toughness properties. Thermal stability and barrier properties were significantly improved by the incorporation of clay particles to epoxy systems.

In recent years hyperbranched polymers (HBPs) have been used as toughness modifiers of epoxy thermosets.[50,51] HBPs are used to improve the toughness of the

epoxy materials due to its high density of functional terminal groups, which allows to tune the interaction with the matrix.[52,53] The incorporation of HBPs into the network structure introduces flexibility and increases the impact resistance without affecting others properties, such hardness, modulus or glass transition temperature. [54] These improvements are attributed either to the flexibilizing effect or to the reduction of the crosslinking densities because the homogeneous incorporation of HBPs or alternatively to local heterogeneities within the crosslinked network due to the formation of phase separated particles.

Since the interaction between phases is an important factor related with fracture mechanism, the structure of the HBP must be tailored in order to improve interfacial adhesion between phases. Thus, the identity of terminal groups seems to have a profound effect on the properties of the materials.

Additionally to HBPs, multiarm star polymers can also be considered as a new class of modifiers for epoxy resins. Meng et al. obtained nanostructured diglycidylether of bisphenol A thermosets using core-crosslinked stars based on poly(styrene) core with poly(ethyleneoxide) or poly(styrene)-*b*-poly(ethyleneoxide) arms.[55] In our research team multiarms stars with poly(ε-caprolactone) (PCL) arms and poly(glycidol) or poly(styrene) core have been used because of PCL has a high chain flexibility and is miscible in most epoxy systems.[56,57] The addition of these modifiers led to homogeneous materials with a more tough fracture without increasing the viscosity of the formulation and reducing the shrinkage on curing. The addition of the star-shaped modifier reduced the shrinkage after gelation in a higher extent than the linear PCL. The detrimental effect on the T_g was lower on adding the multiarm-star modifier whereas impact stress and microhardness were improved much with the star topology.[58]

1.8. Hyperbranched Polymers

Hyperbranched polymers (HBPs) are a special type of dendritic polymers and have as a common feature a very high branching density with the potential of branching in each repeating unit. They are usually prepared in an one-pot synthesis, which limits the control on molar mass and branching accuracy and leads to “heterogeneous” products with a distribution in molar mass and branching. This distinguishes hyperbranched polymers from perfectly branched and monodisperse dendrimers. In the last 20 years, both classes of dendritic polymers, dendrimers as well as hyperbranched polymers, have attracted major attention because of their interesting properties resulting from the branched architecture as well as the high number of functional groups.

Some other topologies are also of interest for several applications, among them star polymers or brush polymers, which are represented in **Figure 18**.

Hyperbranched polymers began to seriously attract the attention of scientists in the early 1990s, although Flory first described the synthesis of highly branched polymers by the self condensation of AB_2 type monomers or condensation of AB and AB_2 type monomers in 1952.[59] The term “hyperbranched” was first coined by Webster and Kim in the late 1980s, referring to a dendrimer-like structure with very high chain branching.[60,61]

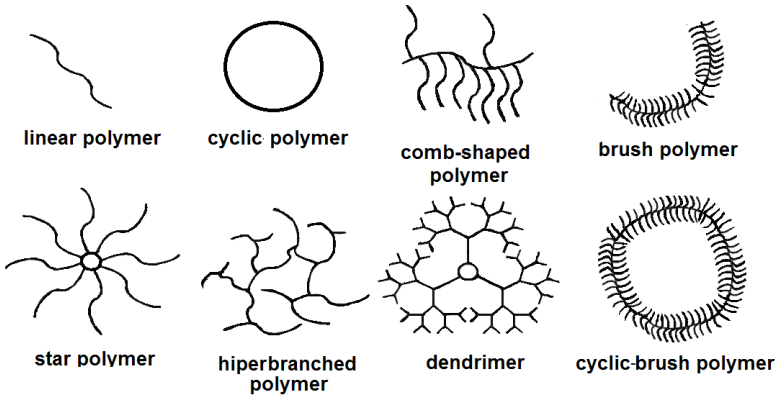

Figure 18. Different types of polymeric topologies

Hyperbranched polymers were not supposed to be very promising at first, probably due to their poor mechanical properties, broad molecular weight distributions, and non-entangled/non-crystalline behaviour.[62,63] However, after realizing the unique properties and developing appropriate techniques for synthesizing dendrimers in the eighty's, hyperbranched molecules started to become an alternative to dendrimers because of their easier preparation and lower cost.[50,64]

Although dendrimers have a well-defined structure, they require a step-wise synthesis, while hyperbranched molecules can be synthesized in one step. They are believed to have properties similar to dendrimers even though they possess some defects on the polymer backbone.[65] Such properties are their low viscosity, good solubility, unique thermal properties and good chemical reactivity.[66] Dendritic molecules have low viscosities because of their low entangled structure due to their spherical shape. Most hyperbranched polymers are amorphous, although crystalline hyperbranched polymers do exist. There are many unreacted chain ends in hyperbranched polymers, and the polymer properties are highly dependent on their nature. Therefore, modifying the end groups provides a viable means of controlling the properties of these polymers.

The growing interest in hyperbranched polymers for technology is due to their unique properties, which make them useful in several applications, such as functional crosslinkers, additives, modifiers in adhesives, coatings, structured hydrogels and dental composites.[67,68,69] Hyperbranched polymers have also become useful in nanotechnology, for use as building blocks for nanoscale reaction parts, in biochemistry and biomedical applications, which include drug and gene delivery components, and finally in organic synthesis such as recyclable catalysts or high-loading supports.[70]

Hyperbranched polymers can be synthesized using condensation polymerization,[60,61] ring opening polymerization,[67,68,69] and addition polymerization.[62] Various types of hyperbranched polymers including polyphenylenes, polyesters,

polyamides, poly(ether imides), polyurethanes, polyureas, and polycarbonates are synthesized using condensation polymerization.[71] As described by Flory, hyperbranched polymers can be prepared by the self-condensation of AB_n type monomers, where A and B groups react with each other and n is equal to or greater than 2.[59]

Specifically, hyperbranched polyesters were prepared by self-condensation of different AB_2 type monomers,[72] condensation of AB_2 type monomer in the presence of a B_f type core molecule, condensation of AB_2/AB_3 type monomers with AB type monomers[62] with different functionalities,[64] or co-condensation of A_2 and B_3 type monomers. Some of these synthetic strategies are represented in **Figure 19**.

AB_n type monomers that contain one "A" functional group and *n*"B" functional groups undergo self-polycondensation or copolymerize with AB type monomers to generate hyperbranched polymers.[59] Polycondensation of AB_n monomers gave rise to various HBPs without the risk of gelation as described by Flory's equation. However, the main problem this methodology presents is the fact that most of AB_n monomers are not commercially available. The formation of bonds through the step-growth reactions are not controlled in any manner and the polydispersity is large. As in the formation of linear step growth polymers high molecular weight species are not created until the conversion is high and even in samples of high molecular weight polymer, monomers and oligomers are still present.

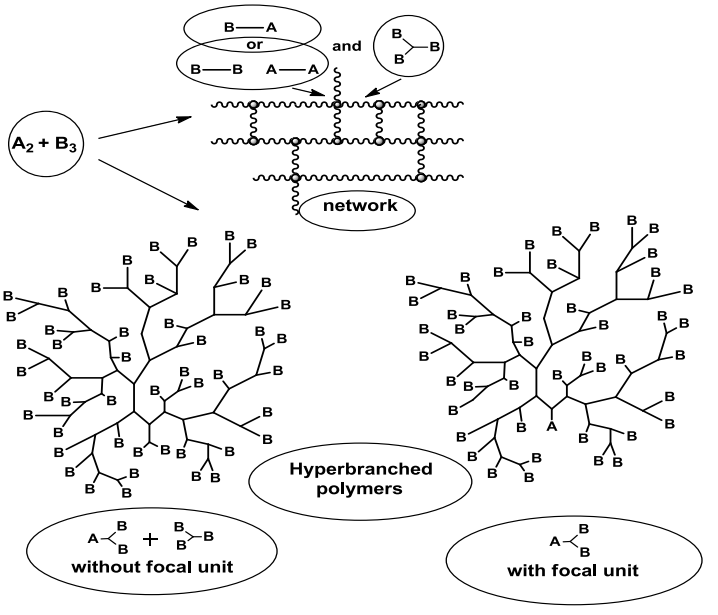

Figure 19. Synthetic methods for hyperbranched polymers.

Schallausky et al.[73] reported the synthesis of an aliphatic aromatic polyester by a AB_2 polycondensation from a commercial diphenol acid compound as depicted in **Figure 20**.

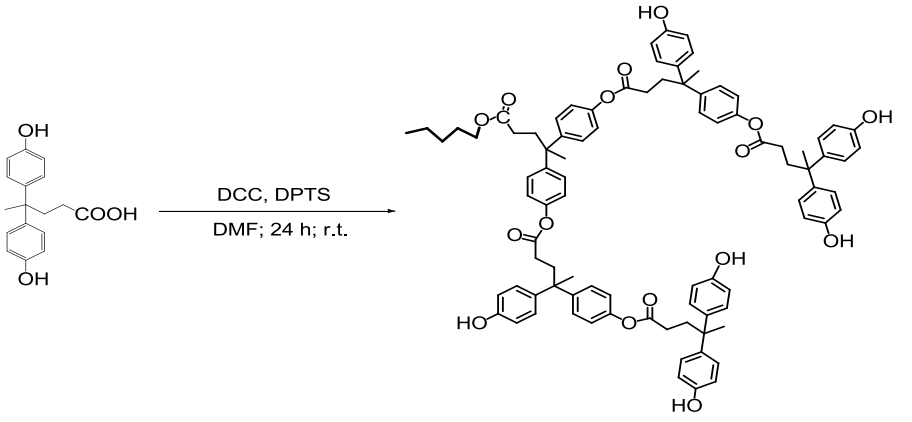

Figure 20. Synthesis of hyperbranched polyester from an AB_2 monomer

Figure 21 collects the mechanism of condensation of acid and alcohol by carbodiimide (DCC). DPTS is the 1:1 complex of 4-(dimethylamino)pyridine (DMAP) and p-TSA and it is required to efficiently suppress the irreversible side reaction leading to N-acylurea (F).[74] Furthermore, successful suppression of this side reaction favours polymerization and consequently high-molecular weight products are achieved.

This mechanism is believed to involve the O-acylisourea intermediate (C),[74,75] which can follow several possible reaction pathways. Bimolecular reaction between the O-acylisourea and a second carboxylic acid leads to the formation of the acid anhydride (E) and urea derivative (D). The extent of urea relative to the anhydride in absence of other nucleophilic species is known to strongly depend on solvent, pK of the carboxylic acid, and pH of the reaction medium.[76] DMAP and DPTS are well known as outstanding catalysts for the acylation of phenols and alcohols by acid anhydrides.[76]

Thus, esterification proceeds through the acid anhydride. Alternatively, it is possible to postulate that DPTS is effective at capturing the O-acylisourea (C) as active N-acylpyridinium intermediate (H). Formation of (H) from (C) involves a series of proton-transfer steps and is accompanied by the generation of urea (D). The acid catalysis may simply facilitate these proton-transfer steps leading to the N-acylpyridiumium (H) species. Reaction of (H) with a nucleophile such as alcohol (I) produces the ester (J) and DPTS (G), which could be involved in a further catalytic cycle.

The in-situ activation of the monomer with DCC in combination with DPTS enables the direct use of AB_2 type monomers and avoids the need to prepare and handle with pretreated (activated or protected) acid derivatives, which are described by Turner et al.[77] and Fréchet and coworkers.[72]

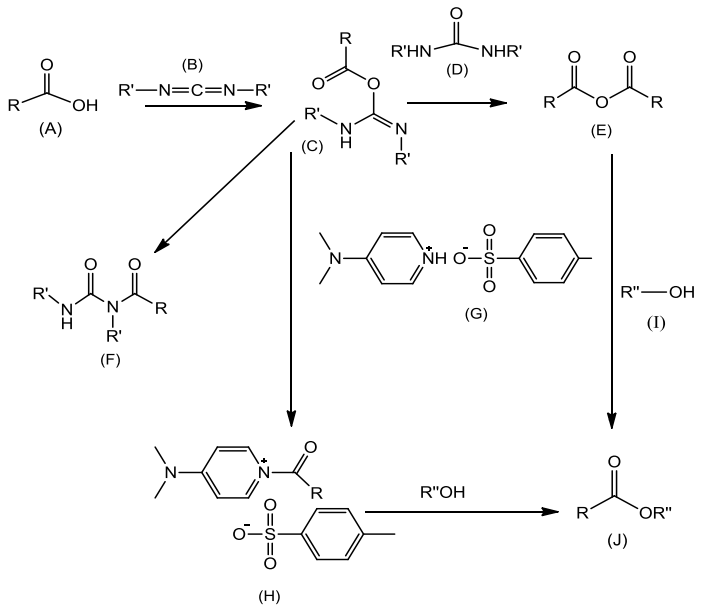

Figure 21. Proposed mechanisms during condensation of acid and alcohol by carbodiimide

Polycondensation of A_2 and B_3 monomers may achieve soluble HBPs with the advantage of commercial availability of monomers. **Figure 22** shows an example of this type of synthesis. It should be noted that high risk of gelation exists during reaction and therefore special skills such as slow addition of A_2 monomers to the diluted solution of B_3 is required. Another possibility is working in non-stoichiometric proportions.

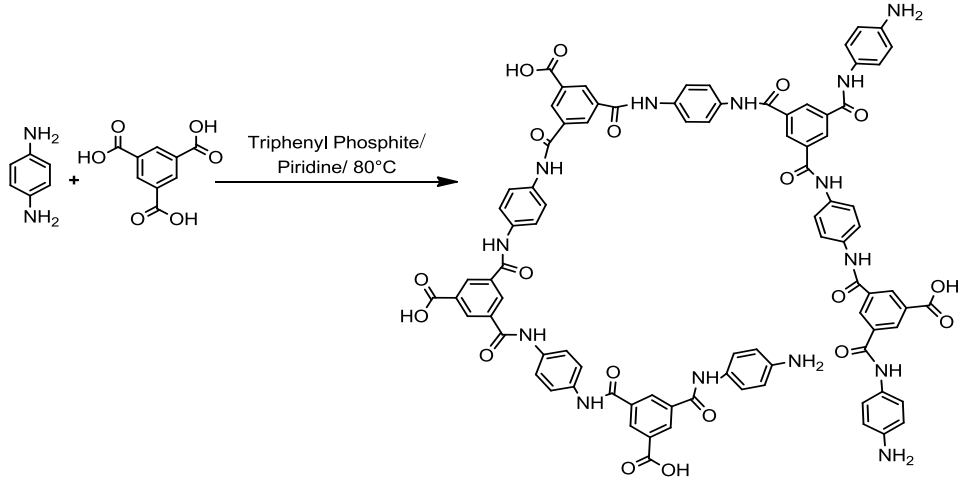

Figure 22. Synthesis of a HBP using the A_2 + B_3 monomer approach

Due to the statistical character of HBP synthesis, unlike dendrimers, they have molecular weight dispersity, isomerism and a degree of branching (DB). As seen in **Figure 23** the simplest HBP present four different units: the focal group, linear (L), dendritic (D) and terminal (T) units. Fréchet and co-workers defined the DB as the fraction of terminal and dendritic units from the total.[72]

$$DB = \frac{D+T}{D+T+L} \qquad (1)$$

Frey has reported the modified definition of DB based on the growth directions, as shown in the next equation[78] where N is the number of molecules.

$$DB = \frac{2D}{2D+L} = \frac{D+T-N}{D+T+L-N} \qquad (2)$$

Equations (1) and (2) give almost the same DBs for the hyperbranched polymers with a high molecular weight since N in equation (2) can be negligible in such cases. Frey also pointed out that DB statistically approaches 0.5 in the case of the polymerization of AB_2 monomers. Most of hyperbranched polymers reported in the literature have actually DBs close to 0.5.

It should be noted that hyperbranched polymer possess many isomers. If propagation reactions proceed symmetrically and DB of the polymer is equal to 1, the architecture of the hyperbranched polymer is eventually the same as that of the corresponding dendron. NMR spectroscopy is a powerful tool to determine the DB of hyperbranched polymers. The structures of the different D, L and T units are represented in the following scheme.

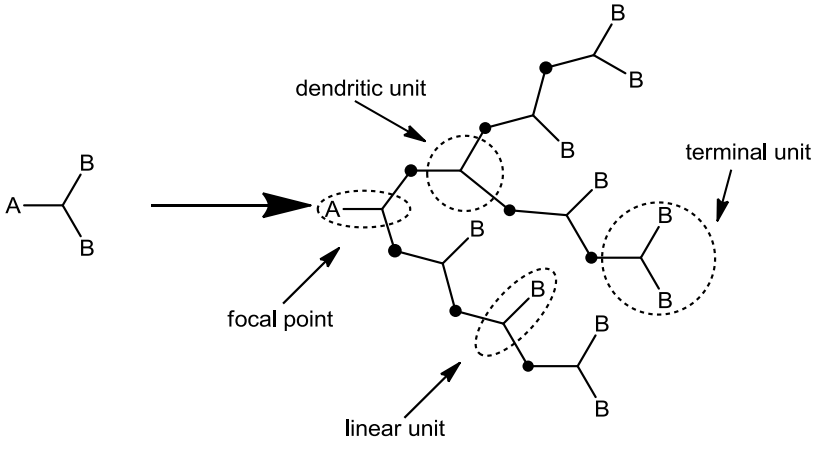

Figure 23. Different units present in a HBP obtained from the polymerization of an AB_2 monomer.

Although the properties of hyperbranched polymers are intermediate between those of dendrimers and linear polymers, the low cost for the synthesis of hyperbranched polymers permits to produce them on a large scale, giving them an advantage over dendrimers in applications. Hyperbranched polymers are thus considered as an alternative to dendrimers for different applications both in academia and in industry.[62,71]

The rheological behaviour is affected by molecular variables such as DB and M_w, however, the molecular architecture appears to be the most important factor determining the nature of the intermolecular interactions and consequently the rheological behaviour. The viscosity of hyperbranched polymers, both in solution and in the molten state have been found to be considerably lower when analysed to their linear analogues.

The intrinsic viscosity as a function of the logarithm molar mass of different polymer architectures is outlined graphically in **Figure 24**. For hyperbranched polymers, the slope is smaller than that for linear polymers although the intrinsic viscosities do increase with increasing molecular weight.

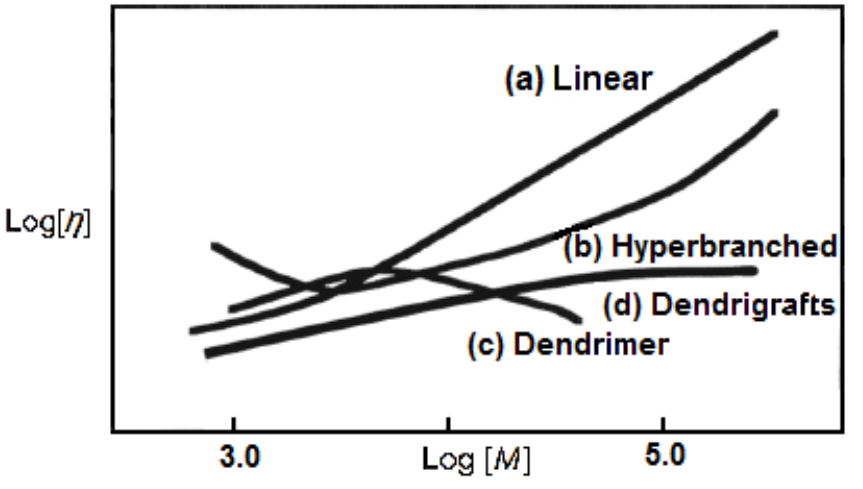

Figure 24. Schematic plots for the relationship between intrinsic viscosity (log[η]) and molecular weight (log[M]) for various polymer topologies.

Hyperbranched macromolecules in solution reach a maximum intrinsic viscosity where their shape changes from an extended to a more compact globular structure, especially at high molecular weights. The melt viscosity for linear polymers increases linearly up to a critical molar mass where the viscosity drastically increases.

This phenomenon is a consequence of the entanglement of polymer chains and is not observed for dendrimers or hyperbranched polymers, which indicates that minimal entanglement of the branched chains occurs.

1.9. Multiarm star polymers

Multiarm star polymers, consisting of a high number of linear homopolymer arms joined covalently to a central core, represent model soft 'hybrid' spheres encompassing both polymeric (arm) and colloidal (core) character. Due to this topology, the single star has a non-uniform monomer density distribution. Linear polymers and colloids represent two of the most studied classes of soft polymeric materials because of their interesting properties and widespread applicability.[79,80] In recent works, poly(ε-caprolactone)[81] have been successfully used for the synthesis of numerous star[82] and multi-arm star polymers.[67,68,69,83]

The main synthetic strategies to access multiarm star polymers are: arm-first and core-first. Arm-first synthesis of a star polymer involves the growth of the linear polymer arms and then cross-linking the ends of the arms together to create the core of the star structure. This is accomplished by creating the polymer arms through a living polymerization technique and then adding a cross-linking agent that has two vinyl groups, such as divinylbenzene. This simple, one-pot synthesis can create polymers with a large number of arms, but it results in a statistical distribution of the number of arms incorporated into each star.[84] Alternatively, preformed linear arms can be attached to a functionalized core.[85]

The core-first method of synthesizing star polymers involves growing the polymer arms starting from the core which contains multiple reactive sites. This allows the synthesis of star polymers with a very well-defined number of arms and core structure.[86] Through the use of reactive sites for orthogonal polymerization reactions, miktoarm star polymers, with arms of different nature, can be synthesized with very high control over the product structure.[87]

A great number of multiarm star polymers with PCL arms have been described.[56,57,88,89,90] It is well known that cyclic esters, like *ε*-caprolactone (*ε*-CL), can be polymerized in a controlled manner using tin catalysts, like for example tin 2-ethylhexanoate ($Sn(Oct)_2$), in combination with initiators like hydroxyl groups (R-OH), or primary amines. Specifically, the polymerization in the presence of the hydroxyl groups begins with the formation of the active species, alkoxide type RO-Sn-Oct or RO-Sn-OR, according to the following equilibrium:

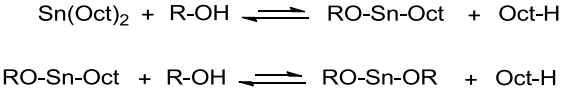

Figure 25. Formation of the active species RO-Sn-Oct and RO-Sn-OR by transfer reactions between $Sn(Oct)_2$ and OH groups. (Oct = $C_4H_9CH(C_2H_5)C(O)O^-$)

In this way, the insertion of the monomer between the bond··Sn-OR with formation of species like··Sn-O-$(CH_2)_5$-C(O)-OR will help propagate the polymerization inserting more monomer. In this way, the transfer reaction occurs again starting from Oct-H present in the medium, protonating the alkoxide in the activated chain and regenerating the catalyst, as detailed in **Figure 26**.

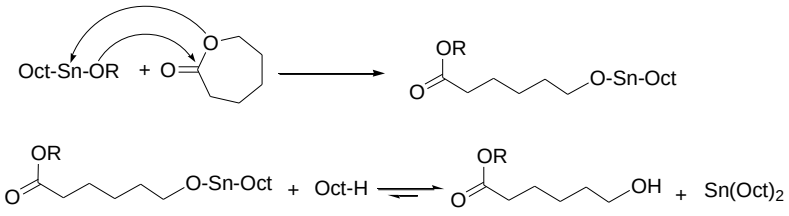

Figure 26. Mechanism of monomer insertion and termination of polymerization by ring opening of ***ε***-caprolactone (***ε***-CL) catalyzed by $Sn(Oct)_2$

In the following figure (**Figure 27**) the main features of dendritic polymers are summarized.

Polymer	**Dendrimer**	**Hyperbranched**	**Stars**
Structure	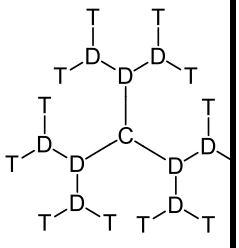	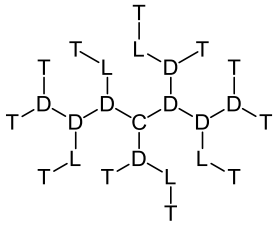	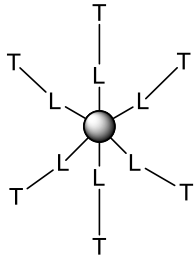
Topology	3D, globular	3D, elipsoidal	3D, globular
Synthesis	Multistep, laborius	One-step	Two-steps
Purification	Chromatography	Precipitation	Precipitation
MW	Same MW	Mixed MWs	Mixed MWs
PDI	1.0 (<1.05)	>3.0	> 1
DB	1	0.4-0.6	-
Entanglement	Very Weak or not	Weak	Weak
Viscosity	Very Low	Low	Very low
Solubility	Very High	High	Very high
Reactivity	Very High	High	High
Strength	Very low	Low	High

Figure 27. Structural characterization and main features of dendritic polymers

1.10. Objectives

Epoxy resins have been widely used in technological applications because of their combination of high strength and stiffness, excellent corrosion resistance and good electrical properties. However, their high crosslink density leads to low impact resistance, which places a limitation on their potential range of applications. On the other hand, at the end of the service life of the epoxy coated devices, it is difficult to recycle or to repair these devices because the epoxy thermoset coating cannot easily be removed by solvents or thermal treatment The main objective of this project is the preparation and characterisation of novel thermosets, based on epoxy resins and dendritic polymers, hyperbranched polymers and multiarm stars, with enhanced toughness and reworkability.

This general objective is achieved through a series of specific objectives:

- To synthesize dihydrazides of different structure and use them as latent curing agent for epoxy resins and as flexibilizing additive.
- To prepare aliphatic-aromatic hyperbranched polyesters with hydroxyl or vinyl groups of different length as chain ends and to study the effect of these modifiers on the curing kinetics, thermal mechanical properties, toughness, and morphology of the epoxy thermosets obtained using dihydrazide as latent curing agent.
- To synthesize new aliphatic-aromatic hyperbranched polyester with vinylic chains of different lengths and use them as non-reactive toughening modifier of epoxy/anhydride systems.
- To synthesize new multiarm star polymers with aromatic or aliphatic-aromatic cores and poly(ε-caprolactone) arms and use them as epoxy/$Yb(OTf)_3$ or epoxy/anhydride modifiers to improve the chemical reworkability and toughness of the resulting thermosets.

Reference

[1] Pascault JP, Sautereau H, Verdu J, Williams RJJ, *Thermosetting Polymers*, Marcel Dekker: New York; 2002.
[2] Mark JE, ed. *Polymer Data Handbook,* Oxford University Press, Inc.: New York; 1999.
[3] Zhang Z-G, Li Y-B, Wu Y, Li F-M, *J Appl Polym Sci* **94**: 2217-2222 (2004).
[4] Mark HF, Bikales NM, Overberger CG, Menges G, eds. *Encyclopedia of Polymers Science and Engineering*, 3rd ed. John Wiley: New York: 1988.
[5] May CA, ed. E*poxy resins. Chemistry and Technology*. 2nd ed. Marcel Dekker: New York; 1988.
[6] Petrie EM. *Epoxy Adhesive Formulations*. McGraw-Hill, New York; 2006.
[7] Castan P, *Swiss Pat*. 211,116 (1940).
[8] Lee H, Neville K, *Handbook of Epoxy Resins*, McGraw-Hill: New York; 1982.
[9] Park S-J, Jin F-L, Lee J-R, Shin J-S, *Eur Polym J* **41**: 231-237 (2005).
[10] Takahashi E, Sanda F, Endo T, *J Polym Sci Part A: Polym Chem* **40**: 1037-1046 (2002).
[11] Ghaemy M, *Eur Polymer J* **34**: 1151-1156 (1998).
[12] Castell P, Galià M, Serra A, Salla JM, Ramis X, *Polymer* **41**: 8465-8474 (2000).
[13] Pearson RG, *J Am Chem Soc* **85**: 3533-3539 (1963).
[14] González L, Ramis X, Salla JM, Mantecón A, *Polym Sci Part A: Polym Chem* **46**: 1229-1239 (2008).
[15] Endo T, Sanda F, *Macromol Symp* **107**: 237-242 (1996).
[16] Crivello JV, Lam JHW in: *The photoinitiated cationic polymerization of epoxy resins, ACS Symposium Series* **114**: 1-16 (1979).
[17] Kubisa P, Penczek S, *Prog Polym Sci* **24**: 1409-1437 (1999).
[18] Matejka L, Chabanne P, Tighzert L, Pascault JP, *J Polym Sci Part A: Polym Chem* **32**: 1447-1458 (1994).
[19] Decker C, Viet TNT, Thi PH, *Polym Int* **50**: 986-997 (2001).
[20] Rozenberg BA, *Adv Polym Sci* **75**: 113-165 (1986).
[21] Leukel J, Burchard W, Krüguer RP, Munch H, Schulz G, *Macromol Rapid Commun* **17**: 359-366 (1996).
[22] Fedtke M, Domaratius *F, Polym Bull* **15**: 13-19 (1986).
[23] Wear SL, *Stable Heat-Curing Epoxy Resin Compositions*. U.S. Patent 2847395 (1958).
[24] Khosravi E, Musa OM, *Eur Polym J* **47**: 465-473 (2011).
[25] Yang S, Chen J-S, Körner H, Breiner T, Ober CK, *Chem Mater* **10***:* 1475-1482 (1998).
[26] Chen J-S, Ober CK, Poliks MD, *Polymer*, **43***:* 131-139 (2002).
[27] Goosey M, ed. *Plastics for electronics.* 2nd ed. Kluwer Academic Publisher: Dordrecht, p. 177; 1999.
[28] Yorkgits EM, Trau C, Eiss NS, Hut TY, Yilgor I, Wilkes GL, McGrath JE, *Adv Chem Ser* **208**:137-161 (1984).
[29] Mijovic J, Pearce EM, Foun CC, *Adv Chem Ser* **208**: 293 (1984).
[30] Kirshenbaum SL, Gazit S, Bell JP, *Adv Chem Ser* **208**: 163 (1984).
[31] Frounchi M, Mehrabzadeh M, Parvary M, *Polym Int* **49**: 163-169 (2000).
[32] McGarry FJ, Sultan JN, *J Polym Sci* **13**: 29-34(1973).
[33] Bucknall CB, Partridge IK, *Polymer* **24**: 639-644 (1983).
[34] Sue HJ, *Polym Eng Sci* **31**: 275-288 (1991).
[35] Lazzeri A, Bucknall CB, *J Mater Sci* **28**: 6799-6808 (1993).
[36] Brydson J.A, *Plastic materials,* Butterworths Heinemann: Oxford, Ch 26; 1999.
[37] Ray SS, Okamoto M. *Prog Polym Sci* **28**: 1539-1641 (2003).
[38] LeBaron PC, Wang Z, Pinnavaia TJ *Appl Clay Sci* **15**: 11-29 (1999).
[39] Alexandre M, Dubois P, *Mater Sci Eng R* **28**: 1-63 (2000).
[40] Pavlidou S, Papaspyrides CD, *Prog Polym Sci* **33**: 1119-1198 (2008).

[41] Ke YC, Stroeve P, *Polymer-layered silicate and silica nanocomposites*, 1st ed. Elsevier: Amsterdam; 2005.
[42] Chazeau L, Cavaille JY, Canova G, Dendievel R, Boutherin B, *J Appl Polym Sci* **71**: 1797-1808 (1999).
[43] Vaia RA, Price G, Ruth PN, Nguyen HT, Lichtenhan J, *Appl Clay Sci* **15**: 67-92 (1999).
[44] Giannelis EP, Krishnamoorti R, Manias E. *Adv Polym Sci* **138**: 107-147. (1999).
[45] Pinnavaia TJ, Beall GW, eds. *Polymer clay nanocomposites*, John Wiley & Sons Inc.: Chichester; 2001.
[46] Giannelis EP, *Appl Organomet Chem* **12**: 675-680 (1998).
[47] Bharadwaj RK, *Macromolecules* **34**: 9189-9192 (2001).
[48] Messersmith PB, Giannelis EP, *J Polym Sci Part A: Polym Chem* **33**: 1047-1057 (1995).
[49] Morgan AB, Wilkie CA, *Flame retardant polymer nanocomposites,* John Wiley & Sons Inc.: Chichester 2007.
[50] Cicala G, Recca A, *Polym Eng Sci* **48**: 2382-2388 (2008).
[51] Ratna D, Varley R, Simon GP, *J Appl Polym Sci* **89**: 2339-2345 (2003).
[52] Mezzenga R, Månson JAE, *J Mater Sci* **36**: 4883-4891 (2001).
[53] Fröhlich J, Kautz H, Thomann R, Frey H, Mülhaupt R, *Polymer* **45**: 2155-2164 (2004).
[54] Boogh L, Pettersson B, Manson JAE, *Polymer* **40**: 2249-2261 (1999).
[55] Meng Y, Zhang XH, Du BY, Zhou BX, Zhou X, Qi GR, *Polymer* **52***:* 391-399 (2011).
[56] Morell M, Foix D, Lederer A, Ramis X, Voit B, Serra A, *J Polym Sci Part A: Polym Chem* **49**: 4639-4649 (2011).
[57] Morell M, Lederer A, Ramis X, Voit B, Serra A, *J Polym Sci Part A: Polym Chem* **49**: 2395-2406 (2011).
[58] Morell M, Ramis X, Ferrando F, Serra A. *Polymer* **52:** 4694-4702 (2011).
[59] Flory P.J, *J Am Chem Soc* **74**: 2718-2723 (1952); Flory PJ, *Principles of Polymer Chemistry*, Cornell University Press: NY; 1953.
[60] Kim YH, Webster OW, *J Am Chem Soc* **112***:* 4592-4593 (1990).
[61] Kim YH, Webster OW, *Macromolecules* **25***:* 5561-5572 (1992).
[62] Hult A, Johansson M, Malmström E, *Adv Polym Sci* **143**: 1-34 (1999).
[63] Jikei M, Chon SH, Kakimoto MA, Kawauchi S, Imase T, Watanebe J, *Macromolecules* **32**: 2061-2064 (1999).
[64] Kricheldorf HR, Zhang QZ, Schwarz G, *Polymer* **23**: 1821-1829 (1982).
[65] Kim YH, in: Salamone JC, ed. *Polymeric Materials Encyclopedia*, CRC Press: New York, pp 3049-3053; 1996.
[66] Jikei M, Kakimoto MA, *High Perform Polym* **13**, S33-S43 (2001).
[67] Burgath A, Sunder A, Frey H *Macromol Chem Phys* **201**: 782-791 (2000).
[68] Mezzenga R, Boogh L, Månson J-AE, *Comp Sci Tech* **61**: 787-795 (2001).
[69] Haag R, *Chem Eur J*, **7**: 327-335 (2001).
[70] Kim YH, *J Polym Sci Part A: Polym Chem* **36**: 1685-1698 (1998).
[71] Gao C, Yan D, *Prog Polym Sci* **29**: 183-275 (2004).
[72] Hawker CJ, Lee RJ, Fréchet JM, *J Am Chem Soc*, **113**: 4583-4548 (1991).
[73] Schallausky F, Erber M, Komber H, Lederer A, *Macromol Chem Phys* **209**: 2331-2338 (2008).
[74] Moore JS, Stupp SI, *Macromolecules* **23**: 65-70 (1990).
[75] Detar DF, Silverstein R, *J Am Chem Soc* **88**: 1013-1019 (1966).
[76] Scriven EFV, *Chem Soc Rev* **12**: 129-161 (1983).
[77] Turner SR, Voit, BI, Mourey TH, *Macromolecules* **26**: 4617-4623 (1993).
[78] Holter D, Burgath A, Frey H, *Acta Polym* **48***:* 30-35 (1997).
[79] de Gennes, P-G, Badoz J. *Fragile objects: Soft Matter, Hard Science and the Thrill of Discovery*, Springer-Verlag: New York; 1996.
[80] Witten TA, Rev *Mod Phys* **71**: S367-S373 (1999).

[81] Lu C, Liu L, Guo S-R, Zhang Y, Li Z, Gu J, *Eur Polym J* **43**: 1857-1865 (2007).
[82] Buwalda SJ, Dijkstra PJ, Calucci L, Forte C, Feijen J, *Biomacromolecules* **11**: 224-232 (2010).
[83] Wolf FK, Frey H, *Macromolecules* **42**: 9443-9456 (2009).
[84] Gao H, Matyjaszewski K, *Macromolculees* **41**: 1118-1125 (2008).
[85] Yen DR, Merrill E, *Polym Prepr (Am Chem Soc Polym Chem*) **38**: 599-600 (1997).
[86] Maier S, Sunder A, Frey H, Mülhaupt R, *Macromol Rapid Commun* **21**, 226-230 (2000).
[87] Miller RD, *Macromolecules*, **34**: 2798-2804 (2001).
[88] Kowalski A, Duda A, Penczek S, *Macromol Rapid Commun* **19**: 567-572 (1998).
[89] Kowalski A, Libiszowski J, Biela T, Cypryk M, Duda A, Penczek S, *Macromolecules* **38**: 8170-8176 (2005).
[90] Acebo C, Fernández-Francos X, Ferrando F, Serra A, Salla JM, Ramis X, *React Funct Polym* **73**: 431-441 (2013).

Chapter 2

Materials and Methods

2. Characterization Techniques

2.1. Differential Scanning Calorimetry (DSC)

A Mettler DSC821e equipped with a robotic arm TSO801RO was used to perform DSC analysis from 30 to 300 ºC. To perform tests under room temperature a Mettler DSC822e cooled with liquid nitrogen. Both calorimeters were calibrated using an indium standard (heat flow calibration) and an indium-lead-zinc standard (temperature calibration). Samples of 5 to 10 mg of weight were placed in covered aluminum pans to perform analysis. **Figure 2.1** shows the calorimeters used.

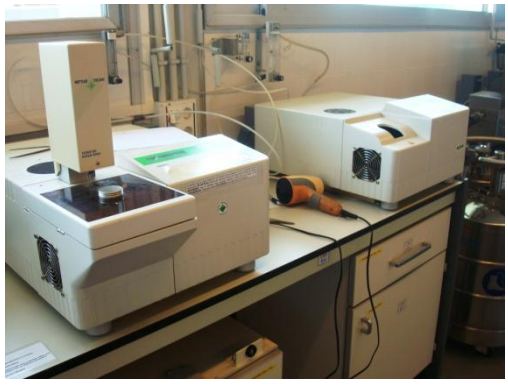

Figure 28. Pictures of the calorimeters and the robot used to study thermal curing systems.

Curing Kinetics

The kinetic study using DSC assumes that the heat released during the reaction is proportional to the degree of conversion and that the heat released *dH/dt*. is proportional to the curing rate *dx/dt* .The integration of this signal, in the case that the reaction is complete, yields the total heat released ΔH_{tot}. Mathematically one can express this as follows:

$$\frac{dx}{dt} = \frac{dH/dt}{\Delta H_{tot}} = \frac{dh/dt}{\Delta h_{tot}}$$

$$x = \frac{\Delta H_t}{\Delta H_{tot}} = \frac{\Delta h_t}{\Delta h_{tot}}$$

where *dh/dt* and Δh_{tot} are the heat releasing rate and the total heat released normalized in respect to the sample size, ΔH_t is the heat released up to a time *t*, and Δh_t is the heat released normalized in respect to the sample size. It can be expressed in J/g or in kJ/ee. Finally *x* is the degree of curing, and can also be expressed as α .

The kinetics of a system can be studied in isothermal or dynamic conditions. In our case we chose to work with dynamic experiments since they present some advantages being the most important the fact that in isothermal conditions it is possible to lose some information of the beginning of the curing and that the curing is not always complete.[1]

2.1.1 Kinetic Analysis

The reaction rate in a condensed phase reaction is usually expressed as $dx/dt = k\,f(x)$ being k the kinetic constant and $f(x)$ a function depending on the conversion. The kinetic constant, k, usually follows the Arrhenius expression:

$$k = Ae^{\frac{-E}{RT}} \tag{2.3}$$

where A is the preexponential factor, E the activation energy, R the gas constant and T the absolute temperature.

A kinetic process can be well characterized if one knows E, A and $f(x)$, the so called kinetic triplet. Although strictly speaking this methodology should only be valid for "single-step" processes it can also be applied in systems where more than one chemical (or physical) process coexists. There are two main approaches in the kinetic analysis:

1. *Isoconversional methods (or model-free)*. They study the apparent activation energy without knowing the kinetic model.
2. *Model-fitting methods*. They search an approximation of the experimental data to a kinetic model, and from that the values of the kinetic triplet are obtained.

The isoconversional methodology assumes that the reaction function $f(x)$ is independent of the heating rate β.[2] On that way the kinetics of a process only depends on the degree of conversion at a certain time. It also requires the performance of series of experiments to determine the apparent activation energy. Those experiments can be, for example, dynamic DSC curing at different heating rates.

Depending on the approach used to determine the apparent activation energy, it is possible to classify isoconversional methodologies between lineal and non-lineal. In turn, lineal methodologies can be divided between differential and integral. In this job the integral methodology has been applied. By integrating $dx/dt = k \cdot f(x)$ considering that the temperature is not constant but $T = T_0 + \beta t$ and applying a change of variables $dt = dT/\beta$ one can obtain the following expression:

$$g(x) = \int_0^t Ae^{-E/RT}\,dt = \int_{T_0}^{T} \frac{A}{\beta} e^{-E/RT} dT = \frac{A}{\beta}\int_{T_0}^{T} e^{-E/RT} dT \tag{2.4}$$

where $g(x)$ is an integral function that describes the reaction as $f(x)$.

Eq. (2.4) can be simplified assuming that only at $T_0 = 0$ the reaction is forbidden:

$$g(x) = \frac{A}{\beta}\int_0^T e^{-E/RT} dT \tag{2.5}$$

To resolve this integral, which has no analytical solution, the best strategy is to make an approximation to a simpler expression. To do so, a variable $y = E/RT$ is defined and the change of variables $dy = -E/RT^2$ and $dT = -(R/E)y^2 dT$ is applied:

$$\int_0^T e^{-E/RT} dT = -\frac{E}{R}\int_{\infty}^{y} \frac{e^{-y}}{y^2} dy = \frac{E}{R}\int_{y}^{\infty} \frac{e^{-y}}{y^2} dy = \frac{E}{R} p(y) \tag{2.6}$$

Finally to determine *p(y)* the solution of Murray and White,[3] $p(y) = e^{-y}/y^2$, which represents the bases of the Kissinger-Akahira-Sunose (KAS)[4,5] methodology, was applied:

$$ln\left(\frac{\beta}{T_{i,x}^2}\right) = ln\left(\frac{A\,R}{g(x)E_x}\right) - \frac{E_x}{RT_{i,x}} \tag{2.7}$$

From that expression the apparent activation energy E_x can be obtained from the slope of the curve $ln(\beta/T_{i,x}^2)$ against $-1/RT_{i,x}$.

Using the model-fitting methodology it is possible to determine a kinetic model. Integrating the expression of the reaction rate depending on the heating rate of the DSC experiment (eq. (2.8)) using the Coats-Redfern[6] approximation the expression eq. (2.9) can be obtained:

$$\frac{dx}{dt} = \beta\frac{dx}{dT} = Ae^{\frac{-E}{RT}}f(x) \tag{2.8}$$

$$ln\left(\frac{g(x)}{T_{i,x}^2}\right) = ln\left(\frac{A\,R}{\beta\,E}\right)\left(1 - \frac{2R\bar{T}}{E}\right) - \frac{E}{RT_{i,x}} \tag{2.9}$$

where $\bar{T}$ is the mean value of temperature of the process and assumes that *A* and E are constant during the experiment. Considering $2R\bar{T} \ll 1$ the eq. (2.9) can be simplified as:

$$ln\left(\frac{g(x)}{T_{i,x}^2}\right) = ln\left(\frac{A\,R}{\beta\,E}\right) - \frac{E}{RT_{i,x}} \tag{2.10}$$

For a given kinetic model, the linear representation of $ln[g(x)/T^2]$ versus $1/T$ makes it possible to determine *A* and *E* from the slope and the ordinate at the origin. . Different models (**Table 2.1**) are compared with the data obtained and the one that present the best fitting and that has an *E* value similar to that obtained isoconversionally (considered to be the effective *E* value) is chosen. Moreover the *k* has been determined by using eq. (2.3) and *A* and *E* values.

Table 1. Kinetics models used to determine the kinetic triplet with the model fitting methodology.[7]

Model	*f(x)*	*g(x)*
D_1	$\frac{1}{2x}$	x^2
D_2	$\frac{1}{\ln(1-x)}$	$(1-x)\ln(1-x)+x$
D_3	$\frac{3}{2}\frac{(1-x)^{2/3}}{(1-(1-x)^{1/3})}$	$(1-(1-x)^{1/3})^2$
D_4	$\frac{3}{2}\frac{(1-x)^{1/3}}{(1-(1-x)^{1/3})}$	$1-\frac{2}{3}x-(1-x)^{2/3}$
R_n (R_2, R_3)	$n(1-x)^{1-1/n}$	$1-(1-x)^{1/n}$
n order	$(1-x)^n$	$-\ln(1-x) \quad (n=1)$ $\frac{1-(1-x)^{1-n}}{1-n} \quad (n\neq 1)$
A_n (A_2, A_3)	$n(1-x)(-\ln(1-x))^{1-1/n}$	$(-\ln(1-x))^{1/n}$
n potence	$nx^{1-1/n}$	$x^{1/n}$
Autocatalytic	$x^m(1-x)^n$	$\frac{1}{n-1}\left(\frac{1-x}{x}\right)^{1-n} \quad (n+m=2; n\neq 1)$ $\frac{1}{n-1}\left(\frac{1-x}{x}\right)^{1-n}+\frac{1}{n-2}\left(\frac{1-x}{x}\right)^{2-n}$ $(n+m=3; n\neq 1{,}2)$

Glass Transition Temperature (T_g)

In order to determine the T_g of the cured materials as well as the T_g of the synthesized hyperbranched polymers DSC experiments were performed in dynamic conditions at 20 ºC/min. The evaluation of the glass transition temperature was carried out using the ASTM methodology.

2.2 Fourier-Transformed Infrared Spectroscopy (FT-IR)

To study thermal curing processes, an FTIR-680PLUS spectrophotometer from JASCO with a resolution of 4 cm^{-1} in the absorbance mode, equipped with an attenuated total reflection accessory (ATR) with thermal control and a diamond crystal (Golden Gate heated single-reflection diamond ATR from Specac-Teknokroma) was used.

Figure 29. IR device used for and thermal curing systems.

The principle which allows following the curing reaction using FT-IR measurements is the Lambert-Beer law, which is as follows:

$$A = \varepsilon \times C \times L \tag{2.12}$$

where *A* is the absorbance of a specie at a certain frequency, ε is the absortivity coefficient, *C* is the concentration and *L* is the optical pathway.

If one can identify a band of a functional group that reacts during the curing process, and therefore disappears, it is possible to follow the curing process. In the case of epoxy resins the band followed is the one of the epoxide group, which is at around 915 cm^{-1} for DGEBA and between 760 and 780 cm^{-1} for the cycloaliphatic epoxy resin.

Since the absorbance is proportional to the optical pathway, *L*, it is necessary to normalize the target band in respect to a reference band that remains unaltered during the curing process. In the case of DGEBA based thermoset the peak at 1508 cm^{-1} corresponding to the phenyl group is chosen whereas in CE based epoxy thermosets the normalization is done in respect to the band of the stretching of ester groups at 1174 cm^{-1}. On that way the conversion *x*, determined by FT-IR measurements can be written as follows:

$$x = 1 - \frac{\overline{A^t}}{\overline{A^0}} \tag{2.13}$$

where $\bar{A}^t$ is the normalized absorbance at a certain time and $\bar{A}^0$ is the initial absorbance that correspond to the maximum.

In the case of UV cured samples, the formulations are coated onto a silicon wafer (about 50 μm thickness) with a wire-wound applicator. The sample can then be exposed simultaneously to the UV beam, which induces the polymerization, and to the IR beam, which analyzes *in situ* the extent of the reaction.

2.3 Dynamic Mechanical Thermal Analysis (DMTA)

Figure 30. DMTA equipments used to study the viscoelastic properties of the prepared thermosets.

To obtain specimens from thermal curable formulations, they were placed in steel templates and cured with the appropriate curing schedule, depending on each material. On that way, samples of around 25 x 5 x 1.5 mm^3 were obtained. In the case of UV curable formulations, they were coated onto poly(propylene) molds with a wire-wound applicator and exposed to UV radiation with a fusion lamp (H-bulb) in air at a conveyor speed of 5 $m \cdot min^{-1}$, with radiation intensity on the surface of the sample of 280 $mW \cdot cm^{-2}$. The dimensions of the samples obtained are 25 x 15 x 3 mm^3.

DMTA studies the viscoelastic nature of a material by applying an oscilatory stress with a fixed frequency to the sample and monitoring its response at different temperatures. Two parameters can be determined: the complex modulus *(E*)* and the loss factor *(tanδ)*. The modulus contains real and imaginary contributions *(E*=E'+i·E'')*. The real part, *E'*, is a measure of the elastic response of the material, while the imaginary part, *E''*, reflects the viscous response. The maximum of the *tanδ* curve is generally accepted as the T_g of a material although it changes with the frequency used in the experiment.

2.4 Rheology

Rheological measurements were carried out in the parallel plates (geometry of 25 mm) mode with an ARG2 rheometer (TA Instruments, **Figure 2.10**), equipped with a Peltier system for controlling the temperature. Curable formulations are placed between two aluminum plates with a distance between plates (gap) of approximately 1000 μm. By rheology it is possible to study the gel time, the conversion at the gel point and the evolution of the shrinkage during curing, as well as determining the viscosity of uncured formulations.

Figure 31. Rheometer ARG2 used, with a magnification of the geometry used.

Rheological measurements are based on monitoring the tension generated in the sample as a response to the application of an oscillatory shear force. The viscoelasticity of a given polymer reflects in the difference in the applied and measured angle δ. As for the case of DMTA, one can define a complex modulus $G^* = G' + i \cdot G''$.The complex viscosity (η*) is determined in multi-frequency experiments at a certain temperature and amplitude. This amplitude must be comprised within the range of linear viscoelasticity.

The gel time is determined in isothermal experiments where the oscillation amplitude changes to adjust to the changes in the material. The point at which *tan δ* is independent of the frequency is defined as the gel point (**Figure 32**). By stopping the experiment at that point and performing a DSC scan to determine the remaining heat it is possible to determine the conversion at gelation.

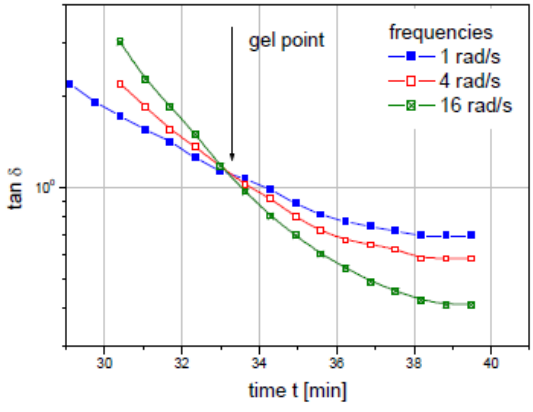

Figure 32. Example of gel time determination in a multifrequency experiment.

Finally, to monitor the shrinkage, as for the case of TMA, an isothermal experiment is performed and a force of 0.01 N applied to monitor the gap between plates, when working under gap control conditions.

2.5 Thermogravimetry (TGA)

A thermobalance Mettler TGA/SDTA 851e (**Figure 32**) was used to analyze the thermal degradation of cured samples and of the synthesized hyperbranched polymers. The degradation was carried out in dynamic conditions, at 10 ºC/min under nitrogen or air, from 30 to 800 ºC. The most important parameters extracted from the analysis of such curves are the initial degradation temperature, the temperature of the maximum degradation rate and the char yield.

Figure 33. Thermobalance used for the thermal stability evaluation.

2.6 Density and Shrinkage Measurements

The density of both formulations and cured samples were determined in a Micromeritics AccuPyc 1330 Gas Pycnometer (**Figure 2.13**) thermostatized at 30 ºC and using helium as gas. The device works by measuring the amount of displaced gas by the sample. The pressures observed upon filling the sample chamber and then discharging it into a second empty chamber allow the determination of the sample volume as follows:

$$V_s = V_c + \frac{V_r}{1-\frac{P_1}{P_2}} \tag{2.15}$$

where V_s is the volume of the sample, V_c is the volume of the empty sample chamber, V_r is the volume of reference (obtained from calibration), P_1 is the pressure of the sample chamber and P_2 the combined pressure after expanding the gas to the second chamber.

Figure 34. Gas pycnometer employed for the density determination.

From the volume measured and knowing the weight, the density of a certain sample can be easily calculated since $\rho = W/V$.

Alternatively, another methodology was used to determine densities. The density of the uncured formulation was measured with a standard pycnometer in a thermostatically controlled bath at 30 ºC. The density of the cured thermosets was determined indirectly by the flotation method. This consists in finding the optimal concentration of KBr in a water solution that makes the thermoset remain in the middle. Then the density of this solution is measured with the pycnometer.

The evaluation of the shrinkage undergone during curing is obtained by comparison of the shrinkage of the curable formulation and the cured thermosets, using the following expression:

$$Shrinkage\ (\%) = \frac{\rho_{polym} - \rho_{mon}}{\rho_{polym}} \times 100$$

2.7 Scanning Electron Microscopy (SEM)

Three different SEM microscopes were used: a Jeol JSM 6400 with 3.5 nm resolution, a FEI Quanta 600 Environmental Scanning Electron Microscope (ESEM) equipped with an X-Ray analyzer and a ZEISS SUPRA™ 40 Field Emission Scanning Electron Microscope (FE-SEM) with a nominal resolution of 1.5 nm. Pictures of two of these equipments can be seen in **Figure 2.14**. For standard SEM analysis, samples were coated with gold while for the FE-SEM analysis with carbon. For ESEM measurements it is not necessary to coat the sample.

SEM is a type of electron microscope that images a sample by scanning it with a high-energy beam of electrons in a raster scan pattern. The electrons interact with the atoms that make up the sample producing signals that contain information about the sample's surface topography, composition, and other properties such as electrical conductivity.

FE-SEM uses a special type of electron gun that allows achieving higher spatial resolutions and minimizes the damaging of the sample. In the case of ESEM the measurements are performed without coating the surface to be observed. This represents an advantage since the same specimens can afterwards be used for other experiments.

Figure 35. SEM equipment used for obtaining surface images.

2.8 Nuclear Magnetic Resonance (NMR)

Two different equipments were used to confirm the chemical structure of the synthesized hyperbranched polymers: a Bruker DRX 500 NMR spectrometer and a Varian Gemini 400 NMR spectrometer of 400 MHz (**Figure 2.16**). The deuterated solvent to dissolve the sample was chosen in each case being the most common ones $CDCl_3$ and DMSO-d_6. The experimental conditions in the case of ^{1}H-NMR measurements where 500 or 400 MHz of magnetic field, 1 s of delay time (D1) and 14 accumulations to obtain quantitative measurements. For ^{13}C-NMR measurements the magnetic field was 125.75 or 100.6 MHz, a D1 of 0.5 s, 0.2 s of acquisition time and 500 spectra were recorded at least.

Figure 36. Picture of the Varian equipment used for the structural identification of the HBPs.

2.9 Size Exclusion Chromatography (SEC)

SEC analyses were carried out with two different equipments:

An Agilent 1200 series system (**Figure 2.17**) with PLgel 3 μm MIXED-E, PLgel 5 μm MIXED-D and PLgel 20 μm MIXED-A columns in series, and equipped with an Agilent 1100 series refractive-index detector. Calibration curves were based in polystyrene standards having low polydispersities. THF was used as the eluent at a flow rate of 1.0 mL/min, the sample concentrations were 5-10 mg/mL, and injection volumes of 100μL were used. With this technique it is possible to determine the molecular weight ($\bar{M}_n$, $\bar{M}_w$) of the synthesized HBPs as well as the molecular weight dispersity ($Đ_M$), by comparing the retention time of a diluted solution of the sample with the solution of standards, which are polymers with different molecular weight and narrow distributions.

Figure 37. GPC chromatograph used for the molecular weight determination

2.10 Impact Test

The impact test was performed at 23 ºC by means of an Zwick 5110 impact tester, according to ASTM D 4508-05 (2008) using prismatic rectangular specimens (ca. 20 x 11 x 2.5 mm^3). The pendulum employed had a kinetic energy of 1 J. A picture of the testing machine can be seen in **Figure 38**.

Figure 38. Impact testing machine

By means of this technique it is possible to determine the impact energy that a sample can absorb, indicating the toughness of the same. The broken samples were afterwards observed by means of SEM in order to correlate the energy value obtained with the impact surface morphology.

2.11 Microhardness

Microhardness was measured with a Wilson Wolpert (MicroKnoop 401MAV) device (**Figure 2.19**) following the ASTM D1474-98 (2002) standard procedure. For each material 10 determinations were made with a confidence level of 95%. The Knoop microhardness (HKN) was calculated from the following equation:

$$HKN = \frac{L}{A_p} = \frac{L}{l^2 \times C_p} \quad (2.17)$$

where, L is the load applied to the indenter (0.025 Kg), A_p is the projected area of indentation in mm^2, l is the measured length of the long diagonal of indentation in mm, C_p is the indenter constant (7.028×10^{-2}) relating l^2 to A_p.This technique is based on measuring the length of the long diagonal produced by the indentation of a rhomboidal tip. The length is related to the hardness of the material: the shorter the diagonal the hardest the material.

Figure 39. Microhardness tester used for the determination of the Knoop hardness of the prepared thermosets.

[1] A. Turi. *Thermal Characterization of Polymeric Materials, 2nd Edition*. Academic Press, San Diego, **1997**.
[2] S. Vyazovkin, C. A. Wight.*Thermochim. Acta* **1999,** *340-341*, 53.
[3] P. Murray, J. White. *Trans. Brot. Ceram. Soc.* **1955,** *54,* 204.
[4] T. Akahira, T. Sunose. *Transactional of Joint convention of Four Electrical Institutes* **1969,** 246.
[5] H. E. Kissinger. *Anal. Chem.* **1957,** *29,* 1702.
[6] A. W. Coats, J. P. Redfern. *Nature* **1964,** *201,* 68
[7] P. Budrugeac, E. Segal, L. A. Pérez-Maqueda, J. M. Criado. *Polym. Degrad. Stab.* **2004,** *84,* 311.

Chapter 3

Dihydrazides as latent curing agents for DGEBA coatings

Chapter 3 - Progress in Organic Coatings 74 (2012) 59–66

THE USE OF DIHYDRAZIDES AS LATENT CURING AGENTS FOR DGEBA COATINGS

Adrian M. Tomuta,[1] Xavier Ramis,[2] Francesc Ferrando,[3] Angels Serra[1*]

[1] Department of Analytical and Organic Chemistry, University Rovira i Virgili, C/ Marcel·lí Domingo s/n, 43007, Tarragona, Spain.

[2] Thermodynamics Laboratory, ETSEIB University Politècnica de Catalunya, C/ Av. Diagonal 647, 08028, Barcelona, Spain.

[3] Department of Mechanical Engineering, University Rovira i Virgili, C/ Països Catalans 26, 43007, Tarragona, Spain.

Abstract

Dihydrazides of different structure were synthesized and tested as curing agents for DGEBA epoxy resin. By calorimetric studies their latent characteristics were proved and the kinetics of the curing was studied. The temperatures of activation are usually dependant on the melting point of the dihydrazide. The acceleration by base and Lewis acids was proved, but the latent character was diminished. FTIR/ATR allowed characterizing the final structures of the thermosets and confirming that the curing process was complete. The thermal stability of the materials and their thermomechanical characteristics were evaluated by TGA and DMTA, respectively. Mechanical properties of the thermosets were also determined. The fracture surface, which reflects the toughness characteristics, was observed by SEM.

Keywords: Epoxy resins, dihydrazide, thermosets, crosslinking

3.1. Introduction

Epoxy resins are one of the most applied thermosets in coatings applications. The curing agent employed in the crosslinking process defines not only the final properties of the thermosets but also the technological conditions of application.[1]

Latent curing agents are those that show no activity under normal conditions but become active by external stimulation. These stimuli are usually heating and photoirradiation, but can also be electron beam or ultrasonic irradiation, among others. Thermal stimulation is easier from the technological point of view, because it allows a complete curing avoiding vitrification and can be applied to thick samples without appearance of inhomogeneities. Latent curing agents simplify the technological curing process because they allow the preparation of one-pot curing mixtures.

Thermal latent curing agents can act mainly by two different mechanisms; the first one is based in their insolubility in epoxy resin, due to their crystalline character, which on melting becomes soluble and active. The second mechanism is based on the use of a precursor compound, inactive at room temperature, but which under stimuli it converts into an active curing agent.[2]

Endo et al.[3,4] reported the use of thermally activated latent cationic initiators in the polymerization of epoxides. They are benzyl sulfonium, ammonium, phosphonium and hydrazinium salts with a counter anion with a low nucleophilicity, such as SbF_6^- or BF_4^-. Diethyl phosphites can also been proposed as precursors of latent cationic systems because they decompose leading to the formation of phosphonic acid.[5] Catalytic curing agents with thermal latent character have been extensively reported in epoxy formulations.[6,7] BF_3 complexes, among latent cationic initiators are the most extended.[8] BF_3·MEA is the only Lewis acid that has achieved a broad industrial use. This complex is solid at room temperature, but melts at 80-85ºC near to its dissociation temperature. After the dissociation, BF_3 gas is formed, which is very active in the curing process.

Among thermal latent curing agents dicyandiamide (DICY) is one of the most employed in epoxy resins technologies.[9] The latent nature is due to its insolubility in epoxy resins at room temperature. Cure of epoxies with DICY occurs only while heating to temperatures of at least 150 ºC[10] and when the heat is removed the curing stops. The curing mechanism is quite complex and includes stepwise and chainwise polymerizations.

Crosslinking density is defined as the number of effective crosslinks per unit of volume.[2] This parameter highly defines the properties of a cured epoxy thermoset and is dependent on the chemical structure of the resin and curing agent and their functionalities and also on the curing mechanism and conditions selected. Catalytic curing agents usually lead to a high crosslinking density which worse the rheological behaviour during curing and the final mechanical properties of the thermosets. Moreover, they generate a large quantity of heat per gram of resin during curing and thus, they are only used in thin films in which the heat produced can be easily evolved. Stoichiometric curing agents have also another advantage, which is that their structure, more or less flexible, greatly affects the curing process and determines some physical characteristics of the cured material such as the T_g. Therefore, stoichiometric curing agents can be more advisable in some technological applications.

The use of dihydrazides as curing agents has been scarcely reported in the scientific literature[11] but it appears in the patent literature[12,13,14] and there are some dihydrazides commercially available as latent curing agents.[15] Dihydrazides cure at lower temperatures than dicyandiamide (DICY), and has been used in powder paints and one-pot adhesives, because of their higher adhesion characteristics.

In the present study, a series of dihydrazides with different structure has been synthesized and their effectiveness tested in the curing of DGEBA resins. The latent characteristics of these agents have been demonstrated and the possible acceleration of the curing by basic and acid catalysts. Aliphatic dihydrazides, on the contrary that aliphatic amines, do not react at room temperature, which is interesting from the point of view of the preparation of one-pot curing systems. Dihydrazides can be easily synthesized from esters of dicarboxylic compounds and hydrazine. The dihydrazides prepared, with aliphatic, cycloaliphatic and aromatic moieties, when used as curing agents allow varying the characteristics of the network structure. Finally it should be mentioned that dihydrazides show no toxicity, making them safe for industrial

applications. Concretely, isophthalic dihydrazide was approved by the FDA for indirect food contact when used to cure epoxy resins.

3.2. Experimental part

3.2.1. Materials

Diglycidylether of bisphenol A (DGEBA, Epikote 828, Hexion, epoxy equivalent 184 g/eq) was used as base resin in all the studies.

Dimethyl isophtalate, adipic acid, dodecanoic acid, 1,4-cyclohexandioic acid, methyl 4-hydroxybenzoate, 1,3-propanediol (Aldrich) were used without further purifications. Hydrazine hydrate (Aldrich) was used as received. Benzyldimethylamine (BDMA) and ytterbium (III) trifluoromethanesulfonate ($Yb(OTf)_3$) from Aldrich were used as received.

Absolute ethanol (Panreac) was used as received and other conventional solvents (from Scharlab) were purified by standard procedures.

3.2.2. General synthetic procedure of dihydrazides

Synthesis of diesters

In a 500 mL round bottomed flask equipped with magnetic stirring and a Dean Stark water separation unit 0.5 mol of the selected dicarboxylic acid were dissolved in 180 mL of absolute ethanol and 90 mL of toluene and 1 g of concentrated sulphuric acid were added to the mixture. The oil bath temperature was set at 115 °C. The mixture was refluxed until no water was evolved (6-10 hours, depending on the carboxylic acid) and then, the excess of ethanol and toluene were eliminated under reduced pressure. The resulting ester was solved in CH_2Cl_2 and washed in a separator funnel two times with a saturated solution of $NaHCO_3$ and then twice with water. The organic layer was dried over anhydrous $MgSO_4$. The evaporation of the solvent leads to the pure diester that was used without further purification in the following step.

Synthesis of dihydrazides

In a three necked 500 mL round bottomed flask provided with a reflux condenser, magnetic stirring and a dropping funnel 0.25 mol of the selected diester were dissolved in 200 mL of absolute ethanol and 0.9 mol of hydrazine hydrate (90 %) were added drop by drop. Once the addition was complete the heating was turned on and the mixture was kept 6 h at reflux. During this time a white precipitate was formed, which was filtrated through a Buchner funnel and then washed twice with cold ethanol. The white powder was dried in the vacuum oven at 50°C. In all cases the obtained yield was higher than 90%. Dihydrazides were purified by recrystallization in methanol or ethanol.

The structure and acronyms of the synthesized dihydrazides are collected in **Scheme 1**. The dihydrazides obtained were characterized by NMR (in DMSO-d_6) and FTIR spectroscopy and the melting points were registered by DSC.

Adipic dihydrazide (AH): ^{1}H NMR (DMSO-d_6, δ in ppm): 8.93 s (2H, NH-); 4.14 s (4H, -NH_2); 1.97 t (4H, -CH_2-) 1.41 m (4H, -CH_2-). ^{13}C NMR (DMSO-d_6, δ in ppm): 171.49 (-CONH-); 33.27 (-CH_2-); 24.99 (-CH_2-). FTIR-ATR (cm^{-1}): 3310, 3288, 3197, 1626, 1529, 1376, 1273, 1166, 1033, 690.[16] m.p. 181-4 ºC (recrystallized from ethanol)

Dodecanoic dihydrazide (DDH): ^{1}H NMR (DMSO-d_6, δ in ppm): 8.89 s (2H, -NH-); 4.12 s (4H, -NH_2); 1.95 t (4H, -CH_2-); 1.45 m (4H, 4H, -CH_2-); 1.21 m (8H, -CH_2-). ^{13}C NMR (DMSO-d_6, δ in ppm): 176.61 (-CONH-) ; 33.41 (-CH_2-) ; 28.76 (-CH_2-) ; 25.23 (-CH_2-). FTIR-ATR (cm^{-1}): 3312, 3288, 3197, 1627, 1531, 1379, 1270, 1161, 1052, 693. m.p. 192-5 ºC (recrystallized from ethanol).

Isophtalic dihydrazide (IPH): ^{1}H NMR (DMSO-d_6, δ in ppm): 9.81 s (2H, -NH-); 8.24 t (1H, -CH- Ar); 7.89 m (2H, -CH- Ar); 7.51 t (1H, -CH- Ar); 4.56 s (4H, -NH_2). ^{13}C NMR (DMSO-d_6, δ in ppm): 165.89 (-CONH-); 133.97 (Ar); 129.78 (Ar) 128.91 (Ar) 126.50 (Ar). FTIR-ATR (cm^{-1}): 3312, 3210, 3056, 1652, 1520, 1342, 1165, 1107, 1016, 683. m.p. 220-4 ºC (recrystallized from ethanol).

1,4-Cyclohexyl dihydrazide (CHH): ^{1}H NMR (DMSO-d_6, δ in ppm): 8.91 s (2H, -NH-); 4.12 s (4H, -NH_2); 1.68 m (2H, -CH-); 1.34 m (8H, -CH_2-). ^{13}C NMR (DMSO-d_6, δ in ppm): 174.89 (-CONH-); (=CH-) 128.97; (=CH-) 126.50; (-CH_2-) 41; (-CH_2-) 28. FTIR-ATR (cm^{-1}): 3297, 3186, 3052, 1624, 1532, 1354, 1222, 1132, 1064, 642. Amorphous solid.

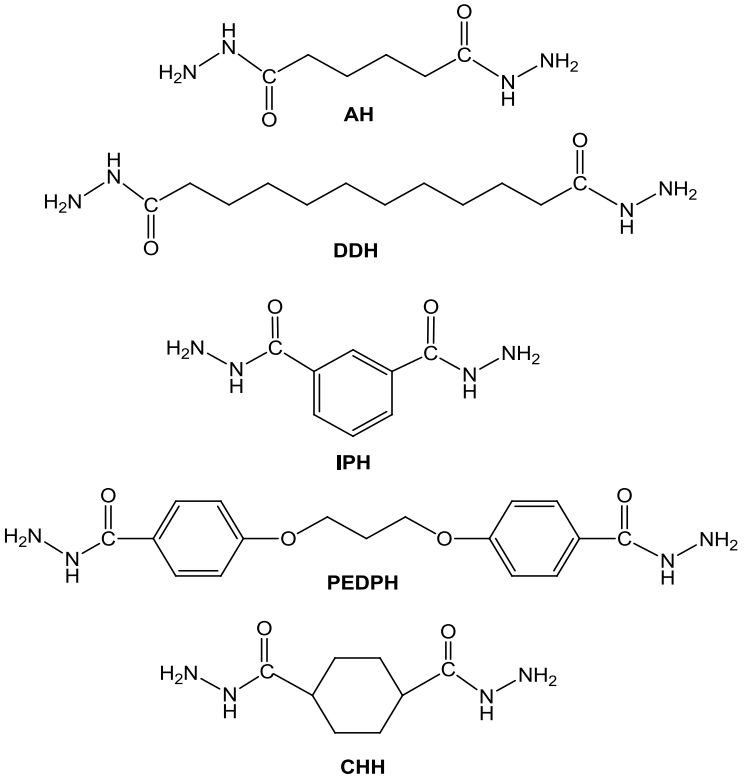

Scheme 1. Structures of the dihydrazides prepared

Synthesis of 4,4'-(propane-1,3-diylbisoxy) dibenzoic dihydrazide (PEDPH)

Propylene glycol (15 mL, 0.2 mol) was added in a 500 mL flask and azeotropically dried in benzene. After most of the benzene was distilled from the flask, 70 mL of anhydrous CH_2Cl_2 was added. The solution was cooled to 0 °C in ice-water bath before triethylamine (80 mL, 0.6 mol) was added. Methanesulfonyl chloride (48 mL, 0.6 mol) was added dropwise into the mixture in 30 min under stirring. After stirring at ambient temperature for 24 h, 150 mL of water were added and the mixture was extracted with CH_2Cl_2. The organic layer was washed firstly with 100 mL 1 M HCl solution in little proportions and secondly with saturated brine. The organic layer was then dried over anhydrous $MgSO_4$ and after filtration was concentrated in vacuum. Yield: 90%.

The mesylated propylene glycol (20 g, 0.08 mol) was dissolved in 150 mL acetone and methyl p-hydroxybenzoate (30 g, 0.2 mol) and K_2CO_3 (28.5 g, 0.2 mol) were added to the solution. The reaction mixture was refluxed for 12 h. After removing the acetone about 200 mL of water were added to the solid product and extracted several times with CH_2Cl_2. The organic layer was dried over anhydrous Mg_2SO_4 and the solvent was evaporated. The product precipitated in 400 mL cold ethanol. Yield 85%.

The ester previously prepared (17.3 g, 0.05 mol) was dissolved in 120 mL anhydrous ethanol and then a mixture of 30 mL (0.6 mol) oh hydrazine hydrate (80%) in 40 mL of anhydrous ethanol was added. The reaction mixture was refluxed for 24 h at 90°C. Most of the ethanol was evaporated under vacuum and then 300 mL of water was added to the resulting solution. The solution was extracted with 300 mL of methylene chloride. The collected organic layer was then washed with 200 mL of water and dried over anhydrous Na_2SO_4, condensed and precipitated over 400 mL of ethyl ether. The precipitate was dried under vacuum. Yield 65 %.

^{1}H NMR (DMSO-d_6, δ in ppm): 9.60 s (2H; -NH-); 7.79 d (4H, Ar); 7.00 d (4H, Ar); 4.40 m (4H, -NH_2); 4.15 t (4H, O-CH_2); 2.18 m (2H, -CH_2-). ^{13}C NMR (DMSO-d_6, δ in ppm): 165.41 (-CONH-); 160.53 (Ar); 128.34 (Ar); 125.34 (Ar); 113.84 (Ar); 64.11 (O-CH_2-); 28.40 (-CH_2-). FTIR-ATR (cm^{-1}): 3297, 3186, 3052, 1624, 1532, 1354, 1222, 1132, 1064, 642. m.p. 231-5ºC.

3.2.3. Preparation of the curing mixtures

The mixtures were prepared by mixing stoichiometric proportions (2:1) of DGEBA and the selected dihydrazide. The mixing was made in a mortar whereas heating (*ca.* 100ºC) until the crystalline product was completely incorporated to the viscous resin. In catalyzed formulations, 1 phr (one part of catalyst for hundred of mixture) of BDMA or $Yb(OTf)_3$ was added after homogenization of DGEBA/AH mixture.

3.2.4. Characterization techniques

^{1}H-RMN and ^{13}C-RMN spectra were recorded at 400 and 100.6 MHz using a Varian Gemini 400 spectrometer with Fourier transform. ^{1}H NMR spectra were acquired in 1 min and 16 scans with a D1 of 1.0 s. ^{13}C NMR spectra were obtained using a D1 of 0.5 s and

an acquisition time of 0.2 s. 500 accumulations were recorded. DMSO-d_6 was used as the solvent and TMS as the internal standard.

FTIR spectrophotometer FTIR-680PLUS from JASCO with a resolution of 4 cm^{-1} in the absorbance mode was used to monitor the isothermal curing process at 120°C. This device was equipped with an attenuated-total-reflection accessory with thermal control and a diamond crystal (Golden Gate heated single-reflection diamond ATR, Specac-Teknokroma). The disappearance of the absorbance peak at 910 cm^{-1} was used to monitor the epoxy equivalent conversion.

Calorimetric studies were carried out on a Mettler DSC-821e thermal analyzer in covered Al pans under N_2 at 100mL/min. The calorimeter was calibrated using an indium standard (heat flow calibration) and an indium-lead-zinc standard (temperature calibration). The samples weighed approximately 7 mg. In the dynamic curing process the degree of conversion by DSC (α_{DSC}) was calculated as follows:

$$\alpha_{DSC} = \frac{\Delta h_T}{\Delta h_{dyn}} \qquad (1)$$

where Δh_T is the heat released up to a temperature T, obtained by integration of the calorimetric signal up to this temperature, and Δh_{dyn} is the total reaction heat associated with the complete conversion of all reactive groups. The precision of the given enthalpies is ± 3%. The glass transition temperature (T_g) for each material was calculated after a complete dynamic curing, by means of a second scan, as the temperature of the half way point of the jump in the heat capacity when the material changed from the glassy to the rubbery state. The precision of the determined temperatures is estimated to be ± 1K.

The kinetic studies were performed at heating rates of 2, 5, 10 and 15 ºC/min in N_2 atmosphere, flow rate 100 ml/min. The kinetic triplet [pre-exponential factor, activation energy and kinetic model of the curing process was determined using integral isoconversional non-isothermal kinetic analysis, Kissinger-Akahira-Sunose equation, combined with the Coats-Redfern procedure. Details of the kinetic methodology are given in previous publications.[17,18]

Thermogravimetric analyses (TGAs) were carried out in a Metler TGA/SDTA 851e thermobalance. Pieces of the cured samples with an approximate mass of 8 mg were degraded between 30 and 600 °C at a heating rate of 10 ºC/min in N_2 (100 mL/min measured in normal conditions) in ceramic crucibles.

Dynamic mechanical thermal analyses (DMTA) were carried out with a TA Instruments DMTA 2980 analyzer. The samples were cured isothermally in a mold at 190 ºC for 1 h and then post-cured for 0.5 h at 200 ºC. Single cantilever bending was performed on prismatic rectangular samples (17.5 mm x 5 mm x 1.2 mm, approx). The apparatus operated dynamically at 3 ºC/min from 30 to 220 °C at a frequency of 1Hz with amplitude of 20 μm.

The impact test was performed at room temperature by means of an Zwick 5110 impact tester, according to ASTM D 4508-05 (2008) using rectangular samples (25.4 mm

x 12.7 mm x 1.5 mm) cured at the same conditions that DMTA samples. The pendulum employed had a kinetic energy of 1 J.

The fracture area of the specimens was observed by scanning electron microscope (SEM). The samples were metalized with gold and observed with a Jeol JSM 6400 with a 3.5 nm resolution.

Microhardness was measured with a Wilson Wolpert (Micro- Knoop 401MAV) device following the ASTM D1474-98 (2002) standard procedure. For each material 10 determinations were made with a confidence level of 95 %. The Knoop microhardness (HKN) was calculated from the following equation:

$$HKN = \frac{L}{A_p} = \frac{L}{l^2 C_p} \qquad (2)$$

where, L is the load applied to the indenter (0.025 Kg), A_p is the projected area of indentation in mm^2, l is the measured length of long diagonal of indentation in mm, C_p is the indenter constant (7.028×10^{-2}) relating l^2 to A_p. The values were obtained from 10 determinations with the calculated precision (95 % of confidence level).

3.3. Results and discussion

3.3.1. Synthesis and characterization of dihydrazides

The synthesis of dihydrazides has been performed following a previously described method.[19] The synthetic procedure is quite easy and implies the preparation of the intermediate diester, which further reacts with hydrazine. The preparation of dihydrazides only failed when a six member cycle can be formed by reaction of both nitrogen of hydrazine, which is the case for diethyl phthalate and triethyl trimellitate. Although the dihydrazides from succinic and malonic acid were prepared, they decompose on heating and therefore cannot be used as curing agents. The products prepared were analyzed by FTIR and NMR spectroscopy. **Figure 1** shows the ^{1}H and ^{13}C NMR spectra of the isophthalic dihydrazide (IPH) in DMSO-d_6 with the corresponding assignments. The most typical FTIR bands for dihydrazides are the ones assignable to the carbonylic absorption at 1652 cm^{-1} for the IPH and 1624-6 cm^{-1} for the other ones and also the N-H absorptions at 3300 and 3197-3052 cm^{-1} which appear as broad bands due to intermolecular association.

The materials obtained are crystalline with the only exception of the 1,4-cyclohexylene derivative, because of the mixture of cis and trans isomers in the initial diacid which prevents the crystalline structure to be adopted. The dihydrazides obtained are only soluble in highly polar solvents such as DMSO, due to the intra/inter molecular hydrogen bonding and their crystalline character. For this reason the preparation of the formulations with the epoxy resin is a quite difficult task and it is necessary to grind the crystalline powder and heat to get a homogeneous mixture.

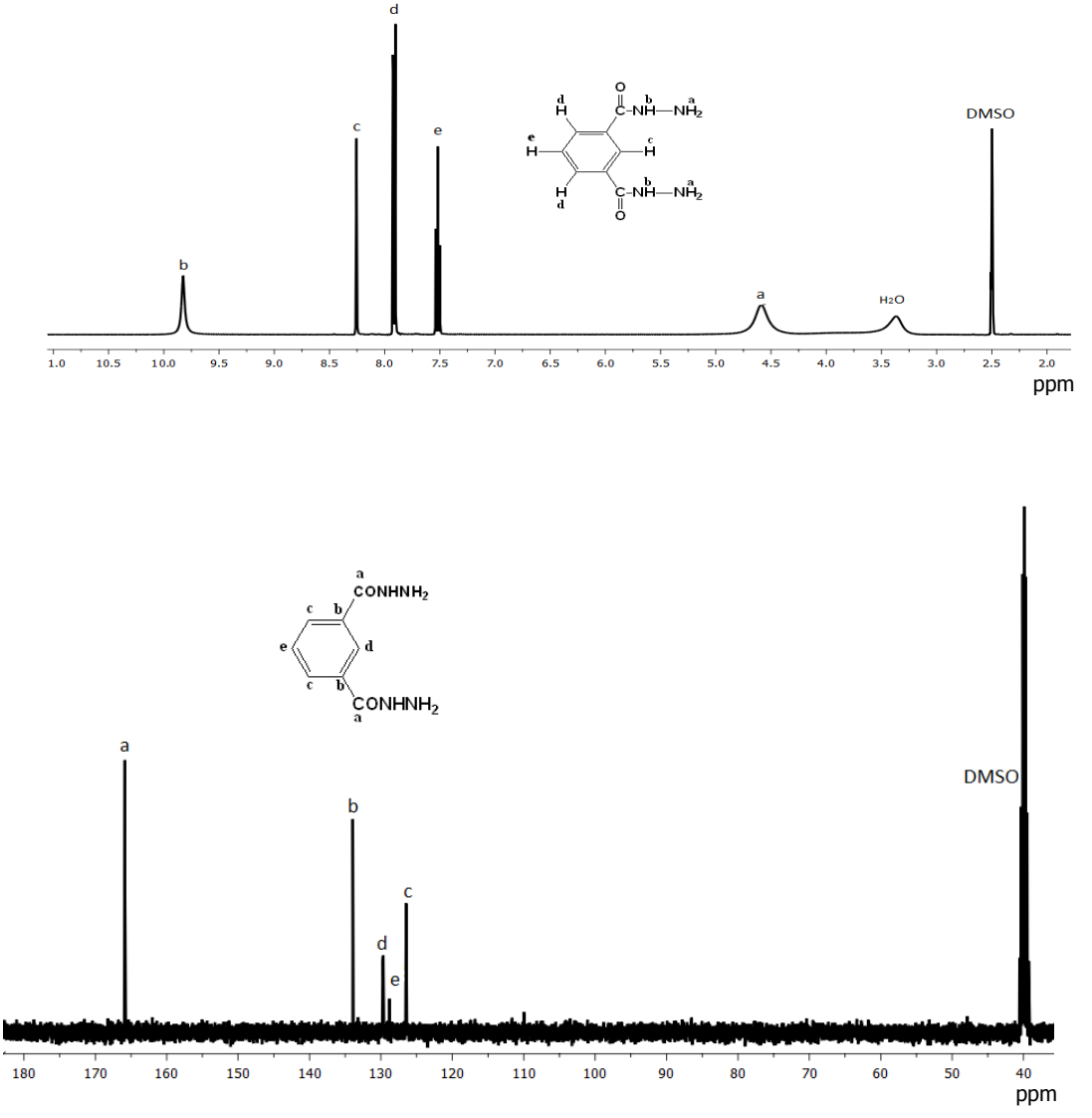

Figure 1. ^{1}H and ^{13}C NMR spectra of isophthalic dihydrazide (IPH) in DMSO-d_6.

In order to further characterize the synthesized dihydrazides, TGA experiments were performed since their thermal stability should be assured to be useful as thermally curing agents at quite higher temperature. All the curves obtained presented two clearly observable degradation processes. **Table 1** shows the thermogravimetric data of these compounds.

As we can see, all of them are stable up to 200 ºC. The most stable dihydrazide is CHH which show no weight loss below 300 ºC and the less one is IPH, although it experiments no degradation below 200 ºC. The temperatures of the two degradation processes are in similar ranges for all the compounds. If we measure the percentage of weight loss after the first degradation step we can calculate that some compounds loss fragments of 60 units, whereas others loss about 80. This could indicate the loss of nitrogen moieties of the dihydrazide groups (60 units) and in some cases an additional water molecule evolution (80 units).

Table 1. Melting temperatures and thermogravimetric data of the synthesized dihydrazides

Curing agent	T_{melt} [a] (°C)	$T_{2\%}$ [b] (ºC)	T_1 [c] (ºC)	T_2 [d] (°C)	$\%_{weight}$ [e]
AH	181-4	253	345	451	46
DDH	192-5	258	348	455	31
IPH	220-4	238	330	460	33
PEDPH	231-5	300	334	446	25
CHH	-	307	351	448	30

a. Obtained by DSC at 10 ºC/min
b. Temperature of 2% of weight loss obtained by TGA in nitrogen atmosphere at 10 ºC/min
c. Temperature of the maximum degradation rate of the first degradation process
d. Temperature of the maximum rate of the second degradation process
e. Weight loss percentage after degradation he first degradation process

3.3.2. Study of the curing process

By calorimetry we studied the curing behaviour of the mixtures with all the dihydrazides prepared. In a preliminary study we determined that the proportion of components in the formulation to reach the maximum degree of curing was DGEBA/dihydrazide 2:1 mol/mol, since this composition leads to a maximum enthalpy release by epoxy equivalent. In this formulation, DGEBA acts as a difunctional monomer and dihydrazide as tetrafunctional in a step growth polymerization mechanism, similar to the conventional epoxy/primary diamine (see **Scheme 2**). It should be commented that only the NH_2 groups are nucleophylic enough to attack oxirane rings.

Figure 2 shows the curing exotherms obtained at 10 ºC/min. As we can see, the curves are sharp and unimodal indicating that the reactions in the curing process take place simultaneously. Depending on the dihydrazide selected the curve occurs at different temperature, but high temperatures of curing are generally required.

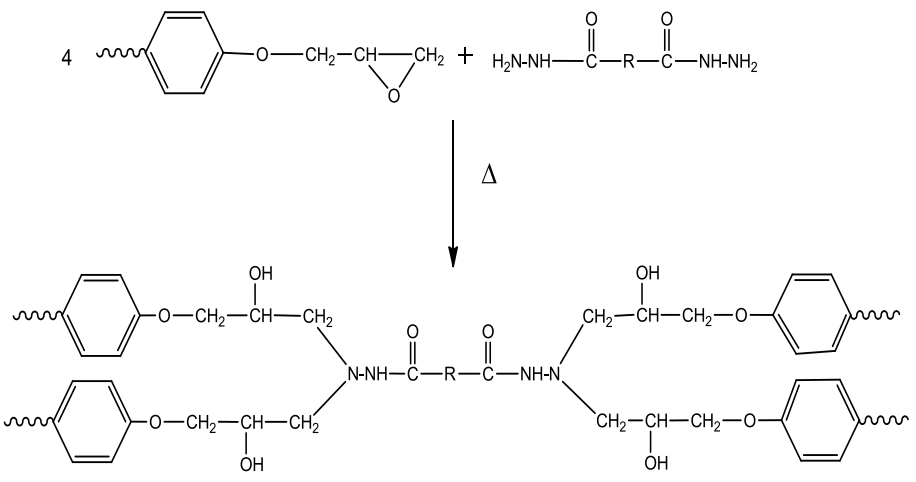

Scheme 2. General structure of the reagents and of the network formed.

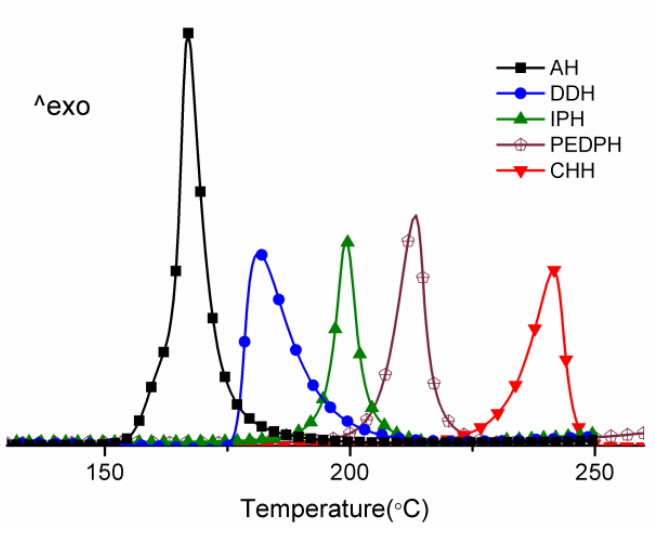

Figure 2. DSC scanning curves for DGEBA/dihydrazide formulations obtained at a heating rate of 10ºC/min

Figure 3 represents the plot of conversion against temperature. All the curing processes show a latent character, because they begin at a definite temperature and once initiated the process occurs very fast. This is an important issue because it allows the preparation of one-pot formulations to be applied at high temperature for a very short time.

As we can see, the aliphatic dihydrazides, ADH and DDH are the ones that lead to the curing at lower temperature. In fact, there is a correlation between melting points and initial curing temperatures, although melting endotherms are rarely detectable by DSC and only at high heating rates (15 ºC/min). The exception to this correlation is CHH, which is an amorphous solid without any detectable *Tg* in the range between 25 and 300 ºC. It is important to notice that whereas aliphatic amines initiate the curing at room temperature, aliphatic dihydrazides react at temperatures much higher than 100 ºC. This can be explained by the lower nucleophilicity of NH_2 groups of dihydrazides, since the nitrogen atom directly linked to this group reduces the electronic density in comparison to that of aliphatic amines. Thus, aliphatic dihydrazides can be advantageous because they introduce flexibility to the epoxy network as the aliphatic amines do, but one-pot formulations could be prepared with these curing agents.

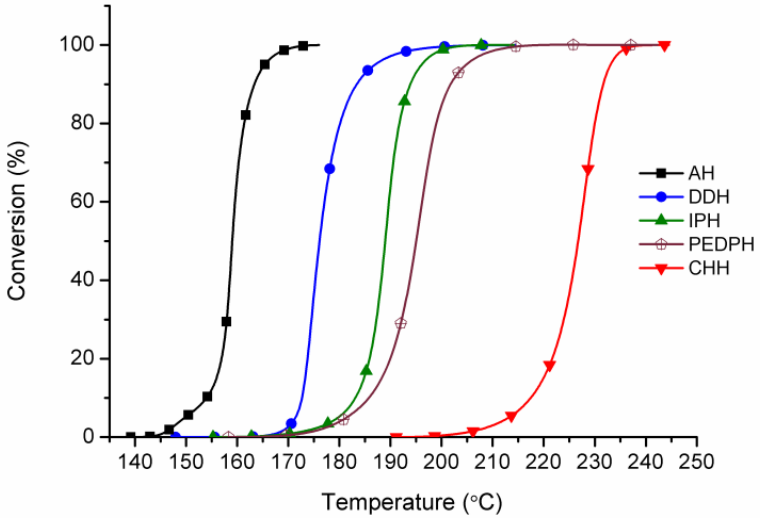

Figure 3. Conversion degree against temperature for the curing of DGEBA/dihydrazide formulations at a heating rate of 10 ºC/min.

Table 2 collects the calorimetric data of the formulations studied. The curing enthalpies per gram are reduced on increasing the molecular weight of the dihydrazide because of the lower epoxy content. However, the released enthalpies per epoxy equivalent are comparable for all the formulations studied although higher for the PEDPH. The values obtained are something lower than the ones described for the curing with amines, which are about 100 kJ/ee.[20] However, by FTIR spectroscopy we could prove that the complete curing was achieved.

The T_gs of the materials obtained in a second scan after dynamic curing in the DSC are quite similar and near to 120 ºC. It seems that the chemical structure of the dihydrazide is not the only factor reflected in this parameter, since the more rigid IPH structure leads to the lowest *Tg* value but the final degree of crosslinking achieved can also influence. The kinetic parameters calculated for all the formulations are collected in **Table 2**.

Table 2. Calorimetric data and kinetic parameters of the DGEBA/dihydrazides

Curing agent	T_{max} [a] (°C)	Δh [b] (J/g)	Δh [b] (kJ/eq)	T_g [d] (°C)	E_a [d] (kJ/mol)	ln$A$ [e] (min^{-1})	$k_{180°C}$ [f] (min^{-1})
AH	165	408	96	128	169.9	46.48	4.926
DDH	181	311	89	122	146.9	38.43	0.569
IPH	196	320	80	118	112.2	28.21	0.206
PEDPH	204	312	106	125	127.4	31.56	0.108
CHH	239	300	76	127	121.1	27.77	0.013

a. Temperature of the maximum of the curing exotherm registered at 10 ºC/min.
b. Enthalpy of the curing exotherm registered at 10 ºC/min.
c. T_g determined after curing in a dynamic scan registered at 20 ºC/min.
d. Values of activation energy at 50% of conversion, evaluated by the isoconversional non-isothermal procedure.
e. Pre-exponential factor calculated for A_4 model with $g(a) = [-\ln(1-a)]^{1/4}$.
f. Values of rate constant at 180°C using the Arrhenius equation at 50% conversion.

The dependence of the apparent activation energy on the degree of conversion calculated by the isoconversional method is presented in **Figure 4**. As we can see, there are no big variations in the activation energy along the curing process, but there are some differences between the values calculated for all the formulations. The activation energies are in the range between 120 and 170 kJ/mol and the higher value corresponds to the adipic dihydrazide. In a previous paper Vyazovkin[21] reported the influence of the nucleophilic character of primary aromatic amines on the activation energy of the amine-epoxy reaction. Normally observed values are of 50-60 kJ/mol but the presence of a substituent of a large negative charge in ortho position causes an increase in the activation energy to 100 kJ/mol approximately. Activation energy values for epoxy-biaguanide curing system were evaluated to be around 60 kJ/mol.[22] The activation energy may afford a relatively straight theoretical interpretation in terms of energy barriers, characterize the temperature sensitivity of the reaction and therefore is a key parameter in practical kinetic predictions. Thus, the higher E_a values obtained for the curing with dihydrazides can be related, in a first approximation, to the reaction taking place at high temperature and with a latent nature.

To calculate the frequency factors, we selected the kinetic model that better fits with the experimental results, which in these formulations was the A_4. Knowing the activation energy and the kinetic model and using the Kissinger-Akahira-Sunose equation,[23] we could obtain the frequency factors for a conversion of 0.5, which are collected in **Table 2**.

The kinetic constants were obtained by the Arrhenius equation. We can see that at 180ºC the constant rate is much higher for the system in which AH is the curing agent. The lowest rate constant was calculated for CHH curing formulation. The magnitude of the rate constants reflect the order of temperatures that initiate the curing for the different

dihydrazides, whereas activation energy does not reflect this effect due to the compensation effect between the activation energy and the frequency factor.[17]

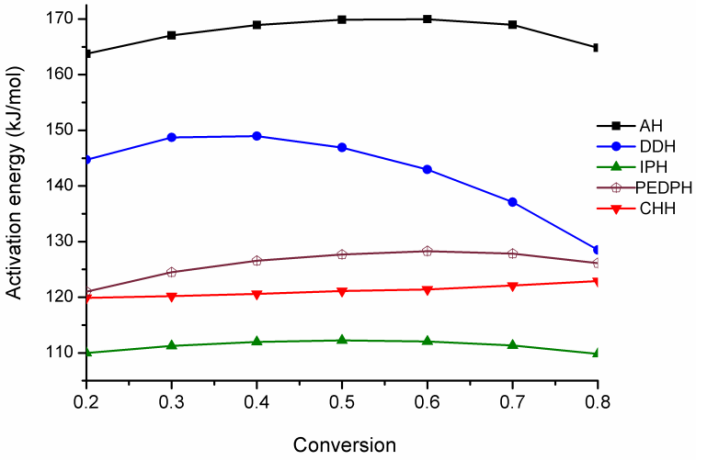

Figure 4. Dependence of activation energy on the conversion degree in the curing of DGEBA/dihydrazide formulations.

In some epoxy-amine formulations the addition of a Lewis acid or a Lewis base can accelerate the curing. However, the chemistry of the cure process becomes more complex because ring-opening homopolymerization can compete with the usual step growth mechanism. The occurrence of both competitive mechanisms depends on the curing temperature.[24] We tested the effect of the addition of catalytic proportions of benzyldimethylamine or ytterbium triflate (1 phr) as base or Lewis acid, respectively. **Figure 5** presents the calorimetric curves for the catalyzed and non-catalyzed AH formulations.

As we can see, the curves broaden and shift to lower temperatures on adding the catalyst and loss the latent character of the curing agent, but the curing enthalpies have similar values. BDMA produces a more important catalytic effect and the reaction occurs before the complete melting of AH, which is visible as an endotherm at about 180 ºC. It must be commented that BDMA alone is not able to cure DGEBA[25] and therefore, the curing exotherm is due to a true catalyzed dihydrazide curing. However, the presence of dihydrazides and especially, the formation of hydroxyl groups during the condensation can favor a slight homopolymerization of epoxides initiated by BDMA. This slight homopolymerization can explain the little endotherm at about 180 ºC, attributable to an excess of adipic dihydrazide. Although $Yb(OTf)_3$ alone can produce the complete curing of DGEBA resins,[26] the shape of the curve and the curing temperatures are quite different, indicating that AH has the role as curing agent in this catalyzed curing process. The addition of these catalysts to DGEBA/AH curing mixtures slightly reduces the T_g of the thermosets. Thus, the material obtained with BDMA presented a T_g of 121 ºC, whereas the value for the thermoset obtained with $Yb(OTf)_3$ was 124 ºC.

The use of $Yb(OTf)_3$ as catalyst was previously reported in the curing of DGEBA with biguanide, which is a latent catalyst usually used in powder coatings.[22,27] In these studies, no variations in the T_g of the materials were observed and the network structure was identical that the one obtained in the non-catalyzed curing. By FTIR spectroscopy we proved that the curing proceed by nucleophilic attack of biguanide nitrogens to epoxy groups.

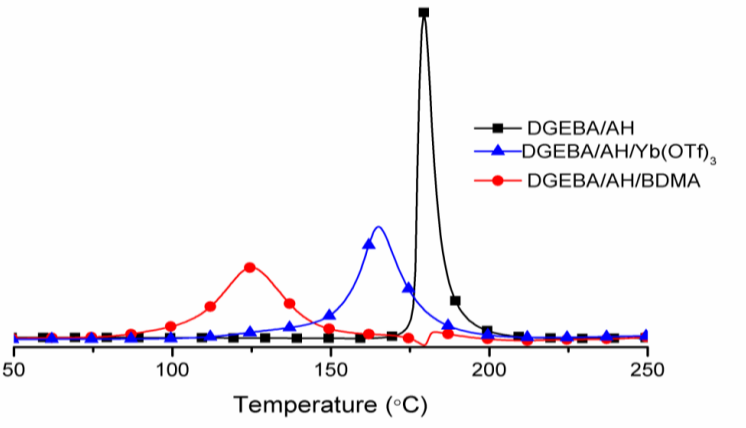

Figure 5. DSC scanning curves for DGEBA/AH formulations without any catalyst or catalyzed by 1 phr of BDMA or $Yb(OTf)_3$ at a heating rate of 10ºC/min.

FTIR spectra allowed us to confirm the complete curing of the DGEBA-dihydrazide formulations. **Figure 6** shows the spectra before and after curing. The most significant signals are the epoxy band at 910 cm^{-1}, which disappears on curing, and the OH broad absorption produced by the attack of NH_2 to the epoxide ring. The band at 1652 cm^{-1} of the carbonyl group of the dihydrazide becomes more visible after the curing has taken place and the broaden C-O st absorptions at about 1100 cm^{-1} increase in size.

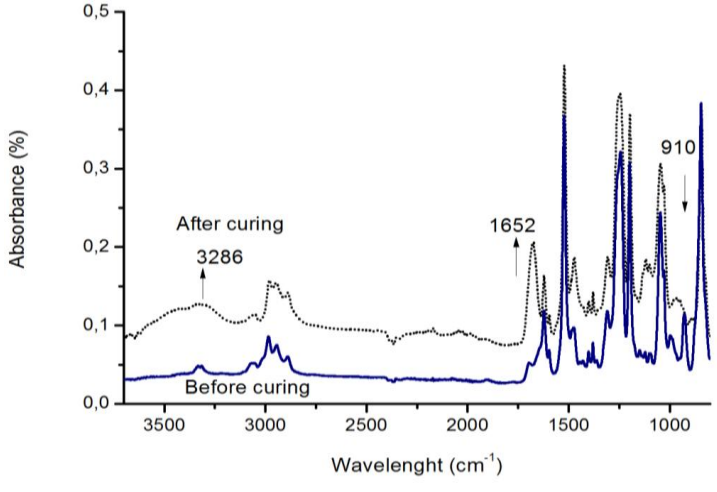

Figure 6. FTIR-ATR spectra of the DGEBA/AH formulation before and after curing at 180ºC

3.3.3 Characterization of the materials

The thermal stability of the thermosets obtained was studied by TGA. The degradation curves of the thermosets show two degradation steps, not as well defined as in pure dihydrazides. This indicates that the loss of nitrogen moieties does not occur by an easy degradative mechanism and the breakage of different bonds and elimination of fragments of different molecular weight takes place simultaneously. **Table 3** collects the main important thermogravimetric data for the thermosets prepared. The material with less thermal stability is the one obtained from AH, but initial temperatures of degradation higher than 280 ºC were determined. The char yield measured reflects the structure of the dihydrazide used. The more aromatic structures of IPH and PEDPH dihydrazides present the highest char yield, whereas the high aliphatic character of DDH leads to the lowest, as expected.

Table 3. Thermogravimetric data for the thermosets prepared

Curing agent	$T_{5\%}$[a] (ºC)	T_{max}[b] (°C)	Char yield[c] (%)
AH	287	344-407	12.2
DDH	293	340-390	8.7
IPH	314	355	18.4
PEDPH	302	400	17,2
CHH	300	347-405	10.8

a. Temperature of a 5% of weight loss
b. Temperature of the maximum degradation rate
c. Residue at 700ºC

Thermomechanical characteristics of the thermosets were studied. The high melting temperature and the low solubility of IPH, CHH and PEDPH in DGEBA and in solvents of low boiling point did not allow the preparation of specimens without defects to perform mechanical and thermomechanical tests. The preparation of such samples requires a homogeneous mixture that should be prepared in special devices, which usually are not disposable in most academic laboratories. However, specimens from formulations DGEBA with AH or DDH could be prepared with an acceptable quality and reproducibility.

Figure 7 shows the DMTA curves for both materials. As expected, the longer aliphatic chain of DDH leads to materials with a lower tan δ temperature than that of AH and also with a lower modulus, both in the glassy and in the rubber state. The lower modulus in the rubbery zone of DDH materials reflects the greater distance between crosslinks. The materials show a unimodal relaxation, indicating their homogeneous character.

The microhardness value, which is a crucial property in coatings technology, was measured by Knoop microindentation. It reflects the capability of the thermoset to resist

static loads or applied at low rates. The values obtained for both materials (see **Table 4**) were similar than previously reported values for epoxy-anhydride thermosets[28] but slightly lower than the values obtained for DGEBA cured by $Yb(OTf)_3$, which corresponds to a more compact structure of the network, due to the homopolymerization process.[29] The microhardness is slightly lower for the specimen obtained from DDH, because of its more flexible structure.

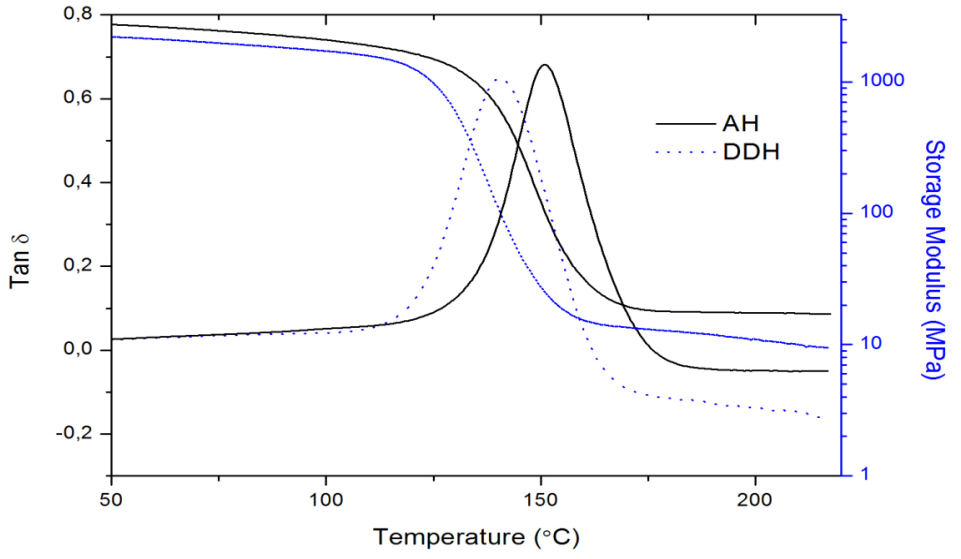

Figure 7. Evolution of tan *δ* and storage modulus against temperature at 1 Hz for the thermosets obtained from AH and DDH.

Table 4. Mechanical properties determined for AH and DDH thermosets

Curing agent	Microhardness (KHO)	Impact strength (J/m^2)
AH	20.7 (± 1.4)	3.4 (± 0.8)
DDH	18.8 (± 1.3)	5.0 (± 0.9)

Impact resistance is a useful measure to evaluate the toughness or brittleness of a material. The measure of this characteristic was done by Izod impact tester. As we can see in the table, the impact resistance is slightly higher for DDH specimen. The flexibilization effect of the longer aliphatic structure of the dihydrazide should be the responsible of this effect. The impact resistance of these cured materials is higher than the measured for epoxy/anhydride thermosets[28] and even two times higher than thermosets obtained by homopolymerization of DGEBA by $Yb(OTf)_3$.[30]

3.4. Conclusions

A series of dihydrazides were prepared by reaction of dicarboxylic diester with hydrazine hydrate in ethanol. These compounds were studied as curing agents in DGEBA/dihydrazide 2:1 (mol/mol) formulations demonstrating their latent character. A relationship between the melting point of the dihydrazide and the initial curing temperature was observed with the exception of CHH dihydrazide, which was amorphous but initiate the cure at the highest temperature. The kinetic parameters for all the curing processes were calculated and the rate constant values agree with reactivity of hydrazide/DGEBA formulations.

The addition of a Lewis acid or a Lewis base as catalyst allowed performing the curing at lower temperature but the latent characteristics was diminished.

Pure dihydrazides showed a definite weight loss that can be explained by the loss of the nitrogen moiety, although they are stable up to 250 ºC. The thermosets obtained showed thermostability at least up to 280 ºC.

The glass transition of the thermosets prepared were around 120 ºC, without a direct relationship with the structure of the dihydrazide.

In the specimens obtained from adipic and dodecanoic dihydazides, thermomechanical characteristics, microhardness and toughness values are related to the flexibility introduced by the dihydrazide structure.

Acknowledgements

The authors would like to thank MICINN (Ministerio de Ciencia e Innovación) and FEDER (Fondo Europeo de Desarrollo Regional) (MAT2008-06284-C03-01 and MAT2008-06284-C03-02) and to the Comissionat per a Universitat i Recerca de la Generalitat de Catalunya (2009-SGR-1512). A.T. acknowledges the grant FI-DGR 2010 from the Catalonian Government.

References

[1]May CA, ed. E*poxy Resins. Chemistry and Technology*. 2nd ed. Marcel Dekker: New York; 1988.
[2] Petrie EM. *Epoxy Adhesive Formulations*. McGraw-Hill: New York; 2006.
[3] Endo T and Sanda F, *Macromol Symp* **107:** 237-242 (1996).
[4] Takahashi E, Sanda F and Endo T. *J Polym Sci: Part A: Polym Chem* **40:** 1037-1046 (2002).
[5] Chiu Y-S, Liu Y-L, Wei W-L and Chen W-Y, *J Polym Sci: Part A: Polym Chem* **41:** 432-440 (2003).
[6] Park S-J, Jin F-L, Lee J-R and Shin J-S, *Eur Polym J* **41:** 231-237 (2005).
[7] Lin R-H, Chen C-L, Kao L-H and Yang P-R, *J Appl Polym Sci* **82:** 3539-3551 (2001).
[8] Matejka L, Chabanne P, Tighzert L and Pascault JP, *J Polym Sci: Part A: Polym Chem* **32:** 1447-1458 (1994).
[9] Güthner T and Hammer B, *J Appl Polym Sci* **50:**1453-1459 (1993).

[10] Raetzke K, Shaikh MQ, Faupel F and Noeske P-LM, *Int J Adhes Adhes* **30:** 105-110 (2010).
[11] Holbery JD and Bordia RK. *J Mater Sci* **36:** 5301-5308 (2001).
[12] Wear SL, Stable Heat-Curing Epoxy Resin Compositions US Patent 2847395 (1958).
[13] Ito N, Takiuchi K, Abe M and Hirai K. Latent Curing Agents for Epoxy Resins US Patent 4448949 (1984).
[14] Hermansen RD and Lau SE. Adhesive of Flexible Epoxy Resin and Latent Dihydrazide. US Patent 6723803 B1 (2004).
[15] Ajinomoto Fine-Techno Company, http://www.aft-website.com [accessed 7 June 2011].
[16] Awasthi S, Rishishwar P, Rao AN, Ganesan K, Malhortra RC, *J Korean Chem Soc* **51:** 506–512 (2007).
[17] Ramis X, Salla JM, Mas C, Mantecón A and Serra A, *J Appl Polym Sci* **92:** 381-393 (2004).
[18] Ramis X, Salla JM, Cadenato A and Morancho JM. *J Thermal Anal Calorim* **72:** 707-718 (2003).
[19] Byrkit GD and Michalek GA, *Ind Eng Chem* **42:** 1862-1875 (1959).
[20] Ivin, KJ in *Polymer Handbook*. Brandrup J, Immergut EH, eds. Wiley: New York; 1975.
[21] Zhang Y and Vyazovkin S. *J Phys Chem B* **111:** 7098-7104 (2007).
[22] García SJ, Serra A, Ramis X and Suay J. *J Therm Anal Calorim* **89:** 223-231 (2007).
[23] Kissinger HE. *Anal Chem* **29**: 1702-1706 (1957).
[24] Pascault JP, Williams RJJ. *Epoxy Polymers. New Materials and Innovations*. Wiley: Weinheim; 2010.
[25] Flores M, Fernández-Francos X, Morancho JM, Serra A and Ramis X, *J Appl Polym Sci* 125: 2779-2789 (2012).
[26] Castell P, Galià M, Serra A, Salla JM and Ramis X. *Polymer* **41:** 8465-8474 (2000).
[27] García SJ, Serra A and Suay J. *J Appl Polym Sci* **105:** 3097-3107 (2007).
[28] Morell M, Ramis X, Ferrando F, Yu Y and Serra A. *Polymer* **50:** 5374-5383 (2009).
[29] González L, Ferrando F, Ramis X, Salla JM, Mantecón A and Serra A. *Prog Org Coat* **65:**175-181 (2009).
[30] Morell M, Ramis X, Ferrando F, Serra A. *Polymer*, **52:** 4694-4702 (2011).

Chapter 4

Influence of end groups in hyperbranched polyesters used as modifiers in the characteristics of epoxy thermosets cured by adipic dihydrazide

Chapter 4 - Express Polymer Letters 7 (2013) 595-606

INFLUENCE OF END GROUPS IN HYPERBRANCHED POLYESTERS USED AS MODIFIERS IN THE CHARACTERISTICS OF EPOXY THERMOSETS CURED BY ADIPIC DIHYDRAZIDE

A. M. Tomuta,[1] X. Ramis[2], S. de la Flor[3], A. Serra[1*]

[1] Department of Analytical and Organic Chemistry, Universitat Rovira i Virgili, C/Marcel·lí Domingo s/n, 43007, Tarragona, Spain.

[2] Laboratory of Thermodynamics, ETSEIB, Universitat Politècnica de Catalunya, Diagonal 647, 08028 Barcelona, Spain

[3] Department of Mechanical Engineering, Universitat Rovira i Virgili, C/ Països Catalans 26, 43007, Tarragona, Spain.

Abstract

Mixtures of diglycidylether of bisphenol A (DGEBA) resin and different ratios of aliphatic-aromatic hyperbranched polyester (HBP) were cured by a latent curing agent, adipic dihydrazide (AH). The HBPs prepared have hydroxyl groups or 10-undecenoyl or allyl groups as chain ends. The curing mixtures were investigated by differential scanning calorimetry (DSC) to study the curing process and to evaluate the kinetic parameters of the different formulations. These studies suggest that HBPs decrease the curing rate of epoxy/AH in the case of vinyl terminated HPB, whereas OH terminated HBP accelerates the first stages and delays the lasts.

The thermosets obtained showed an improvement in microhardness and impact strength without any reduction of the T_g and thermal parameters. Microparticle phase separation was observed with the undecenoyl HBP derivatives or when a 10% of allyl HBP derivative was in the formulation.

Keyword: Thermosetting resins, toughness, hyperbranched polymers, latency, dihydrazides.

4.1. Introduction

Epoxy resins are widely used in several applications: adhesives, coatings, castings, electric laminates, encapsulation of semiconductor devices, matrix materials for composites, structural components and engineering, [1,2] because of their good characteristics such as adhesion and chemical resistance. However, due to their high cross-link density they are inherently brittle, which limits their applicability. With the aim to increase their toughness different types of modifiers have been added to epoxy formulations such as rubber, thermoplastic and core-shell particles. The addition of liquid rubbers and thermoplastics was one of the first attempts to improve toughness, but usually this method has a detrimental effect on the thermomechanical characteristics of the thermosets and the processability of the formulation, [3] which is a drawback for coatings applications.[4,5] To solve the limitations related to processability, hyperbranched polymers (HBPs) were introduced as toughness modifiers.[6,7,8] The advantage is that their

highly branched structure prevents entanglement, reducing the viscosity of the formulation in comparison to the use of their linear analogues. Moreover, the great number of terminal groups has a significant effect on the reactivity, can increase the compatibility with the resin and helps to maintain thermomechanical characteristics.[9,10] Based on their unique properties, HBPs have been applied not only as toughening for thermosets but also in cross-linking or adhesive agents,[11] compatibilizers,[12] dispersers,[13] processing aids, and rheology modifiers.[14,15]

One of the most effective methods of inhibiting crack growth after impact is the addition of a second phase that induces the formation of particles that absorb the impact energy and deflect the crack.[5] Usually, the particles are generated from a homogeneous solution composed of the resin, curing agent and modifiers, which on curing causes a reaction-induced phase separation (RIPS) to take place. The phase separated morphology is highly dependent on the kinetics of curing and on the dynamics of the phase separation process.

The synthesis and characterization of aromatic-aliphatic hyperbranched polyesters modified with long and short vinylic chains and their use as modifiers of DGEBA thermosets cured with hexahydro-4-methylphthalic anhydride was reported by us.[16] The addition of these modifiers led to significantly increased rates of cure. However, the materials obtained were homogeneous and the increase in impact strength was only modest. In addition, the HBPs led to a plasticization and to a considerable decrease in the T_g.

In a previous paper we demonstrated the latent character of a series of dihydrazides in the thermal curing of DGEBA.[17] Several dihydrazides were synthesized and used as stoichiometric curing agents of epoxy resins. From the dihydrazides synthesized, AH was the one that leads to curing at the lowest temperature (maximum of the curing exotherm at 165ºC) and led to materials with good characteristics. However, dihydrazides possess a high crystalline character and they are difficult to disperse or dissolve, because on melting (at 181-184ºC) the curing process is extremely fast.

In the present work, the influence of the addition of aromatic-aliphatic hyperbranched polyesters modified with long and short vinylic chains (see **Figure 1**) to the epoxy formulation has been studied with two different aims: to increase toughness and help to disperse AH in the DGEBA resin. In addition, it was expected from the fast curing process caused by the dihydrazides at the appropriate temperature that could induce phase separated morphologies, when the HBP structure cannot be covalently incorporated to the epoxy matrix, because of its solubility and the end group characteristics.

4.2. Experimental

4.2.1. Materials

4,4-Bis(4-hydroxyphenyl) valeric acid, N,N'-dicyclohexylcarbodiimide (DCC), triethyl amine, allyl bromide, 10-undecenoyl chloride, diethyl adipate and hydrazine hydrate were purchased from Sigma Aldrich (St. Louis, MO, USA) and used without further purification.

Diglycidyl ether of Bisphenol A (DGEBA) Epikote Resin 828 was provided by Momentive Speciality Chemicals Inc. (Barbastro, Spain) with an epoxy equivalent of 184 g/eq and was dried in vacuum before use. All the organic solvents were purchased from Scharlab and purified by standard procedures. 4-(N,N-dimethylamino) pyridinium p-toluenesulfo-nate (DPTS) was prepared as described in the literature.[18]

4.2.2. Synthesis of adipic dihydrazide (AH)

50.5 g (0.25 mol) of the diethyl adipate were dissolved in 200 mL of absolute ethanol and 0.9 mol of hydrazine hydrate (90 %) were added drop by drop. Once the addition was complete the heating was turned on and the mixture was kept 6 h at reflux. During this time a white precipitate was formed, which was filtered through a Buchner funnel and then washed twice with cold ethanol. The white powder was dried in the vacuum oven at 50°C. The obtained yield was higher than 90%. m.p. 181-4 ºC (recrystallized from ethanol). ^{1}H NMR (DMSO-d_6, δ in ppm): 8.93 s (2H, -NH-); 4.14 s (4H, -NH_2); 1.97 t (4H, -CH_2-) 1.41 m (4H, -CH_2-); ^{13}C NMR (DMSO-d_6, δ in ppm): 171.49 (-CONH-); 33.27 (-CH_2-); 24.99 (-CH_2-). FTIR-ATR (cm^{-1}): 3310, 3288, 3197, 1626, 1529, 1376, 1273, 1166, 1033, 690.

4.2.3. Hyperbranched polyester synthesis (HBP-OH) (Figure 1)

The HBP-OH was synthesized according to a previously described procedure[19] from 4,4-bis(4-hydroxyphenyl) valeric acid as AB_2 monomer. The ^{1}H and ^{13}C NMR data are in accordance with those published.[20]

M_n: 8700 g/mol, M_w: 12300 g/mol. T_g 121 ºC (by DSC). The amount of hydroxyl groups was determined according to ISO 2554-1974 standards. The number of hydroxyl groups per molecule found by titration was 36.[16]

4.2.4. Derivatization of HBP-OH with 10-undecenoyl chain ends (HBP-Und) (Figure 1)

The derivatization was done from HBP-OH synthesized previously by reacting with 10-undecenoyl chloride in the presence of triethylamine, as previously described.[16] The product was dried in a vacuum oven at 50 °C overnight and a pale brown viscous liquid was obtained. Yield: 94% T_g 18 ºC (by DSC).

^{1}H NMR (400 MHz, $CDCl_3$), δ (ppm): 1.26 m (-CH_2-); 1.41 m (-CH_3); 1.68 m (-CH_2-); 2.06 m (-CH_2-); 2.34 m (-CH_2-); 2.55 m (-CH_2-); 5.10 dd (CH_2=); 5.87 m (=CH-); 7.11 m (CH Ar).

^{13}C NMR (100.6 MHz, $CDCl_3$), δ (ppm): 24.7 (-CH_2-); 27.6 (-CH_2-); 28.9 (-CH_2-); 33.6 (-CH_2-); 34.3 (-CH_2-) 36.2 (-CH_2-); 45.4 (=C=); 113.9 (CH_2=); 121.2 (Ar) ; 128.2 (Ar); 139.0 (=CH-); 145.6 (Ar); 148.6 (Ar); 172.3 (C=O).

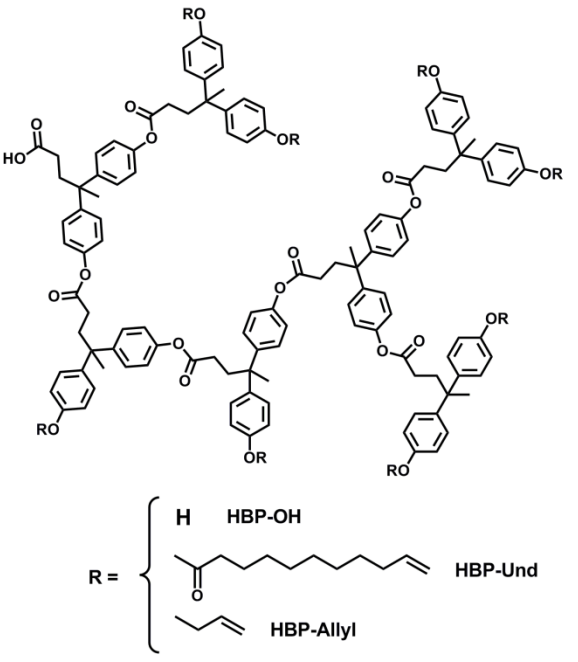

Figure 1. Structure of the HBP modifiers added to the formulations.

4.2.5. Derivatization of HBP-OH with allyl chain ends (HBP-Allyl) (Figure 1)

The derivatization was performed by nucleophylic substitution on allyl bromide by the phenolate end groups, formed by treating HBP-OH with K_2CO_3 in a mixture of THF and acetone, as previously reported.[16] HBP-Allyl was obtained by precipitating the THF solution on water. The polymer was dried in a vacuum oven at 50 °C overnight and a white powder was obtained. Yield: 90%. T_g 81 ºC (by DSC).

^{1}H NMR (400 MHz, $CDCl_3$), δ (ppm): 1.65 s ($-CH_3$); 2.36 m ($-CH_2-$); 2.53 ($-CH_2-$); 4.53 s ($-CH_2-$); 5.35 dd ($CH_2=$); 6.07 m (=CH-); 6.8-7.2 m (CH Ar).

^{13}C NMR (100.6 MHz, $CDCl_3$), δ (ppm): 28.0 ($-CH_2-$); 30.6 ($-CH_2$); 36.6 ($-CH_2-$); 45.1 (=C=); 68.9 ($-CH_2-$); 114.3 (Ar); 117,9 ($CH_2=$); 128.4 (Ar); 133.5 (=CH-); 141.2 (Ar); 156.9 (Ar); 172.5 (C=O).

4.2.6. Preparation of the curing mixtures

The neat DGEBA/AH formulation was prepared by adding the stoichiometric amounts of each reactant to a mortar and homogenizing them by mechanical mixing while heating at 90ºC.

For the preparation of the formulations with the HBP modifiers, first of all the corresponding proportion was dissolved in DGEBA by adding a little amount of THF. The solvent was then eliminated in vacuum at 50 ºC overnight and then the stoichiometric amount of AH was added and homogenized by mixing in a mortar while heating at 90ºC. The proportions of HBPs added were a 5 and 10% w/w in reference to DGEBA. AH was added in a molar proportion to DGEBA of 1:2.

4.2.7. Measurements

The 400 MHz ^{1}H-NMR and 100.6 MHz ^{13}C-NMR spectra were obtained with a Varian Gemini 400 spectrometer with Fourier Transformed (Palo Alto, California USA). ^{1}H-NMR spectra were acquired in 1 min and 16 scans with a 1.0 s relaxation delay (D1). ^{13}C NMR spectra were obtained using a D1 of 0.5 s and an acquisition time of 0.2 s. A total of 500 accumulations were recorded. $CDCl_3$ was used as a solvent and tetramethylsilane (TMS) as internal standard.

Calorimetric analyses were carried out on a Mettler DSC-821e calorimeter (Greifensee, Switzerland). Samples of approximately 10 mg were cured in aluminium pans in a nitrogen atmosphere. Non-isothermal experiments were performed from 0 to 225ºC at heating rates of 2, 5, 10, and 15 ºC/min to determine the reaction heat and the kinetic parameters. In the non-isothermal curing process, the degree of conversion at a given temperature *T* was calculated as the quotient between the heat released up to *T* and the total reaction heat associated with the complete conversion of all reactive groups. The precision of the given enthalpies is ±3%. The T_gs of the cured materials were determined with a second scan at 20 ºC/min after dynamic curing by the mid-point method and the error is estimated to be approximately ±1°C. The T_gs of the pure HBPs were determined by a similar procedure.

Dynamic mechanical thermal analysis (DMTA) was carried out with a TA Instruments DMTA 2980 analyzer (New Castle, USA). The samples were cured isothermally in a mould at 190 ºC for 1 h and then post-cured for 0.5 h at 200 ºC. Before the samples were prepared, they were degassed in a vacuum oven at 50 ºC for 3 h. Single cantilever bending at 1 Hz was performed at 3ºC/min from 30 to 220 ºC on prismatic rectangular samples (1.5 x 20 x 5 mm^3).

Thermogravimetric analysis was carried out with a Mettler-Toledo TGA/SDTA 851e thermobalance (Greifensee, Switzerland). Cured samples with an approximate mass of 5 mg were heated from 30 to 800ºC at a heating rate of 10 ºC/min in a nitrogen atmosphere.

Impact tests were performed at room temperature by means of a Zwick 5110 impact tester (Altamonte Springs, USA) according to ASTM D 4508-05 using rectangular samples (25 x 12 x 2.5 mm^3). The pendulum employed had a kinetic energy of 1 J. For each material, 9 determinations were made. The impact strength (IS) was calculated from the energy absorbed by the sample upon fracture as:

$$IS = \frac{E - E_0}{S} \qquad (1)$$

where E and E_0 are the energy loss of the pendulum with and without sample respectively, and S is the cross-section of the samples.

The fracture area of impacted samples was metalized with gold and observed with a scanning electron microscope (SEM) Jeol JSM 6400 (Tokyo, Japan).The kinetic triplet [pre-exponential factor, activation energy, and the kinetic model] of the curing was determined using integral isoconversional non-isothermal kinetic analysis, Kissinger-Akahira-Sunose equation, combined with the Coats-Redfern procedure. Details of the kinetic methodology are given in previous studies.[21]

Microhardness was measured with a Wilson Wolpert (Micro-Knoop 401MAV) device (Massachusetts, USA) following the ASTM D1474-98 (2008) standard procedure. For each material 10 determinations were made with a confidence level of 95%. The Knoop microhardness (HKN) was calculated from the following equation:

$$\mathrm{HKN} = \frac{L}{A_P} = \frac{L}{l^2 C_p} \qquad (2)$$

where L is the load applied to the indenter (0.025 kg), A_p is the projected area of indentation in mm^2, l is the measured length of long diagonal of indentation in mm, and C_p is the indenter constant (7.028×10^{-2}) relating l^2 to A_p. The values were obtained from 10 determinations with the calculated precision (95% of confidence level).

4.3. Results and discussion

4.3.1. Calorimetric study of the curing process and the thermosets obtained

In the preparation of epoxy thermosets, the selection of the curing agent is crucial to obtaining good thermoset properties but especially when a HBP modifier is added to the formulation, because of the role played by the chemistry of the curing agent in the possible reaction of the terminal groups in the HBP structure. A number of authors used primary amines as curing agents, which did not allow the covalent incorporation of hydroxyl terminated HBPs to the epoxy matrix and thus microphase separation in the final material could be observed.[22,23]

In the present study, the addition of a 5 or 10% in weight of HBP-OH and its derivatives with allyl and 10-undecenoyl chain ends should not react with dihydrazides and phase separation could also be expected. However, not only the chemistry of the terminal groups but also the structure of the HBP and the curing rate can influence the phase separation process.In a previous paper, we reported the study of the curing process of DGEBA with some dihydrazides and concluded that the stoichiometric proportion is 2 mol of DGEBA per each mol of dihydrazide. The structure of the network formed was confirmed by FTIR analysis and is represented in **Figure 2**.

The curing could be catalyzed by acidic and basic catalysts but the latent character was reduced, and therefore some effects on the curing evolution can be expected on adding HBP modifiers. We studied the curing process by non-isothermal scanning calorimetry. The calorimetric curves collected in **Figure 3** show the curing exotherms for all the formulations studied.

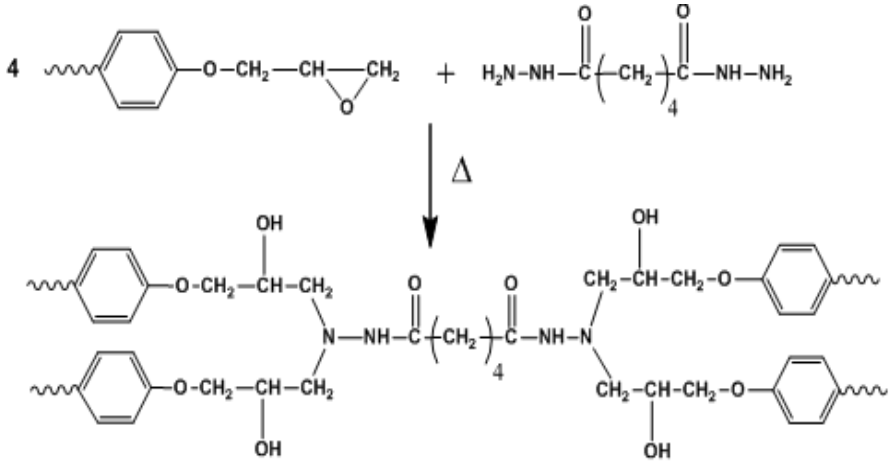

Figure 2. Structure of the network formed by reaction of the epoxy resin and the adipic dihydrazide.

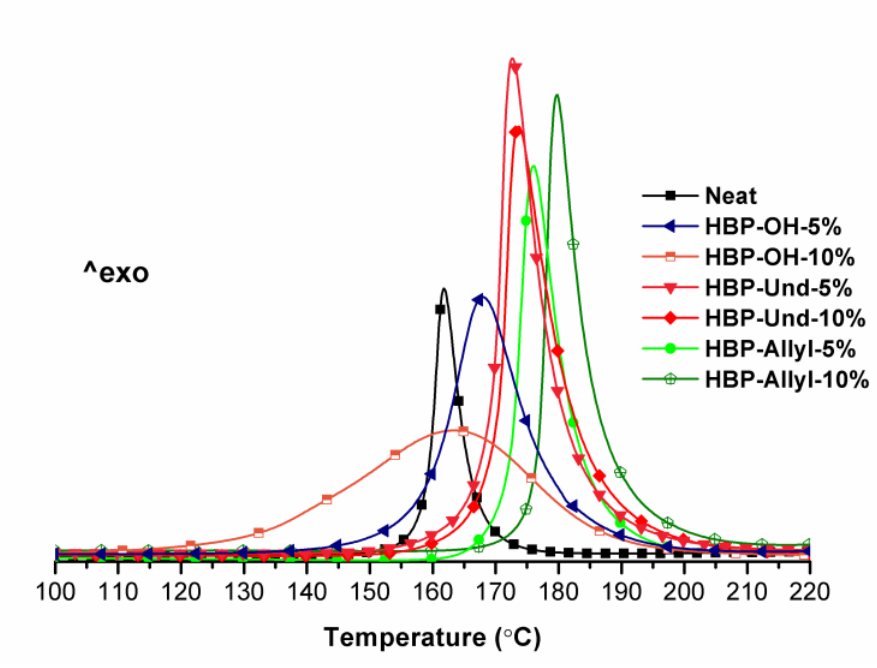

Figure 3. Calorimetric curves for the formulations studied obtained in DSC scans at 10ºC/min under N_2.

The plot of conversion against temperature for all the studied formulations is represented in **Figure 4** and the calorimetric data are collected in **Table 1**. In this plot, we can observe that the latent character of the curing of the neat formulation is slightly reduced on adding the HBP modifiers. The effect on the latency seems to be more noticeable on adding HBP-OH, which catalyzes the first stages of the curing process. However, a delay is observed at higher conversions. The catalytic effect is increased with the proportion of HBP-OH in the formulation. This can be explained by the presence of phenolic groups, which can facilitate the nucleophylic attack of the nitrogen on the epoxy ring by the formation of hydrogen bonds, as is described for epoxy-amine formulations.[24] Since during curing of epoxy resins with active NH_2 moieties OH groups are always formed, the effect of the phenolic groups of the HBP is not as noticeable when the conversion reaches a certain extent. Moreover, the viscosity of the reactive mixture increases and can delay the curing process. The addition of HBP-Und and HBP-Allyl leads to a significant reduction of the curing rate, and higher temperatures are needed to cure these formulations. However, there is not a clear dependence of the curing rate with the amount of modifier. In a previous study in epoxy-anhydride thermosets with both modified HBPs an acceleration of the curing was observed in spite of the higher viscosities of the formulations. This acceleration was attributed to the presence of carboxylic groups in the focal point of the HBPs, which can catalyze the curing process.[16] In the present case using dihydrazides, the dilution effect on adding the modifiers and the increase in the viscosity seem to greatly influence the curing rate in comparison to the acidic catalysis produced by carboxylic groups.[17]

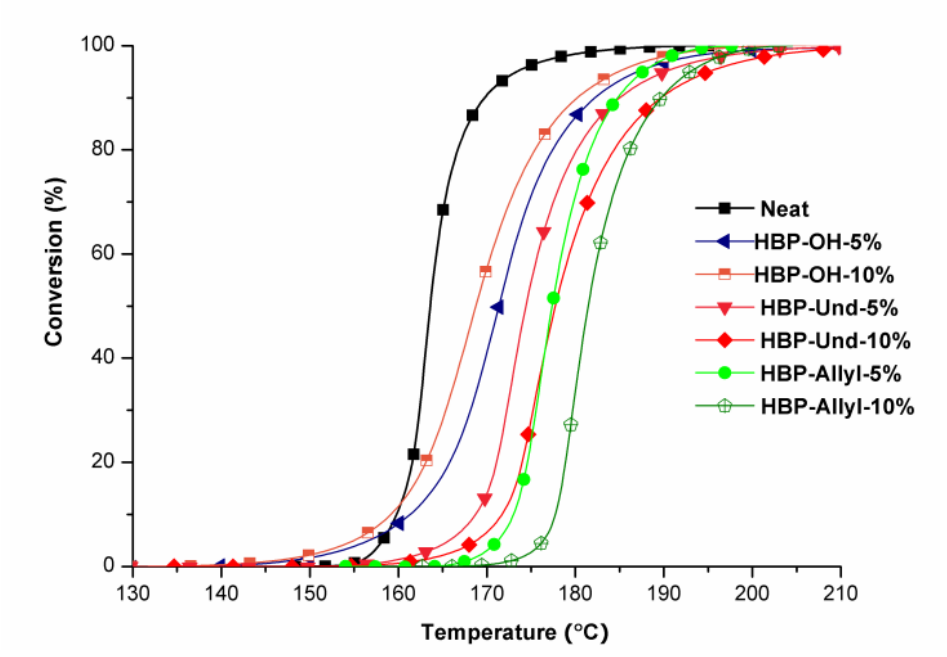

Figure 4. Conversion against temperature of the dynamic curing at 10ºC/min of all the formulations studied.

Table 1. Calorimetric data and kinetic parameters obtained in the curing of all the formulations

Thermoset	T_{max} [a] (°C)	Δh [b] (J/g)	Δh [b] (kJ/eq)	T_g [c] (°C)	T_{gFox} [d] (°C)	E_a [e] (kJ/mol)	ln$A$ [f] (s^{-1})	$k_{170°C}$ [j] (min^{-1})
Neat	165	408	96	128	128	170	49.2	21.3
HBP-OH-5%	170	352	90	130	128	114	33.0	7.1
HBP-OH-10%	167	331	89	138	127	99	29.0	7.3
HBP-Und-5%	172	355	91	127	121	117	33.4	5.0
HBP-Und-10%	176	327	88	123	113	117	33.1	4.5
HBP-Allyl-5%	180	273	70	123	125	161	45.3	4.7
HBP-Allyl-10%	177	285	78	128	121	127	35.7	3.0

a. Temperature of the maximum of the curing exotherm registered at 10°C/min.
b. Enthalpy of the curing exotherm registered at 10°C/min
c. T_g determined after curing in a dynamic scan registered at 20°C/min.
d. T_g calculated by the Fox equation
e. Values of activation energy at 50% of conversion, evaluated by the isoconversional non-isothermal procedure.
f. Pre-exponential factors calculated for autocatalytic model (n=2.1, m=0.9) with $g(\alpha)=\left[(1-\alpha)\alpha^{-1}\right]^{-0.9}(0.9)^{-1}$
g. Values of rate constants at 170°C using the Arrhenius equation at 50% conversion.

From the values in **Table 1** we can observe that the curing enthalpy of the formulations containing HBP modifiers is somewhat lower than that measured for the neat formulation, but in all cases the curing was complete, as identified by the complete disappearance of the band at 910 cm^{-1} in the FTIR of the final thermosets. It should be stressed that the T_g measured for the modified thermosets does not decrease significantly, and even increases in the case of adding HBP-OH to the formulation. If we consider the T_gs of the different hyperbranched T_g^{HBP} and the T_g of the neat material and apply these values and the corresponding proportions (w) in the Fox equation[25] we can predict the T_g values of the homogenously blended modified thermosets.

$$\frac{1}{T_g}=\frac{w}{T_g^{HBP}}+\frac{1-w}{T_g^{neat}} \qquad (3)$$

As can be seen in **Table 1**, only the thermoset with a 5% of Allyl-HBP has an experimental value of T_g similar to that predicted by this equation, whereas the addition of the other vinylic modified HBPs does not significantly influence the T_g determined for the neat material. This result can be explained by a phase separation of the HBPs due to the incompatibility produced during the curing reaction, which will be further confirmed by SEM.

Since the initial solution was fully compatible, the separation of the particles is originated by a reaction-induced phase separation process (RIPS), which is highly dependent on the kinetics of curing and on the dynamics of the phase separation process. It should be pointed out, that the same HBP-Allyl and HBP-Und were used as modifiers of DGEBA/anhydride thermosets, leading to completely homogeneous materials.[16]

The higher curing rate when dihydrazides are used as curing agents and the highly polar structure of the network produced with this agent could both be responsible for the phase separation process, since these HBPs cannot be chemically incorporated into the epoxy network and have non-polar characteristics, especially in case of HBP-Und, as a result of the presence of the long aliphatic chains. Thus, the addition of a 5% of HBP-Allyl to the formulation leads to a homogeneous material because of its higher compatibility, due to its shorter aliphatic structure. On adding HBP-OH to the formulation, the T_g of the final thermosets is even higher than that predicted by the Fox equation. This unexpected result in fully homogeneous materials can be rationalized by the reduction in free volume due to the hydrogen bonding established between the OH groups of HBP and the epoxy-dihydrazide network.[26]

In **Table 1**, the kinetic parameters calculated for the curing of the different formulations are collected. The kinetics of these systems was studied by the non-isothermal isoconversional procedure, as explained in the experimental part and in a previous article.[21] **Figure 5** shows the evolution of the activation energy against conversion for the formulations studied.

As is shown in the **Figure 5**, the activation energy remains, during curing, nearly constant for all formulations. This result suggests that the reaction mechanism is the same in the whole range of curing and only a single kinetic model is needed to describe the curing.

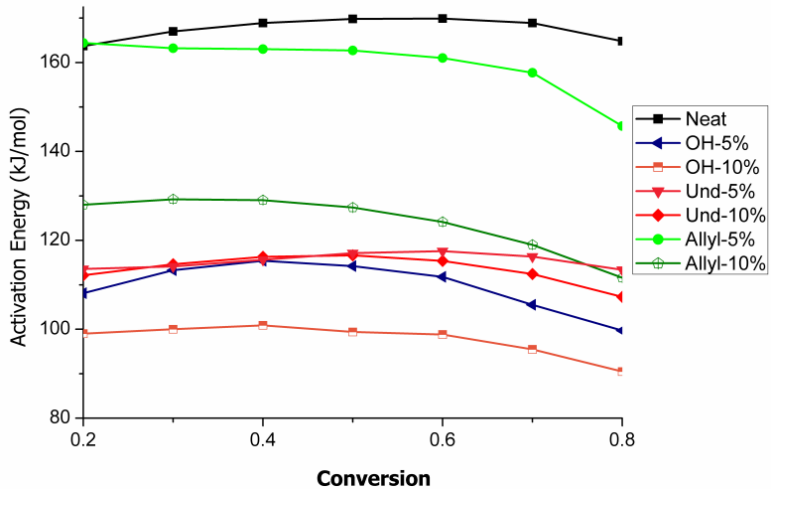

Figure 5. Apparent activation energies against conversion of all the formulations studied.

In many reaction processes the values of activation energy, due to the compensation effect between the activation energy and the pre-exponential factor,[27] do not reflect exactly the reaction rate and it is better to discuss the rate constants calculated using the Arrhenius equation and the aforementioned kinetic parameters. To calculate the frequency factors, we selected the kinetic model that best fits the experimental data, which for all formulations was the autocatalytic kinetic model with n=2.1 and m=0.9. This kinetic model is consistent with the accelerative effect of the hydroxyl groups generated during curing.

The calculated values of the rate constants (**Table 1**) illustrate the order of reactivity on curing at a conversion of 0.5 and agree with the experimental conversion-temperature curves. In this conversion, all the HBP modifiers show a delaying effect on the curing rate, as can be also observed in **Figure 4**. However, this effect is not produced at the beginning of curing in the case of the formulations containing HBP-OH, where hydroxyl terminal groups accelerate the curing.

4.3.2. Characterization of the materials by TGA and DMTA

Table 2 and **Figure 6** present the thermogravimetric data and the derivatives of the TGA curves, respectively.

Table 2. Thermogravimetric data for all the thermosets obtained

Thermoset	$T_{5\%}$ [a] (°C)	T_{max} [b] (°C)	Char Yield [c] (%)
Neat	287	337-390	12.2
HBP-OH-5%	292	344-407	13.2
HBP-OH-10%	290	352-398	14.1
HBP-Und-5%	293	355-404	14.5
HBP-Und-10%	291	356-402	14.6
HBP-Allyl-5%	297	360-400	13.7
HBP-Allyl-10%	296	350-410	13.8

a. Temperature of the 5% of weight loss in N_2 atmosphere
b. The temperature of the peaks of the derivative on the thermogram registered in N_2 atmosphere.
c. Char yield after a dynamic scan until 600 °C in N_2 atmosphere.

The thermosets obtained show a higher resistance to thermal degradation than the neat material, since the ester groups introduced are aromatic and therefore there is no *β*-elimination process that finally leads to the formation of little fragments that can be lost on heating. There is also no effect on the temperature of the maximum degradation rate, but the shape of the curves changes on modifying the materials. As we can see, all the degradation curves are bimodal, indicating two different degradative processes. In case of the neat material, the peak at lower temperature is more pronounced than the one occurring at higher temperature, whereas in case of the material containing a 10% of HBP-Und the contrary trend is observed. This can be related to the lower proportion of OH groups in the latter.

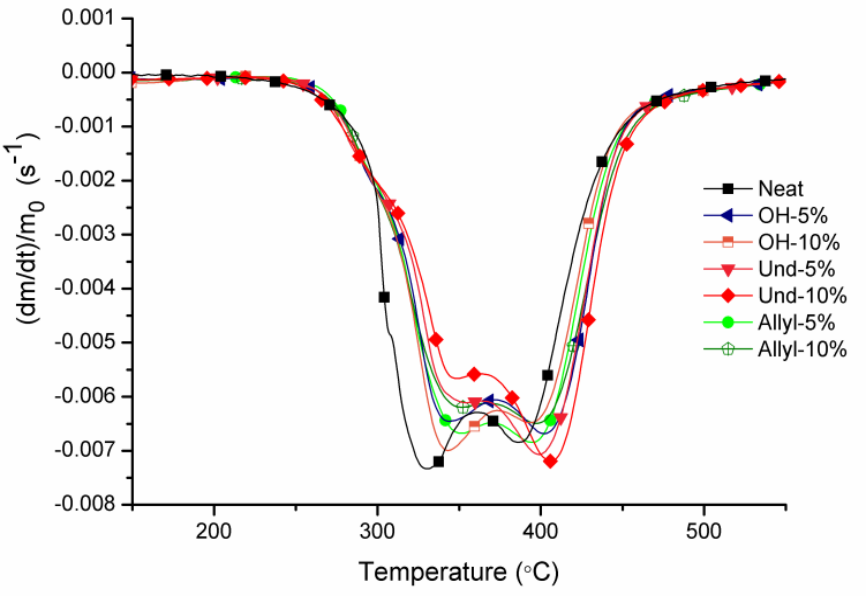

Figure 6. Derivatives of the TGA curves in N_2 atmosphere for the thermosets obtained.

Figures 7 and **8** show the curves of the storage modulus and tan *δ*, respectively, for all the thermosets prepared obtained by DMTA.

In **Figure 7** we can see that the modulus in the rubbery state is similar for the neat and HBP-OH formulations, which seems to indicate that the crosslinking density, either covalently or by hydrogen bonding, is quite similar. On the contrary, the presence of HBP-Ally and HBP-Und leads to a reduction of the modulus.

From **Figure 8**, it can be seen that the temperature of the maximum of the tan *δ* peak is quite similar for all the thermosets studied, but the values are higher than those obtained by DSC, because of the differences in the frequency applied in DMTA technique. It should be noted that the materials containing a 10% of HBP-Allyl or HBP-Und show a much broader curve indicating their lower homogeneity

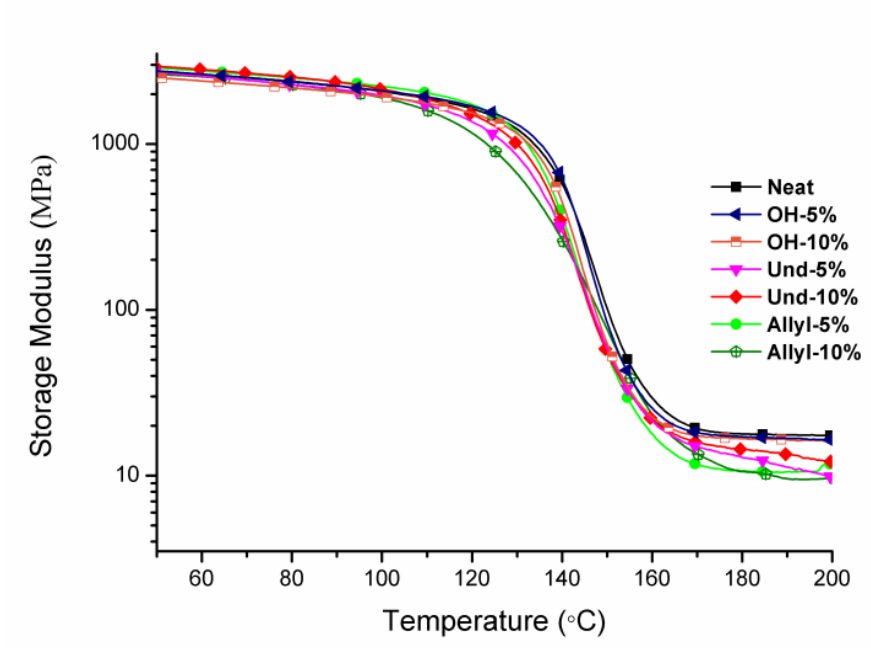

Figure 7. Evolution of storage modulus against temperature at 1 Hz for all the thermosets obtained.

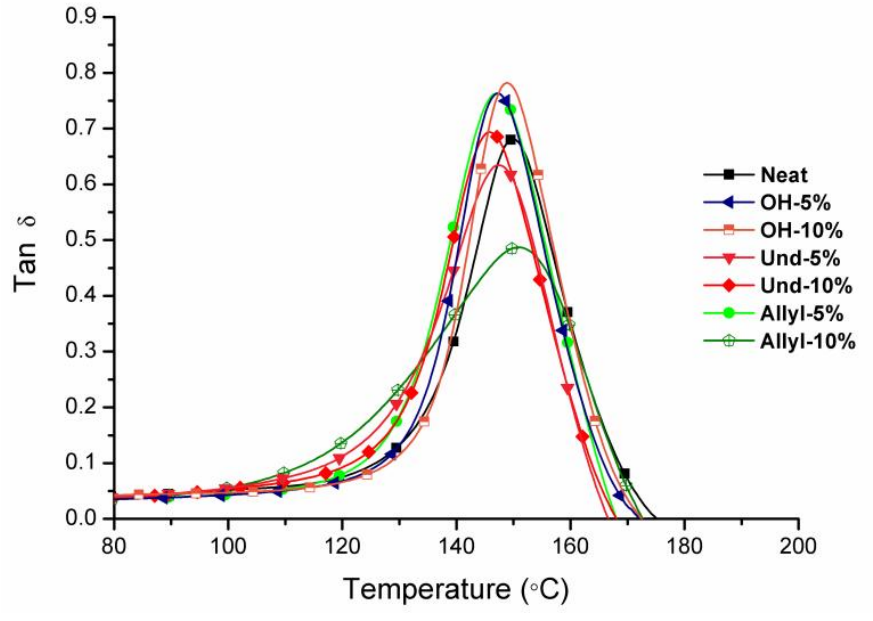

Figure 8. Evolution of tan *δ* against temperature at 1 Hz for all the thermosets obtained.

4.3.3. Mechanical and morphological characterization

Microhardness measurements are very useful in rating coatings on rigid substrates as a measure of the resistance that one body offers against penetration by another under static loads. These measurements were carried out with a Knoop microindenter and the results are shown in **Figure 9**.

As can be seen, the addition of all the HBP modifiers does not reduce this parameter but even increases it, which is advantageous in the performance of the coatings. The best formulation in terms of microhardness enhancement is the one containing a 10% of HBP-Allyl.

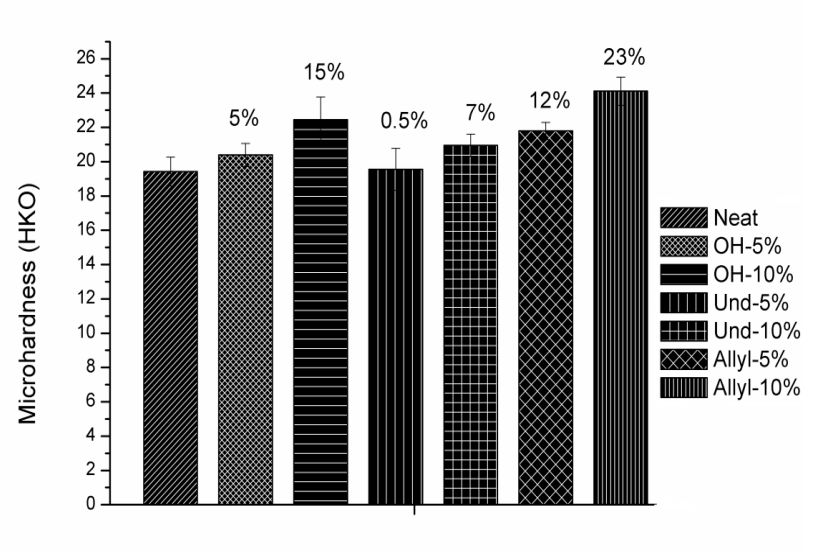

Figure 9. Microhardness values of the thermosets prepared. The increase in microhardness respect to the neat formulation is also indicated.

The results of the impact tests are collected in **Figure 10** for all the materials prepared. The values correspond to the energy absorbed by the material during crack propagation. It is possible to prove that the modification of DGEBA/AH thermosets with all the HBPs synthesized improves this value, as it was reported in previous publications on epoxy/amine or anhydride systems.[28]

As we can see, all the modified thermosets present a higher value than the neat material. The highest values were obtained with a 10% of HBP-Und or a 5% of HBP-Allyl. In reference to the impact strength values, it should be pointed out that the neat system is tougher than the DGEBA/MHHPA neat material studied in a previous publication (2.4 to 3.9 kJ/m^2).[16] This illustrates the important role of the curing agent in the characteristics of the thermosets. Moreover, the addition of HBP-Und and HBP-Allyl to DGEBA/dihydrazide materials results in a greater improvement of the toughness characteristics in comparison with DGEBA/MHHPA thermosets.

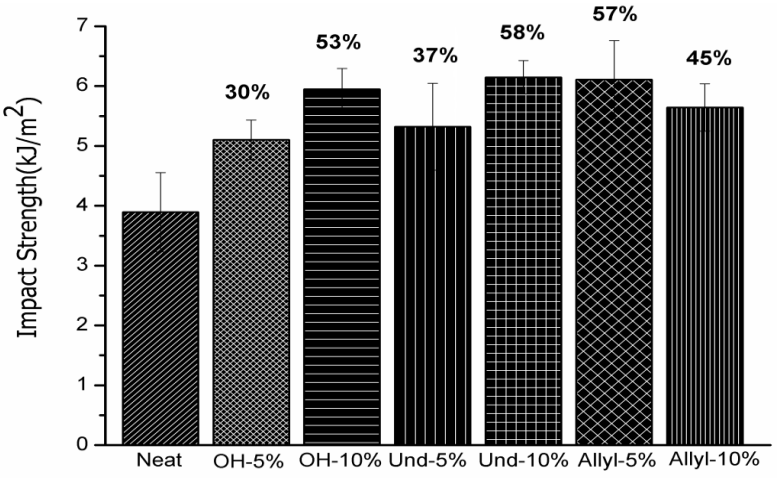

Figure 10. Impact strength values of the thermosets prepared.

The SEM micrographs of the impacted fracture surfaces are collected in **Figure 11**. These show a fracture surface with cracks and river-line structures in different planes in the neat material in accordance with the impact strength measured. In agreement with our earlier interpretations, on comparing the experimental T_gs which are higher than those predicted by the Fox equation, materials containing a 5 % of HBP-Und or a 10 % of both vinylic modifiers show a clear phase separation of the HBP from the epoxy matrix. Usually, particle phase separated materials have enhanced toughness characteristics.[5, 29] However, the thermoset containing a 10% of HBP-OH shows a notable improvement in impact strength, quite similar to phase separated materials, but it presents a homogeneous appearance with a patterned roughness. This type of morphology was previously observed by us in materials obtained with 1-methylimidazole, which cured very fast as is also the case here.[30]

The T_g measured for this thermoset does not indicate plasticization, related to ductility, that dictate its toughness characteristics.[31] However, the rougher surface appearance observed in the fractographs containing HBP-OH blends, suggests that the impact specimens experienced more plastic deformation during fracture in comparison with the unmodified epoxy network.

As we can see, materials with a 5 or a 10% in weight of HBP-Allyl show very different fracture morphologies. Whereas the first one, present a homogeneous appearance with unidirectional cracks, river-line structures and striations, the second present nanoparticles (of about 300 nm) distributed in the surface, which leads to high expanded cracks. In both materials containing HBP-Und a microphase separation is observed which stops or deflects the crack propagation. In both cases, the size of the particles has a broad distribution, and more particles with a bigger size (average about 1.5 μm) can be observed for the material containing a larger proportion of modifier.

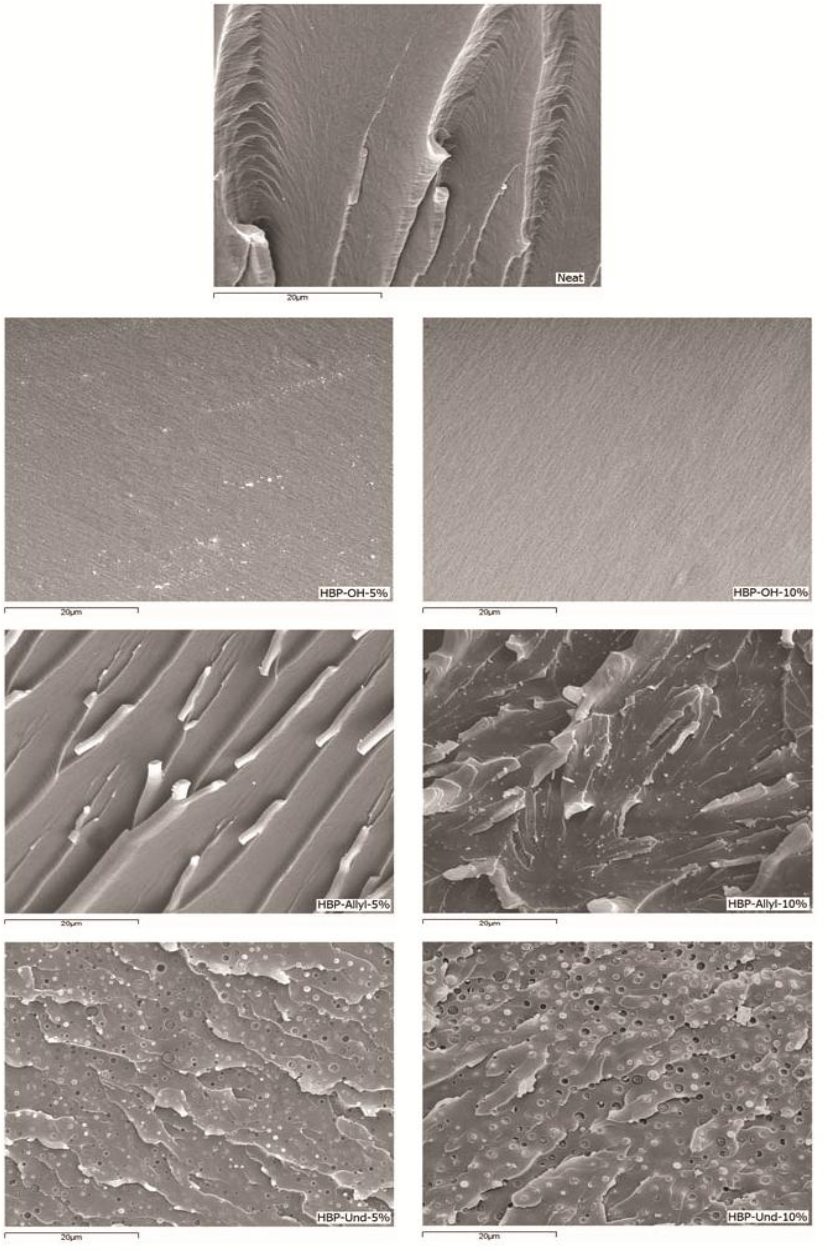

Figure 11. SEM micrographs from impacted fracture surfaces of the thermosets prepared at 2000 magnifications.

In **Figure 12**, a more detailed micrograph of the fracture surface for the material containing a 10 % of HBP-Und is shown. As we can see, when the crack reaches the particle, it terminates and the energy is dissipated around the particle of HBP. This indicates that there is no interfacial adhesion between epoxy network and HBP-Und as expected as a result of the loss of hydrogen bonding by derivatization of phenolic groups. Some authors reported that the improvement in the interfacial adhesion of epoxy resin and HBP particles contributes to an improvement of the facture behaviour of epoxy resin/HBP blends.[28] According to that argument, the nano/microphase separation reached in the present study does not very effectively enhance the toughness, as was expected. HBP-OH modifiers do not separate because of the compatibility with the epoxy matrix. However, the improvement in toughness is achieved in all the materials obtained in the present work without any decrease of T_g or deterioration of the thermal characteristics and microhardness without forgetting that the addition of HBPs helps to reach a good dispersion of the dihydrazide in the formulation.

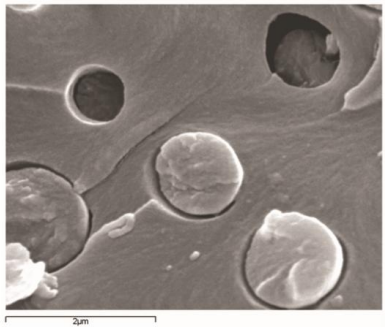

Figure 12. SEM micrograph of the impacted fracture surface for the thermoset containing a 10 % of HBP-Und at 20000 magnifications.

4.4. Conclusions

A series of HBPs with OH or vinyl groups of different length as chain ends were synthesized and used as modifiers in DGEBA/AH formulations. The addition of the HBPs helped to disperse and to compatibilize the crystalline dihydrazide in the reactive mixture.

The addition of HBP-OH to the formulation increased the curing rate at the beginning of the curing but decreased it at high conversion, and slightly reduced the latency of the adipic dihydrazide as DGEBA curing system. The addition of HBP-Allyl and HBP-Und led to a significant reduction of the curing rate and higher curing temperatures were needed to reach the complete curing of these formulations.

The T_g values of the modified thermosets were not significantly lower than that of the neat material and were even higher when HBP-OH was blended in the thermoset. This was attributed to the hydrogen bonding of the phenolic groups with the epoxy matrix. When 5% or 10% of HBP-Und or 10% of HBP-Allyl was incorporated into the material a nano or microphase separation was observed by SEM, which explains why no

reduction in the T_g was observed. The materials showed a higher resistance to thermal degradation on adding the modifiers.Microhardness and impact strength values were improved by adding all the HBP modifiers to the formulations.

Acknowledgements

The authors would like to thank MINECO (MAT2011-27039-C03-01, MAT2011-27039-C03-02) and Generalitat de Catalunya (2009-SGR-1512) for giving financial support. A.T. acknowledges the grant FI-DGR 2010 given by the Generalitat de Catalunya.

References

[1] May CA, ed. *Epoxy Resins. Chemistry and Technology*. 2nd ed. Marcel Dekker: New York; 1988.
[2] Petrie EM. *Epoxy Adhesive Formulations*. McGraw-Hill, New York; 2006.
[3] Zheng S. *Nanostructured Epoxies by the Use of Block Copolymers.* in *Epoxy Polymers. New Materials and Innovations*. Pascault JP, Williams RJJ, eds. Wiley-VCH: Weinheim, 81-108; 2010.
[4] Pearson RA, Yee AF. *Polymer* **34**: 3658-3670 (1993).
[5] Bagheri R, Marouf BT, Pearson RA. *J Macromol Sci Part C: Polymer Rev* **49**: 201-225 (2009).
[6] Ratna D, Varley R, Simon GP. *J Appl Polym Sci* **89**: 2339-2345 (2003).
[7] Boogh L, Pettersson B, Månson J-AE. *Polymer* **40**: 2249-2261 (1999).
[8] Mezzenga R, Boogh L, Månson J-AE. *Compos Sci Technol* **61**: 787-795 (2001).
[9] Morell M, Erber M, Ramis X, Ferrando F, Voit B, Serra A. *Eur Polym J* **46**: 1498-1509 (2010).
[10] Foix D, Khalyavina A, Morell M, Voit B, Lederer A, Ramis X, Serra A. *Macromol Mater Eng* **297**: 85-94 (2012).
[11] Emrick T, Chang H-T, Fréchet JMJ, Woods J, Baccei L. *Polym Bull* **45**: 1-7 (2000).
[12] Jannerfeldt G, Boogh L, Månson J-AE. *J Polym Sci Part B: Pol Phys* **37**: 2069-2077 (1999).
[13] Star A, Stoddart JF. *Macromolecules* **35**: 7516-7520 (2002).
[14] Kim YH, Webster OW. *Macromolecules* **25**: 5561-5572 (1992).
[15] Hong Y, Cooper-White JJ, Mackay ME, Hawker CJ, Malmström E, Rehnberg N. *J Rheol* **43**: 781-793 (1999).
[16] Tomuta AM, Ferrando F, Serra A, Ramis X. *React Funct Polym* **72**: 556-563 (2012).
[17] Tomuta AM, Ramis X, Ferrando F, Serra A. *Prog Org Coat* **74**: 59-65 (2012).
[18] Moore JS, Stupp SI. *Macromolecules* **23**: 65-70 (1990).
[19] Schallausky F, Erber M, Komber H, Lederer A. *Macromol Chem Phys* **209**: 2331-2338 (2008).
[20] Schmaljohann D, Komber H, Voit B. *Acta Polym* **50**: 196-204 (1999).
[21] Ramis X, Salla JM, Mas C, Mantecón A, Serra A. *J Appl Polym Sci* **92**: 381-393 (2004).
[22] Zhang J, Guo G, Fox B. *J Polym Sci Part B: Pol Phys* **48**: 417-424 (2010).
[23] Cicala G, Recca A, Restuccia C. *Polym Eng Sci* **45**: 225-237 (2005).
[24] Schechter L, Wynstra J, Kurkjy RE. *Ind Eng Chem* **48**: 94-97 (1956).
[25] Fox TG. *Bulletin American Physical Society*. **1**: 123 (1956).
[26] Abate L, Blanco I, Cicala G, Recca G, Scamporrino A. *Polym Eng Sci* **49**: 1477-1483 (2009).
[27] Vyazovkin S, Wight CA. *Annu Rev Phys Chem* **48**: 125-149 (1997).
[28] Xu G, Shi W, Gong M, Yu F, Feng J. *Polym Advan Technol* **15**: 639-644 (2004).
[29] Brooker RD, Kinloch AJ, Taylor AC. *J Adhesion* **86**: 726-741 (2010).
[30] Morell M, Ramis X, Ferrando F, Serra A. *Macromol Chem Phys* **213**: 335-343 (2012).
[31] Levita G, Petris SD, Marchetti A, Lazzeri A. *J Mater Sci* **26**: 2348-2352 (1991).

Chapter 5

Aromatic-aliphatic hyperbranched polyesters with vinylic end groups of different length as modifiers of epoxy/anhydride thermosets

Chapter 5 - Reactive & Functional Polymers 72(2012) 556-563

NEW AROMATIC-ALIPHATIC HYPERBRANCHED POLYESTERS WITH VINYLIC END GROUPS OF DIFFERENT LENGTH AS MODIFIERS OF EPOXY/ANHYDRIDE THERMOSETS

Adrian Tomuta,[a] Francesc Ferrando,[b] Àngels Serra,[a] Xavier Ramis[c]

[a]Department of Analytical and Organic Chemistry, Universitat Rovira i Virgili, Marcel·lí Domingo s/n, 43007 Tarragona, Spain

[b]Department of Mechanical Engineering, Universitat Rovira i Virgili, Països Catalans 26, 43007 Tarragona, Spain

[c]Laboratory of Thermodynamics, ETSEIB, Universitat Politècnica de Catalunya, Diagonal 647, 08028 Barcelona, Spain

Abstract

The synthesis and characterization of two new aromatic-aliphatic hyperbranched polyesters modified with long and short vinylic chains was reported. These hyperbranched polymers were used as toughening modifiers of epoxy/anhydride thermosets. The curing of mixtures of diglycidyl ether of bisphenol A and hexahydro-4-methylphtalic anhydride with different proportions of both hyperbranched polymers using *N,N*-benzyldimethylamine as catalyst was investigated by differential scanning calorimetry. The kinetic of curing process was established using an isoconversional pintegral procedure. The characterization of these materials was done by means of several thermal analysis techniques and their morphology was investigated by electron microscopy. The addition of highly branched structures led to homogeneous morphologies and a more toughening fracture of the thermosets in comparison to the neat epoxy/anhydride material. The modified thermosets presented slightly lower glass transition temperature than the unmodified one and the thermal stability barely changed by the addition of the modifiers.

Keywords: epoxy, anhydride, aromatic-aliphatic polyester, hyperbranched, toughness

5.1. Introduction

Epoxy thermosets present good overall properties, although they also present some drawbacks. In terms of structural applications, epoxy systems are in general rigid and brittle. While rigidity and strength are desired, brittleness reduces their applicability. As a result, considerable efforts have been made on improving the toughness of the materials during the past decades and many reviews in this area are available.[1,2]

There are many approaches to improve toughness in epoxy resins. One of the most classical is based on increasing the flexibility of the final network by decreasing the crosslinking density or the rigidity of the epoxy backbone. This procedure leads to thermosets with low glass transition temperature, Young's modulus and thermal stability. However, the most successful route towards toughness improvement is the incorporation

of a dispersed second phase that absorbs energy. Among the second phases used stand out rubbers, thermoplastics and hard inclusions such as silica, glass and beads.[3,4,5]

In the last years hyperbranched polymers (HBPs) and more recently other dendritic highly branched polymeric structures with a large number of chain ends have demonstrated to be very interesting epoxy toughners.[6] They have been found to give enhanced flexibilities and increased toughness to thermosets without affecting other properties, such as hardness, modulus and glass transition temperature.[7] Improved toughness is due to local inhomogeneities in the crosslinked network caused by the chemical or physical incorporation of HBP molecules into the matrix or to the formation of phase separated nanoparticles with good interfacial adhesion between the separated phases.[8] It has also been described that toughness improvement can be reached through an *in situ* homogeneous reinforcing and toughening mechanism. The compatibilization between the modifier and the matrix through different physical chemical interactions may be the responsible of this mechanism.[9]

In previous works, we studied the curing of different mixtures of epoxy matrices and HBPs or star polymers.[10,11]The composition of the mixtures, the curing conditions, the curing agent used and the structure and chemical composition of the dendritic polymers (molecular weight, degree of branching, amount and type of terminal groups, length of the arms) are the parameters that control the structure of the network formed, the curing evolution and the final properties. In terms of improvement of toughness we achieved the best results when the modifier was initially miscible in the precursor and phase-separated during curing.[12] Phase-separated materials were obtained with unreactive modifier or when the modifier had only a small amount of residual reactive groups that enhanced the compatibility between the phases by the formation of an interphase.[13] Although to a lesser extent, we obtained improvements in toughness with systems that did not phase separate because of a high physical compatibility between the modifier and the matrix or because of the modifier was chemically incorporated into the network structure.[10,11,14,15]

The thermal stability and the glass transition temperature of the epoxy thermosets was not compromised by the addition of aliphatic-aromatic hyperbranched polyester hydroxyl terminated as reactive modifier, when $Yb(OTf)_3$ was selected as cationic initiator.[16] Although morphology was not studied in this work, it was expected that the materials were homogeneous without phase-separation due to the presence of hydroxyl chain-ends in the HBP that allows the modifier to be covalently linked to the epoxy matrix. In another study, commercial Boltorn H30 was esterified with long aliphatic chains having vinyl or epoxy terminal groups and used as toughness modifier of epoxy thermosets with the same curing system.[13] Whereas epoxy terminated HBP reached a completely miscible and homogeneous network, vinyl terminated HBP showed a limited solubility in the epoxy matrix and phase separated during curing. Taking into account these previous results, the aim of the present work is the synthesis of two new dendritic structures that combine the characteristics of the previously described HBPs.

The novel HBPs are formed by an aliphatic-aromatic hyperbranched polyester core and a shell with aliphatic chains of different lengths (the longest, 10-undecenoyl moieties and the shortest, allyl groups). It should be noticed that the modification with allyl groups is quite easy because allyl bromide experiments nucleophylic attack by phenolate groups of the HBP, formed in a weak basic medium. The acylation with 10-undecenoyl chloride follows a typical acylation procedure, and also takes place with a high yield. The modification of the HBP with aliphatic chains of different length can influence the final morphology and mechanical characteristics of the HBP.

Another purpose of this study is to show the effect of these novels HBPs on the curing of epoxy/anhydride systems, the kinetics of the curing process, the dynamomechanical properties, the impact behaviour and the morphology of the resulting materials. **Scheme 1** depicts the structure of the HBPs used as modifiers (HBP-Allyl and HBP-Und, with allyl and undecenoyl chains respectively).

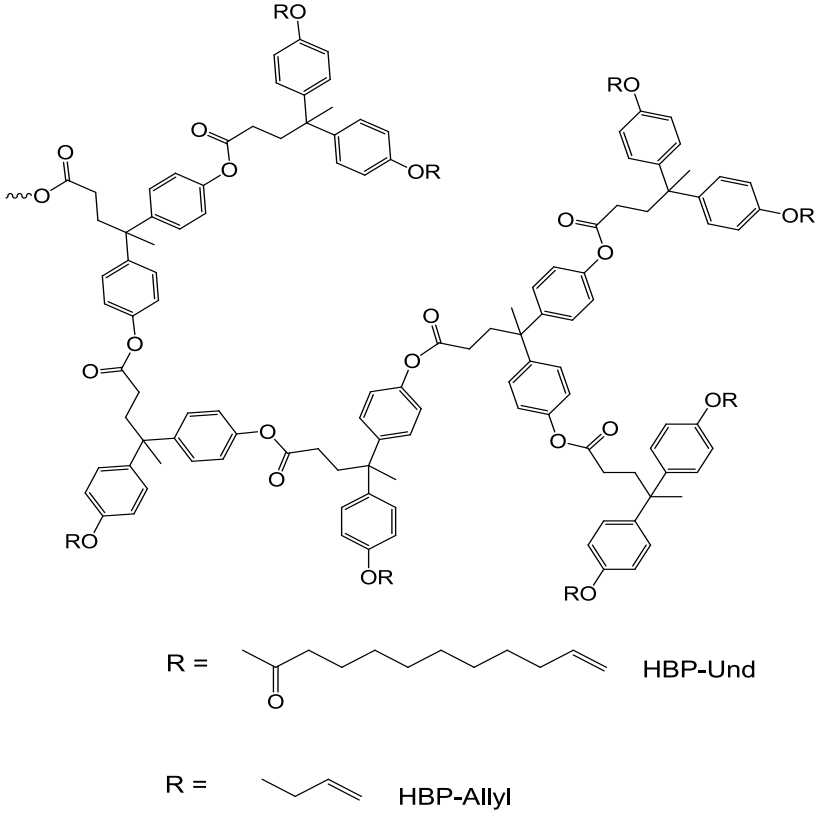

Scheme 1. Chemical structure of HBP-Und and HBP-Allyl.

5.2. Experimental

5.2.1. Materials

4,4-Bis(4-hydroxyphenyl) valeric acid, *N,N'*-dicyclohexylcarbodiimide (DCC), triethyl amine, allyl bromide, 10-undecenoyl chloride, hexahydro-4-methylphtalic anhydride (MHHPA) and *N,N*-dimethylbenzylamine (BDMA) were purchased from Aldrich and used without further purification. Diglycidyl ether of Bisphenol A (DGEBA) Epikote Resin 828 was provided by Shell Chemicals with an epoxy equivalent of 184 g/eq and was dried in vacuum before use. Methanol, N,N-dimethylformamide (DMF) and tetrahydrofurane (THF) were purchased from Scharlab and purified by standard procedures. 4-(N,N-dimethylamino) pyridinium p-toluenesulfonate (DPTS) was prepared as described in the literature.[17]

5.2.2. Hyperbranched polyester synthesis (HBP-OH*)*

The HBP-OH was synthesized according to a previously described procedure.[18] In a 500 ml two-necked round-bottomed flask, 50 g (1 eq) of 4,4-bis(4-hydroxyphenyl) valeric acid and 7.64 g (0.2 eq) of DPTS were dissolved in 200 mL of anhydrous DMF. Then, 43.24 g (1.2 eq) of DCC were added in portions and the mixture was kept under argon atmosphere for 24 hours at room temperature. Then, the precipitate was filtered off and the solution was poured in methanol (1200 mL) to obtain a white powder after drying in a vacuum oven overnight at 60ºC. Yield 37 g (conversion: 80%).

The ^{1}H and ^{13}C NMR data are in accordance with those published.[19]

Mn: 8700 g/mol, Mw: 12300 g/mol. T_g 121ºC (by DSC).

The amount of hydroxyl groups was determined according to ISO 2554-1997 standards.

An acetylating solution was prepared by dissolving 11.8 mL of acetic anhydride in 100 mL of pyridine. About 0.4–0.6 g of the polymer sample was dissolved in 5 mL of the acetylating solution. The mixture was stirred for 20 min at 130 °C.

Thereafter, at the same temperature, 8mL of water was added in order to hydrolyze the excess acetic anhydride. Finally, the solution was titrated with 1N ethanolic KOH solution to determine the equivalence point. An analogous ‘‘blank experiment’’ was performed without the polymer sample with exactly the same amount of the acetylating mixture. The hydroxyl number (HN) was calculated from the results of both titrations using the formula:

$$HN = \frac{(V_0 - V_1) \cdot C \cdot M_{KOH}}{m} + AN \qquad (1)$$

where V_0 and V_1 are the equivalence titration volume of KOH in mL from the blank experiment and from the sample titration, respectively, C is the concentration of KOH in

eq/L, M_{KOH} is the molecular weight of KOH in g/mol, m is the mass of polymer sample in grams and *AN* is the acid number, which has not been taken into account in this case because it is very low. The number of hydroxyl groups per molecule found by titration was 36.

5.2.3. HBP-Undecenoyl synthesis (HBP-Und)

In a 500 mL three-necked round bottomed flask 10 g (0.04 mol of hydroxyl groups) of HBP-OH were placed and dissolved in 200 mL of THF and 15 mL (0.08 mol) of triethylamine were added. Under gentle magnetic stirring, 12 mL (0.06 mol) of 10-undecenoyl chloride were slowly added using a dropping funnel. The reaction was kept at room temperature for 48 h under argon atmosphere. Then, the precipitate was filtered off and the solution was precipitated twice into methanol. The product was dried in a vacuum oven at 50 °C overnight and a pale brown viscous liquid was obtained. Yield: 94%. T_g 18ºC (by DSC).

^{1}H NMR (400 MHz, $CDCl_3$), δ (ppm): 1.26 m ($-CH_2-$); 1.41 m ($-CH_3$); 1.68 m ($-CH_2-$); 2.06 m ($-CH_2-$); 2.34 m ($-CH_2-$); 2.55 m ($-CH_2-$); 5.10 dd ($CH_2=$); 5.87 m (=CH-); 7.11 m (CH ar).

^{13}C NMR (100.6 MHz, $CDCl_3$), δ (ppm): 24.7; 27.6; 28.9; 33.6; 34.3; 36.2; 45.4; 113.9; 121.2; 128.2; 139.0; 145.6; 148.6;172.3.

5.2.4. HBP-Allyl synthesis (HBP-Allyl)

In a 500 mL two-necked round bottomed flask 10 g of HBP-OH (0.04 mol of hydroxyl groups) were dissolved in 100 mL of THF and 100 mL of acetone. Then, 15 g of fine powdered K_2CO_3 (0.10 mol) were added to the flask and 10 mL (0.10 mol) of allyl bromide were added drop by drop under stirring.

The reaction was kept at reflux for 12 hours at 83º C. The product was filtered off and the solvent was evaporated. The product was dissolved in 25 mL of THF and precipitated in water. Finally, the polymer was dried in a vacuum oven at 50 °C overnight and a white powder was obtained. Yield: 90%. Tg 81ºC (by DSC).

^{1}H NMR (400 MHz, $CDCl_3$), δ (ppm): 1.65 s ($-CH_3-$); 2.36 m ($-CH_2-$); 2.53 ($-CH_2-$); 4.53 s ($-CH_2-$); 5.35 dd ($CH_2=$); 6.07 m (=CH-); 6.8-7.2 m (CH ar).

^{13}C NMR (100.6 MHz, $CDCl_3$), δ (ppm): 24.7; 30.6; 36.6; 45.1; 69.0; 114.5; 117.9; 121.3; 128.4; 138.6; 141.2; 148.8; 156.9; 172.5.

5.2.5. Preparation of the curing mixtures

The DGEBA/MHHPA formulations were prepared by adding the appropriate amounts of each reactant and catalyst to a vial and homogenizing them by mechanical stirring. For the preparation of the formulations with HBP-Und and HBP-Allyl, appropriate amounts of DGEBA and HBP were heated up to 150 ºC with a thermal gun and the mixture was homogenized by mechanical stirring; after cooling down, anhydride was added and the resulting mixture was homogenized. Finally, the adequate proportion of catalyst was added and the mixture was homogenized again. For all formulations, the

amount of catalyst was 1 phr (parts per hundred grams) with respect to the anhydride. **Table 1** shows the notation and composition of the different formulations studied.

Table 1. Composition and notation of the formulations studied in this work with different percentage of HBP (indicate in the first column) in equivalent ratio X_{eq} and by total weight percentage (wt.%) of the mixture.

Formulation	Notation	DGEBA		MTHPA		BDMA	
		X_{eq}	(Wt.%)	X_{eq}	(Wt.%)	X_{eq}	(Wt.%)
DGEBA/MTHPA	Neat	1.00	52.0	1.00	48.0	0.0065	0.53
DGEBA/MTHPA/Allyl-5%	Allyl-5%	0.95	49.4	0.95	45.6	0.0061	0.50
DGEBA/MTHPA/Allyl-10%	Allyl-10%	0.90	46.8	0.90	43.2	0.0061	0.50
DGEBA/MTHPA/Und-5%	Und-5%	0.95	49.4	0.95	45.6	0.0061	0.50
DGEBA/MTHPA/Und-10%	Und-10%	0.90	46.8	0.90	43.2	0.0061	0.50

5.2.6. Measurements

The 400 MHz ^{1}H-NMR and 100.6 MHz ^{13}C-NMR spectra were obtained with a Varian Gemini 400 spectrometer with Fourier Transformed. ^{1}H-NMR spectra were acquired in 1 min and 16 scans with a 1.0 s relaxation delay (D1). ^{13}C NMR spectra were obtained using a D1 of 0.5 s and an acquisition time of 0.2 s. A total of 500 accumulations were recorded. $CDCl_3$ was used as a solvent and tetramethylsilane (TMS) as internal standard.

Calorimetric analyses were carried out on a Mettler DSC-821e calorimeter. Samples of approximately 10 mg in weight were cured in aluminium pans in a nitrogen atmosphere. Non-isothermal experiments were performed from 0 to 225 ºC at heating rates of 2, 5, 10, and 15 ºC/min to determine the reaction heat and the kinetic parameters. In the non-isothermal curing process, the degree of conversion at a given temperature T was calculated as the quotient between the heat released up to T and the total reaction heat associated with the complete conversion of all reactive groups. The T_gs of the cured materials were determined with a second scan at 20 ºC/min after dynamic curing by the mid-point method and the error is estimated to be approximately ±1°C. The T_gs of the pure HBPs were determined by a similar procedure.

Dynamic mechanical thermal analysis (DMTA) was carried out with a TA Instruments DMTA 2980 analyzer. The samples were cured isothermally in a mould at 120 ºC for 2 hours and then postcured at 150ºC for 2 hours. Before the samples were prepared, they were degassed in a vacuum oven at 50ºC for 3 h. Single cantilever bending at 1 Hz was performed at 3ºC/min from 30 to 220ºC on prismatic rectangular samples (1.5 x 20 x 5 mm^3).

Thermogravimetric analysis was carried out with a Mettler-Toledo TGA/SDTA 851e thermobalance. Cured samples with an approximate mass of 5 mg were heated from 30 to 800ºC at a heating rate of 10 ºC/min in a nitrogen atmosphere.

Impact tests were performed at room temperature by means of a Zwick 5110 impact tester according to ASTM D 4508-05 (2008) using rectangular samples (25 x 12 x 2.5 mm^3). The pendulum employed had a kinetic energy of 1 J. For each material, 9 determinations were made. The impact strength (IS) was calculated from the energy absorbed by the sample upon fracture as:

$$IS = \frac{E - E_0}{S} \qquad (2)$$

where E and E_0 are the energy loss of the pendulum with and without sample respectively, and S is the cross-section of the samples.

The fracture area of impacted samples was metalized with gold and observed with a scanning electron microscope (SEM) Jeol JSM 6400.

The kinetic triplet [pre-exponential factor, activation energy, and the kinetic model] of the curing was determined using integral isoconversional non-isothermal kinetic analysis, Kissinger-Akahira-Sunose equation, combined with the Coats-Redfern procedure. Details of the kinetic methodology are given in previous studies.[20]

5.3. Results and discussion

The hyperbranched structures used as modifiers in the present work were synthesized by an easy modification procedure from a pre-formed phenol-ended hyperbranched polymer. The synthetic way is represented in **Scheme 2**. The preparation of the HBP-OH from an AB_2 monomer had been previously reported.[18] The presence of phenol terminal groups allows the modification reaction by esterification with 10-undecenoyl chloride, following the similar procedure we used in the modification of Boltorn type hyperbranched polyesters.[13]

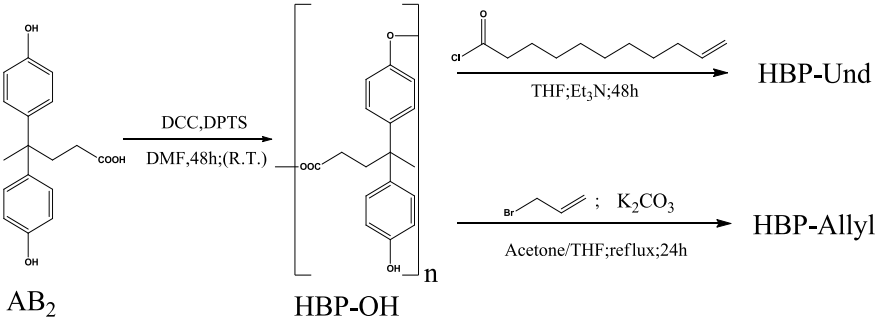

Scheme 2. Synthetic route to HBP-Und and HBP-Allyl**.**

The characterization of the esterified HBP has been carried out by NMR spectroscopy. **Figure 1** shows the ^{1}H-NMR spectrum of HBP-Und with the corresponding assignments. Alternatively, the acid character of the phenol leads to phenolate end-groups in the presence of a weak base, which can act as nucleophiles in front of allyl bromide giving the corresponding ether. In this way, short vinylic chains can be introduced. **Figure 2** shows the assigned ^{1}H-NMR spectrum of HBP-Allyl. Both reactions take place quantitatively. This has been confirmed by the complete disappearance of the aromatic signals of the spectrum of HBP-OH as it is shown in **Figure 3**. The complete conversion of phenolic groups to unreactive vinylic units was planned to avoid the chemical linkage of the HBP modifier to the epoxy matrix, which can be originated by reaction with the curing agent selected. In the present study hexahydro-4-methylphthalic anhydride (MHHPA) catalyzed by benzyldimethylamine (BDMA) has been the curing system employed.

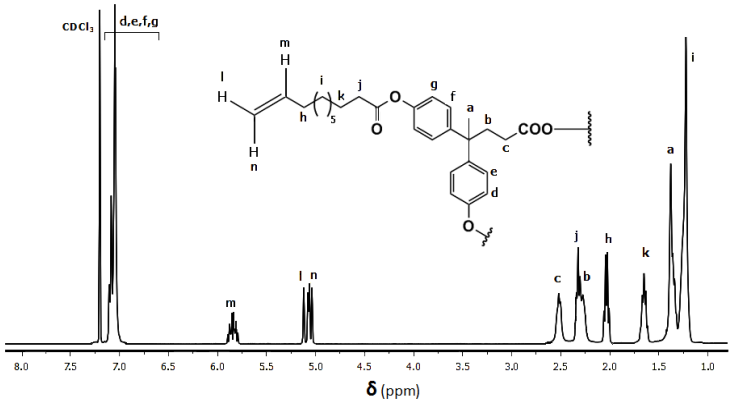

Figure 1. ^{1}H NMR spectra of HBP-Und in $CDCl_3$

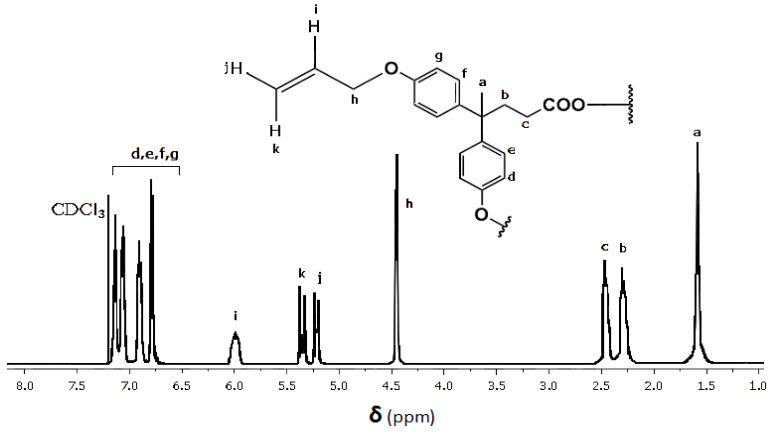

Figure 2. ^{1}H NMR spectra of HBP-Allyl in $CDCl_3$

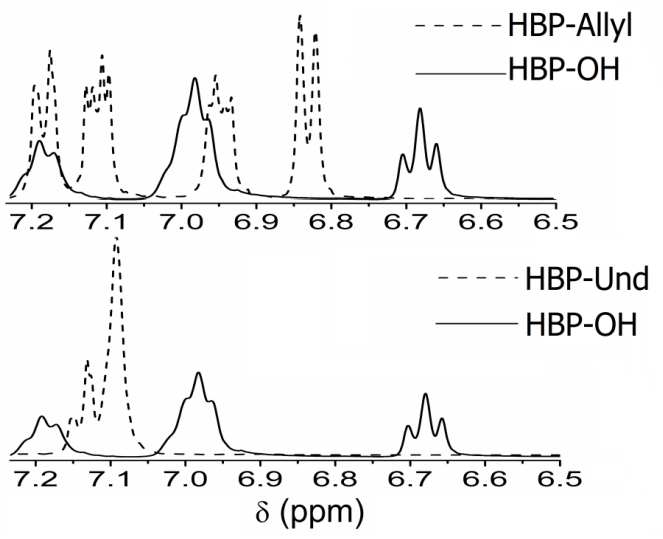

Figure 3. Aromatic region of de ^{1}H NMR spectra of HBP-OH, HBP-Und and HBP-Allyl in $CDCl_3$.

In absence of hydroxyl groups the reaction of DGEBA with anhydrides is slow and needs a catalyst to initiate the curing process at moderate temperatures. In this work we used BDMA since we obtained good curing conditions in a previous work.[10] In the presence of a tertiary amine, the following ideal reaction mechanism takes place:[21] a) alkoxide formation by nucleophilic attack of the tertiary amine to the epoxy ring, b) propagation of this alkoxide anion by anionic polyesterification with anhydride giving rise a carboxylate and c) propagation of the carboxylate anion formed by attack to another epoxy leading to a new alkoxide. Although, it is generally accepted that the propagation of epoxy-anhydride formulations catalyzed by tertiary amines follows an alternating mechanism, some side reactions such as the attack of carboxylate formed to an anhydride group, can lead to inhomogeneous networks due to non-alternating mechanism.[22]

The curing of DGEBA/MHHPA with different amounts of HBP-Und and HBP-Allyl using 1 phr of BDMA as initiator was studied to obtain new thermosets with enhanced toughness. **Table 2** collects the main features and the kinetic parameters of the curing process. The similarity between enthalpies per epoxy equivalent and the reported for other epoxy systems indicates that epoxides have reacted almost completely.[23]

FTIR spectra of cured samples showed that the absorbance bands at 915 cm^{-1} and at 1860-1780 cm^{-1}, due to the oxirane and anhydride group respectively, disappeared completely, which accounts for a complete reaction during curing.

Figure 4 shows the DSC conversion degree against temperature recorded at 10 ºC/min for all formulations studied. It can be observed that all modifiers produce a significant accelerative effect in all stages of the curing. Although it is not clear how this effect is originated, since HBP slightly increases the viscosity of the reactive mixture and reduces the concentration of reactive groups, the combination of some effects could explain this experimental behaviour. The existence of residual carboxylic acid as the focal point of the HBP, which is expected by the condensation reaction of 4,4-bis(4-hydroxylphenyl)valeric acid used as AB_2 monomer can accelerate the curing in two ways: 1) acidic groups can initiate the polycondensation mechanism in the same way as hydroxyl groups and b) carboxylic acids can act as epoxy resin hardener. In this complex mechanism the crosslinking process is accompanied with the regeneration of the tertiary amine, which can restart a new growing chain, reducing the crosslink density and accelerating the curing.[24] On the other hand, the viscosity of the mixture can also contribute to the final reaction rate. The low viscosity of the neat formulation allows the acid-base transfer reaction between the quaternary ammonium salts and the alkoxides and carboxylates of the long growing chain, leading to inactive chains. On the contrary the addition of HBPs to the curing mixture increases the viscosity and reduces the mobility of the long growing chains, avoiding the transfer reactions previously described.

Table 2. Calorimetric,kinetic and DMTA data of the formulations studied in this work.

Thermoset	T_{max} [a] (°C)	Δh [b] (J/g)	Δh [b] (kJ/eq)	T_g [c] (°C)	$T_{g,Fox}$ [d] (°C)	$T_{g,tan\delta}$ (°C)	E_a [e] (kJ/mol)	ln$A$ [f] (s^{-1})	$k_{150ºC}$ [g] (min^{-1})
Neat	159.3	293.4	105	142	142	150	86.9	23.9	0.4955
Allyl-5%	142.4	283.7	102	135	138	120	77.6	21.9	0.9401
Allyl-10%	143.8	288.6	103	132	135	115	76.8	21.6	0.9091
Und-5%	147.5	273.2	98	133	133	116	75.7	21.1	0.6880
Und-10%	146.8	267.1	96	127	125	110	76.2	21.3	0.7326

a. Temperature of the maximum of the curing exotherm registered at 10°C/min.
b. Enthalpy of the curing exotherm registered at 10°C/min.
c. T_g determined after curing in a dynamic scan registered at 20°C/min.
d. T_g predicted using the Fox equation.
e. Values of activation energy at 50% of conversion, evaluated by the isoconversional non-isotermal procedure.
f. Pre-exponential factor calculated for the n=0.5; m=1.5 kinetic model with $g(\alpha)=[(1-\alpha)\alpha^{-1})]^{-0.5}(0.5)^{-1}$.
g. Values of rate constant at 150°C using the Arrhenius equation at 50% conversion.

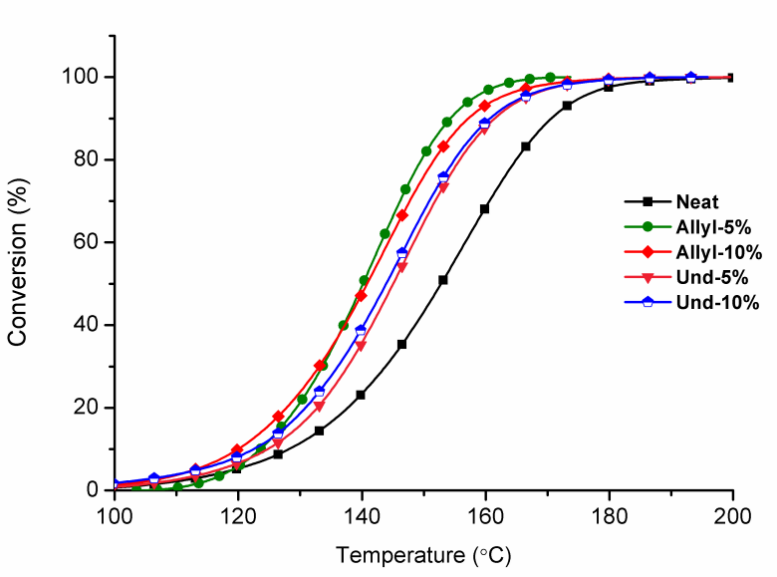

Figure 4. Conversion against temperature of the dynamic curing at 10 ºC/min of the formulations studied in this work.

Due to the complexity of the curing process the kinetics was studied by the non-isothermal integral isoconversional procedure. **Figure 5** shows the evolution of the activation energy during curing for all the formulations studied. In general, the values of activation energy approximately agree with conversions curves shown in **Figure 4.** Neat formulation has a higher activation energy than HBP-formulations, according to the accelerative effect that exert the modifier. Moreover neat formulation presents a constant value of activation energy in all range of conversion, whereas in formulations containing HBP the activation energy is higher at the first stages of the curing process and then diminishes slightly.

These variations on the activation energy values suggest a more complex curing process when HBP is added. In many reaction processes the values of activation energy, due to the compensation effect between the activation energy and the pre-exponential factor,[25] do not reflect exactly the reaction rate and it is better to discuss the rate constants calculated using the Arrhenius equation and the aforementioned kinetic parameters. The calculated values of rate constants (**Table 2**) demonstrate the accelerative effect of HBPs, according to the calorimetric data (**Figure 4**). Concretely, HBP-Ally accelerates in a higher extent than HBP-Und, probably due to the different viscosity of the mixtures and to the different proportion of residual carboxylic acid of the focal point of the HBP.

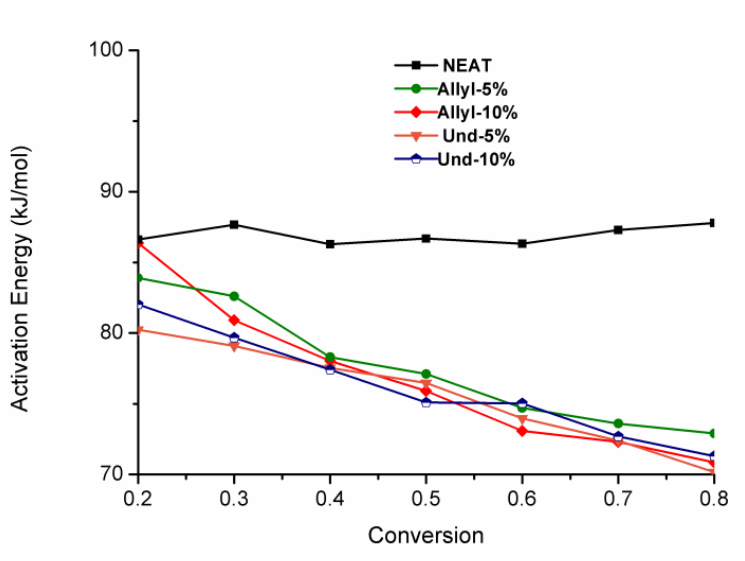

Figure 5. Apparent activation energy against conversion of the formulations studied in this work.

The T_g of the cured systems was determined using DSC and DMTA (**Table 2**). The presence of HBP-Und and HBP-Allyl leads to a progressive decrease in T_g with increasing modifier content. No relaxation at lower temperature was observed for HBP-Und and HBP-Allyl formulations. This result indicates that both modifiers do not induce phase separation during curing, and consequently a homogeneous microstructure is expected, as it will be able to see by microscopy. In **Table 2** we can also see how materials containing HBP-Allyl present slightly higher values of T_g than those containing HBP-Und. In order to understand the effect of HBP-Und and HBP-Allyl on the matrix, the Fox equation was used to predict the T_g of the cured materials considering a mixture of neat DGEBA/MTHPA network and pure HBP-Und or HBP-Allyl:

$$\frac{1}{T_g} = \frac{w}{T_{g,HBP}} + \frac{1-w}{T_{g,DGEBA/MTHPA}} \qquad (3)$$

where $T_{g,HBP}$ is the glass transition of the neat HBP, 18ºC for HBP-Und and 81ºC for HBP-Allyl, $T_{g,DGEBA/MTHPA}$ is the glass transition of the neat DGEBA/MTHPA and w is the weight fraction of the HBP in the formulation. If we compare the T_g values determined experimentally with those calculated by the Fox equation we can observe that HBP-Allyl estimated values are higher than the experimental ones, while the calculated for HBP-Und formulations fit quite well the experimental data.

It can therefore be deduced that while HBP-Und and DGEBA/MHHPA form a single homogeneous network, some part of HPB-Allyl, unappreciated by SEM, can form a separated phase or that this modifier changes the crosslink density of the DGEBA/MHHPA network. The regeneration of the catalyst or the amount the acid-base transfer reaction to form inactive chain when allyl-modifier is used, may explain this behaviour.

Table 2 and **Figure 6** show the results obtained by DMTA. It can be seen how $T_{g,tan\delta}$ shows similar trend than calorimetric glass transition, although the values are a little different. These differences should be attributed to the different curing schedule of DSC and DMTA samples and to the frequency applied in DMTA technique. As the proportion of HBP increases, the maximum of the tan δ-temperature curves moves toward smaller temperature. This effect is consistent with the lower value of T_g revealed by DSC and the possible flexibilizing effect, although in a different extent, of both HBPs. As we said above, no relaxation is observed at 18ºC or 81ºC related with a second phase. **Figure 6** shows unimodal and symmetrical relaxation curves for all the materials prepared, which can be associated to a relatively homogeneous structure.

Tan δ value at the maximum and the area under the loss tanδ curve slightly decrease when HBP is added and when the amount of HBP is increased. This result would be in agreement with a higher crosslinking density and lower damping properties in formulations with HBP and apparently in disagreement with the plasticizing effect expected. The antiplasticization effect, described by several authors,[26, 27] as a consequence of both changes of the network structure and incorporation of miscible additives, may explain the dynamomechanical behaviour. When a plasticization takes place, α-transition (glass transition temperature) decreases and sometimes if antiplasticization effect occurs, this diminution is accompanied by an increase of elastic modulus (decrease of damping properties) in the temperature interval between β- and α-relaxations, due to the fact that the modifier causes the disappearance or the decrease of the secondary relaxation.

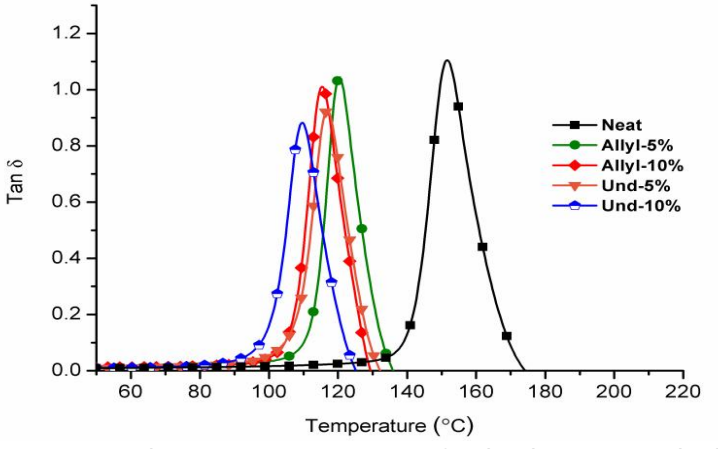

Figure 6. Tan δ against temperature at 1 Hz for the thermosets obtained.

The results of the impact tests are collected in **Figure 7** for all the materials prepared. As we can see, on increasing the proportion of HBP in the thermosets, impact strength slightly increase and all HBP-formulations show higher impact than neat DGEBA/MHHPA sample, as it is expected taking into account the globular architecture of the HBP. Comparing both HBPs, the addition of HBP-Allyl leads to a higher improvement. Although the opposite result could be expected, because of the higher T_g of the HBP-Allyl and lower length of its chains, the different relation between the plasticization and antiplasticization effect in both HBPs can justify the observed behaviour. Probably, HBP-Und exerts a higher plasticizing effect on the α-relaxation and lower antiplastizicing effect on the β-relaxation than HBP-Allyl.

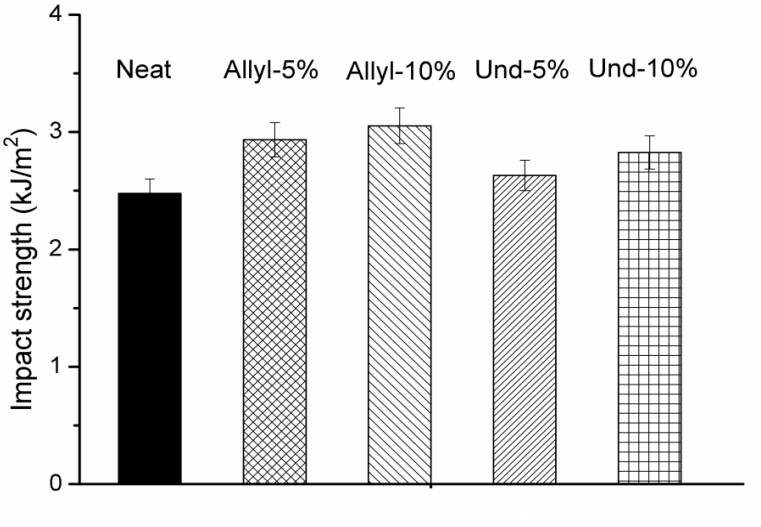

Figure 7. Impact strength for the thermosets obtained**.**

The toughness behaviour of DGEBA/MHHPA and HBP thermosets can be explained in terms of the morphologies observed by SEM. The fracture surfaces after impact tests were investigated by this technique. **Figure 8** shows the SEM micrographs for the fracture surfaces of all the thermosets prepared. As it can be seen, all the micrographs present a homogeneous appearance without any sign of phase separation. It can also be observed that the neat formulation shows a more fragile fracture than the modified materials. The rougher surface and the high amount of cracks and their thickness seen in the microfractographs of the HBP-modified materials, suggest that the fracture surface of these materials broke more yieldingly than that of the unmodified neat network. All these observations agree with the impact strength values measured (**Figure 7**). Since there is no phase separation in the modified materials, the toughness improvement reached by adding HBP-Allyl and HBP-Und should be based on *in situ* homogeneous reinforcing and toughening mechanism.[9,28]

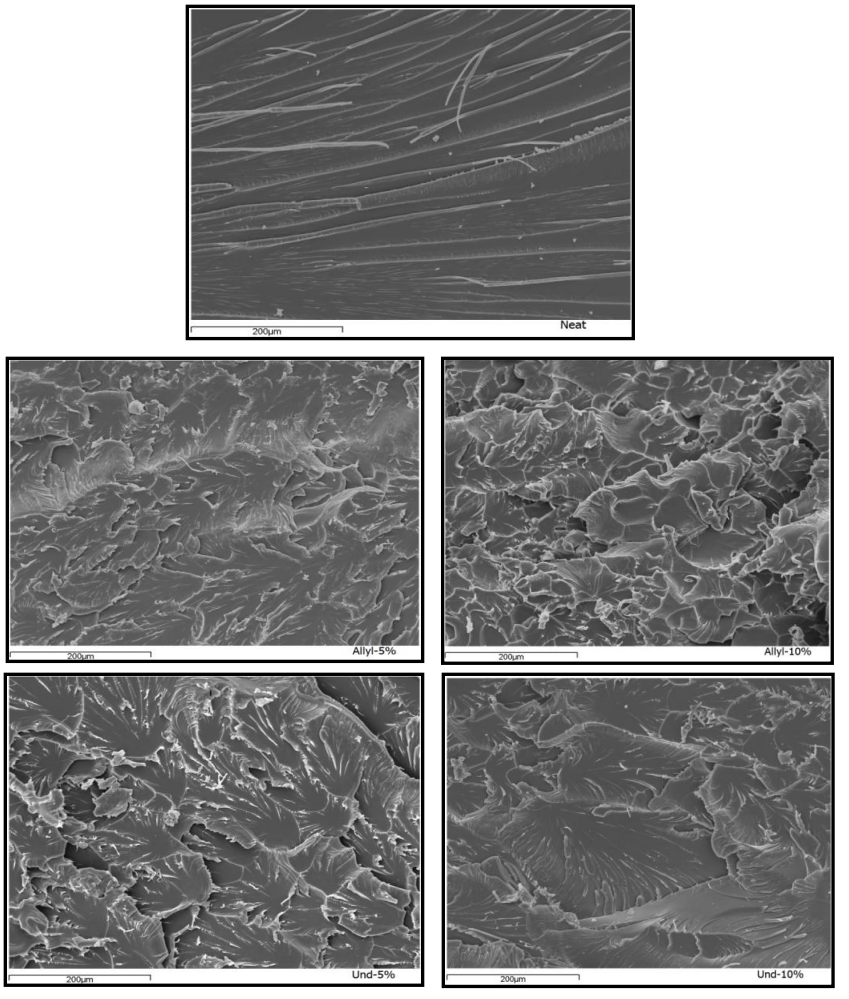

Figure 8. SEM micrographs for impacted fractured surfaces of the thermosets obtained.

The thermal stability of the thermosets was studied by TGA. **Table 3** collects the temperature of the initial decomposition calculated at a 5% of weight loss and the temperature of the maximum degradation rate. The shape of the derivative TGA curves for all the thermosets studied (figure not shown) was unimodal, indicating that there were no regions or structures in the material with significant differences in thermal stability. Some HBPs containing ester groups used as modifier to improve toughness of the epoxy systems compromise their good thermal stability due to the β-elimination reaction that take place through labile ester groups.[29] As we can see in **Table 3**, the addition of HPBs hardly modify the decomposition temperatures and even HBP-Und seems to slightly increase the thermal stability. Similar behaviour was obtained previously using an aliphatic-aromatic HBP polyester similar to the core of the HBP used in this work.[16] This result was rationalized on the fact that the aromatic ring directly bonded to the ester group avoids the β-elimination reaction, responsible of the thermal degradation starting at low temperatures.

Table 3. Thermogravimetric data of the formulation studied in this work.

Thermoset	$T_{5\%}$[a] (°C)	T_{max}[b] (°C)	Char Yield[c] (%)
Neat	346	410	4.6
Allyl-5%	341	410	4.6
Allyl-10%	345	412	5.3
Und-5%	340	410	4.6
Und-10%	351	412	5.1

a. Temperature of a 5% of weight loss.
b. Temperature of the maximum degradation rate.
c. Residue at 800 °C.

5.4. Conclusions

Novel modified aliphatic-aromatic hyperbranched polyester with vinylic chains of different lengths have been synthesized and used as non-reactive toughening modifier of epoxy/anhydride systems.

The addition of these novel HBPs synthesized to epoxy/anhydride systems, in the presence of a tertiary amine as catalyst, increases significantly the curing rate. The kinetics of curing has been established using an isoconversional integral procedure.

New thermosetting materials with improved toughness were obtained by adding the HBP synthesized to DGEBA/MHHPA systems with hardly compromise the thermal stability and the glass transition temperature, which only slightly decreases. The new thermosets obtained are homogenous without any phase separation, and their fracture surface suggests a significant increase in matrix yielding. The best improvement in impact resistance was obtained with the addition of a 10% of HBP-Allyl.

Although the length of the aliphatic chain and the amount of modifier play a role in the curing and in the final properties of the cured materials, the main differences were obtained between neat and modified formulations, independently of the type and amount of modifier used.

Acknowledgements

The authors would like to thank MINECO (Ministerio de Economia y Competitividad) and FEDER (Fondo Europeo de Desarrollo Regional) (MAT2011-27039-C03-01 and MAT2011-27039-C03-02) and to the Comissionat per a Universitats i Recerca del DIUE de la Generalitat de Catalunya (2009-SGR-1512). Adrian Tomuta acknowledges the grant FPI-DGR 2010 from the Catalonian Government.

References

[1] Arends CB, ed. *Polymer Toughening*, Marcel Dekker: New York; 1996.
[2] Kroschwitz JI, *High Performance Polymers and Composites*, John Wiley & Sons: New York; 1991.
[3] McGarry FJ, Sultan JN, *J Polym Sci* **13**: 29-34(1973).
[4] Becker O, Simon GP, *Adv Polym Sci* **179**: 29-82 (2005).
[5] Bagheri R, Marouf BT, Pearson RA, *J Macromol Sci Part C: Polym Rev* **49**: 201-225 (2009).
[6] Boogh L, Petterson B, Månson JAE, *Polymer* **40**: 2249-2261 (1999).
[7] Fu JF, Shi L-Y, Yuan S, Zhong Q-D, Zhang D-S, Chen Y, Wu J, *Polym Adv Technol* **19**: 1597-1607 (2008).
[8] Karger-Kocsis J, Fröhlich J, Gryshchuk O, Kautz H, Frey H, Mülhaupt R, *Polymer* **45**: 1185-1195 (2004).
[9] Xie XL, Tjong SC, Li RKY, *J Appl Polym Sci* **77**: 1975-1988 (2000).
[10] Morell M, Ramis X, Ferrando F, Yu Y, Serra A, *Polymer* **50**: 5374-5383 (2009).
[11] Morell M, Ramis X, Ferrando F, Serra A, *Polymer* **52**: 4694-4702 (2011).
[12] Morell M, Ramis X, Ferrando F, Serra A, *Macromol Chem Phys* **213**: 335-343 (2012).
[13] Fernández-Francos F, Foix D, Serra A, Salla JM, Ramis R, *React Funct Polym* **70**: 798-806 (2010).
[14] Morell M, Erber M, Ramis X, Ferrando F, Voit B, Serra A, *Eur Polym J* **46**: 1498-1509 (2010).
[15] Foix D, Ramis X, Ferrando F, Serra A, *Polym Int* **61**: 727-734 (2012).
[16] Foix D, Erber M, Voit B, Lederer A, Ramis X, Mantecón A, Serra A, *Polym Degrad Stab* **95**: 445-452 (2010).
[17] Moore JS, Stupp SI, *Macromolecules* **23**: 65-70 (1990).
[18] Schallausky F, Erber M, Komber H, Lederer A, *Macromol Chem Phys* **209**: 2331-2338 (2008).
[19]Schmaljohann D, Komber H, Voit B, *Acta Polym* **50**: 196-204 (1999).
[20] Ramis X, Salla JM, Mas C, Mantecón A, Serra A, *J Appl Polym Sci* **92**: 381-393 (2004).
[21] Okaya T, Tanaka T, Yuki K, *J Appl Polym Sci* **50:** 745-751 (1993).
[22] Dusek K, Plestil J, Lednický F, Lunak S, *Polymer* **19**: 393-397 (1978).
[23] Ivin KJ, in: Brandrup J, Immergut EH, eds. *Polymer Handbook*, Wiley: New York; 1975.
[24] Pham M-P, *Theorethical Estudies of Mechanisms of Epoxy Curing Systems*, University of Utah: Salt Lake City; 2011.
[25] Vyazovkin S, Wight CA, *Annu Rev Phys Chem* **48**: 125-149 (1997).
[26] Pascault JP, Saurereau H, Verdu J, Williams RJJ, *Thermosetting Polymers*, Marcel Dekker: New York, pp 234-236; 2002.
[27] Nielsen LE, Landel RF, *Mechanical Properties of Polymers and Composites*, Marcel Dekker: New York, pp 181-188; 1994.
[28] Zhang D, Jia D, *J Appl Polym Sci* **101**: 2504-2511 (2006).
[29] Fernández-Francos X, Salla JM, Cadenato A, Morancho JM, Serra A, Mantecón A, Ramis X, *J Appl Polym Sci* **111**: 2822-2829 (2009).

Chapter 6

New chemically reworkable epoxy coatings obtained by the addition of polyesters with star topologies to DGEBA resins

Chapter 6 - Progress in Organic Coatings 76 (2013) 1616-1624

NEW CHEMICALLY REWORKABLE EPOXY COATINGS OBTAINED BY THE ADDITION OF POLYESTERS WITH STAR TOPOLOGIES TO DIGLYCIDYL ETHER OF BISPHENOL A RESINS

Adrian M. Tomuta,[1] Xavier Ramis,[2] Xavier Fernández-Francos,[1]

Francesc Ferrando,[3] Angels Serra[1*]

[1] Department of Analytical and Organic Chemistry, Universitat Rovira i Virgili, C/Marcel·lí Domingo s/n, 43007, Tarragona, Spain.

[2] Laboratory of Thermodynamics, ETSEIB, Universitat Politècnica de Catalunya, Diagonal 647, 08028 Barcelona, Spain

[3] Department of Mechanical Engineering, Universitat Rovira i Virgili, C/ Països Catalans 26, 43007, Tarragona, Spain.

Abstract

A new multiarm star with hyperbranched aromatic-aliphatic polyester core and poly(ε-caprolactone) arms (HBPCL) was synthesized and characterized. Mixtures of diglycidylether of bisphenol A (DGEBA) resin and different proportions of this star type modifier were cured using a thermal cationic curing agent, $Yb(OTf)_3$. The HBPCL prepared has hydroxyl groups as chain ends, which are capable of chemically incorporating to the epoxy matrix by means of the monomer activated mechanism. This, together with the chemical structure of the modifier, allowed the preparation of new homogeneous thermosets for coating applications. The curing mixtures were investigated by differential scanning calorimetry (DSC) to study the curing process and evaluate the kinetic parameters of the formulations. These studies demonstrated that HBPCL decreased the curing rate and affected the gelation process. The thermosets obtained showed an improvement in impact strength with a discrete reduction of the T_g. The modified coatings showed an increased reworkability in alkaline solution with the maintenance of thermal stability.

Keywords: Epoxy resins, toughness, star polymers, degradability, cationic, crosslinking.

6.1. Introduction

Epoxy thermosets are ideal materials for coatings applications with a widespread use due to their excellent adhesive and thermomechanical properties, as well as their easy processing.[1,2,3] Once cured, these resins form highly crosslinked networks with a high thermal stability, which can be disadvantageous from an ecological point of view. The reuse of the coated metals or the reparation of electrical and electronic devices requires degradable thermosets, able to be eliminated from the substrate when their service life is over. Because of the need of the electronic devices to be reused, some authors applied the term “reworkable” to this type of epoxy coatings. However, it does not mean that the thermoset, applied as the coating, can be reused or recycled and the concept is only based on the ability of the network structure to break-down under

controlled conditions in order to remove it from the substrate.[4] Under these degradation conditions the crosslinking density will be diminished and subsequently their mechanical properties, allowing an easy elimination by mechanical procedures.

The most extended and easiest approach to prepare reworkable epoxy coatings introduces thermally labile ester groups in the epoxy monomer structure.[5] Among the research groups that follow this route it should be considered the work reported by Ober,[4] Sastri[6] and Wong.[7]

Our research team adopted the strategy of including ester groups to the structure of the network, but on the basis of the most popular and extended in use DGEBA epoxy resin. Thus, we copolymerized this resin with lactones[8,9] and Meldrum acid derivatives[10] or we modified it by reacting with hyperbranched polyesters.[11] These types of modifications constitute a more versatile strategy and improve some other properties such as impact strength or shrinkage during curing.

Many efforts have been done in the last decades to improve toughness of epoxy materials. For this purpose, rubbers, elastomers or some particles able to stand deformation during the impact were added to the formulations.[12,13] However, these strategies result in a high increase in the viscosity of the uncured blends or to a decrease in the T_g of the thermosets, which is a drawback for coatings applications.[14] In the last years, the use of hyperbranched and multiarm star polymers has been proposed to overcome the limitations of traditional modifiers.[15,16,17] The advantage of these dendritic polymers is their low viscosity compared to linear analogues, due to the low entanglement between molecules caused by their highly branched architecture.[18,19,20] Depending on the chemical structure of the dendritic modifier and its proportion, the type of resin and the curing agent selected different properties can be improved.[21] Among them, thermal or chemical reworkability have been increased without compromising thermomechanical characteristics.[11,19,21] Moreover, impact resistance has been highly improved.[22]

In the present study, we report the synthesis and characterization of a new multiarm star polymer with a hyperbranched aromatic-aliphatic polyester core and poly(ε-caprolactone) arms (HBPCL) (see **Scheme 1**). This dendritic polymer has been added in several proportions to diglycidylether of bisphenol A resin (DGEBA) and cured using a thermal cationic curing agent, $Yb(OTf)_3$.

The kinetics of the curing process has been studied by calorimetry and the gelation by rheometry, whereas the global shrinkage on curing was calculated from the densities of the material before and after curing. Thermomechanical characteristics of the materials obtained were analyzed by DMTA and their high thermal stability proved by TGA. The chemical reworkability was studied by treating the materials in a basic medium. The presence of ester in the multiarm star structure facilitates the saponification by base. Mechanical characteristics such as Young modulus, microhardness and impact resistance have also been determined.

6.2. Experimental

6.2.1. Materials

4,4-Bis(4-hydroxyphenyl) valeric acid, N,N'-dicyclohexylcarbodiimide (DCC), tin 2-ethylhexanoate ($Sn(oct)_2$) and ytterbium (III) trifluoromethanesulfonate ($Yb(OTf)_3$) were supplied by Sigma-Aldrich and used without further purification. ε-Caprolactone (CL, Sigma-Aldrich) was dried over CaH_2 and subsequently distilled under vacuum. Diglycidyl ether of Bisphenol A (DGEBA) Epikote Resin 828 was provided by Shell Chemicals with an epoxy equivalent of 184 g/eq and was dried in vacuum before use. All the organic solvents were purchased from Scharlab and purified by standard procedures. 4-(N,N-dimethylamino) pyridinium p-toluenesulfonate (DPTS) was prepared as described in the literature.[23]

6.2.2. Hyperbranched polyester synthesis (HBP-OH) (Scheme 1)

HBP-OH was synthesized as previously described[24] from 4,4-bis(4-hydroxyphenyl) valeric acid as AB_2 monomer. The ^1H and ^{13}C NMR data are in accordance with those published.[25] $\overline{M_n}$ =12,300 g/mol, $\overline{M_w}$ = 23,500 g/mol and molecular weight dispersity 1.9 (by SEC). T_g = 124ºC (by DSC). The amount of hydroxyl groups was determined according to ISO 2554-1974 standards. The number of hydroxyl groups per molecule was 46.

6.2.3. Synthesis of the multiarm star polymer with poly(ε-caprolactone) arms (HBPCL) (Scheme 1)

In a 25 mL round bottomed flask 5.1 g (0.4146 mmol) of HBPOH were dissolved in 15.39 g (0.135 mol) of ε-caprolactone at 130 °C under argon atmosphere, under gentle stirring for 1 hour. Then, 4 drops of tin 2-ethylhexanoate were added to the mixture and the temperature was raised to 150 °C and kept for 24 hours.

After the reaction, the polymer mixture was dissolved in 50 mL of THF and precipitated twice in 500 mL of cold diethyl ether. After filtration, the polymer was dried at 40 °C overnight in a vacuum oven. Conversion: 96 %. T_g = - 30 ºC and *Tm* = 62ºC (by DSC). $\overline{M_n}$ =39,500 g/mol, $\overline{M_w}$ = 88,100 g/mol and molecular weight dispersity 2.2 (by SEC). $\overline{M_n}$ = 49,350 g/mol calculated from the $\overline{M_n}$ of the HBPOH core, 5 as the number of arms per molecule and 65 as the average polymerization degree of the arms, both determined by ^1H-NMR analysis.

^1H NMR (400 MHz, $CDCl_3$), δ (ppm): 1.37 m ($-CH_2-$); 1.39 m ($-CH_3$); 1.64 m ($-CH_2-$); 2.16 m ($-CH_2-$); 2.31 m ($-CH_2-$); 4.05 m (CH_2); 5.8-7.4 broad band (CH Ar).

^{13}C NMR (100.6 MHz, $CDCl_3$), δ (ppm): 24.7; 25.6; 28.4; 33.6; 34.2; 64.3; 113.9; 121.2; 128.4; 139.0; 145.6; 148.6; 172.7.

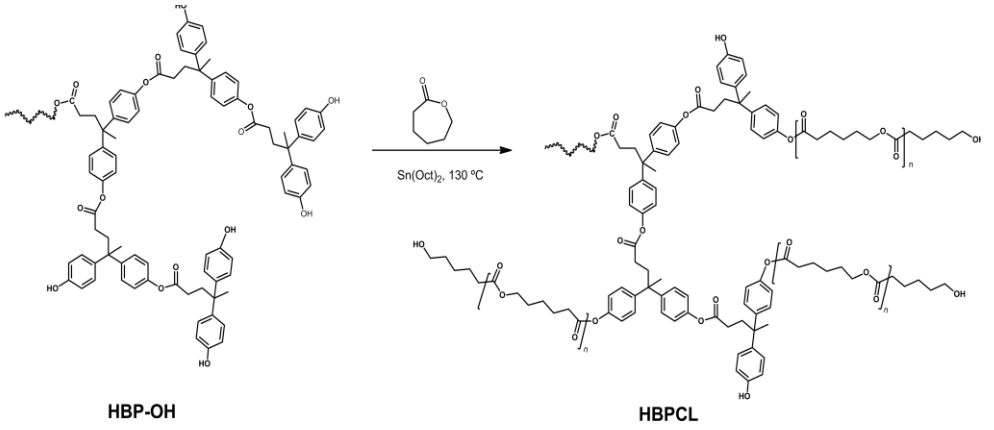

Scheme 1. Representation of the synthetic route to multiarm star HBPCL.

6.2.4. Preparation of the curing mixtures

The mixtures were prepared by mixing DGEBA resin with 5% or 10% w/w of the multiarm star synthesized. The mixing was made in a mortar while heating (ca. 80ºC) until the modifier was completely incorporated to the viscous resin. As for the curing agent, 1 phr (one part of initiator for hundred of mixture) of $Yb(OTf)_3$ was added after homogenization of DGEBA/multiarm star polymer mixture.

6.2.5. Measurements

The 400 MHz ^{1}H-NMR and 100.6 MHz ^{13}C-NMR spectra were obtained with a Varian Gemini 400 spectrometer with Fourier Transformed. ^{1}H-NMR spectra were acquired in 1 min and 16 scans with a 1.0 s relaxation delay (D1). ^{13}C NMR spectra were obtained using a D1 of 0.5 s and an acquisition time of 0.2 s. A total of 500 accumulations were recorded. $CDCl_3$ was used as a solvent and tetramethylsilane (TMS) as internal standard.

Calorimetric analyses were carried out on a Mettler DSC-821e calorimeter. Samples of approximately 10 mg in weight were cured in aluminium pans in a nitrogen atmosphere. Non-isothermal experiments were performed from 0 to 225ºC at heating rates of 2, 5, 10, and 15 ºC/min to determine the reaction heat and the kinetic parameters. In the non-isothermal curing process, the degree of conversion at a given temperature *T* was calculated as the quotient between the heat released up to *T* and the total reaction heat associated with the complete conversion of all reactive groups. The precision of the given enthalpies is ±3%. The T_gs of the cured materials were determined with a second scan at 20 ºC/min after dynamic curing by the mid-point method and the error is estimated to be approximately ±1°C. The T_gs of the pure HBPs were determined by a similar procedure.

The T_gs of the modified materials were predicted by using the Fox equation for homogeneously blended thermosets.[26]

$$\frac{1}{T_g} = \frac{w}{T_g^{HBPCL}} + \frac{1-w}{T_g^{neat}} \qquad (1)$$

, where T_g^{HBPCL} and T_g^{neat} are the glass transition absolute temperatures for the multiarm star and the neat thermoset and *w* is the proportion of the modifier in weight.

The kinetic triplet [pre-exponential factor, activation energy, and the kinetic model] of the curing reaction was determined using integral isoconversional non-isothermal kinetic analysis, Kissinger-Akahira-Sunose equation, combined with the Coats-Redfern procedure. Details of the kinetic methodology are given in previous studies.[27]

Rheometric measurements were carried out in the parallel plates (geometry of 25 mm) mode with an ARG2 rheometer (TA Instruments, UK, equipped with electrical heated plates, EHP). Complex viscosity (η^*) of the pre-cured mixtures was recorded as function of angular frequency (0.05 – 100 rad/s) with a constant deformation of 50 % at 40 ºC. The curing was monitored at 100ºC in order to determine the gel point and the conversion at gelation. Because the viscosity of the system changes significantly during the curing process, a control program was used in which the oscillation amplitude diminishes with an increase in the applied stress. Gel time was taken as the point where *tan δ* is independent of frequency.[13] The conversion at the gelation (α_{gel}) was determined by stopping the rheology experiment at gelation and performing a subsequent dynamic DSC scan at 10K/min of the gelled sample.

Dynamic mechanical thermal analysis (DMTA) was carried out with a TA Instruments DMTA 2980 analyzer. The samples were cured isothermally in a mould at 140 ºC for 1 h and then post-cured for 1 h at 170 ºC. Single cantilever bending at 1 Hz was performed at 3ºC/min from 30 to 220ºC on prismatic rectangular samples (1.5 x 20 x 5 mm^3).

A three point bending assembly was used to obtain the Young modulus in a non-destructive flexural test at room temperature. The support span of the assembly was 10 mm and a load rate of 3 N/min was used. The Young modulus is calculated using the slope of the load deflection curve in accordance with Eq. (2).

$$E_f = \frac{L^3 m}{4bd^3} \qquad (2)$$

where E_f is the Young modulus (MPa), *L* the support span (mm), *b* is the width of test beam (mm), *d* is the depth of tested beam (mm) and *m* is the gradient (i.e., slope) of the initial straight-line portion of the load deflection curve (P/D) (N/mm).

The overall shrinkage was calculated from the densities of the materials before and after curing, which were determined using a Micromeritics AccuPyc 1330 Gas Pycnometer thermostatized at 40ºC. The shrinkage during curing was determined as:

$$\%shrinkage = \frac{\rho_\infty - \rho_0}{\rho_\infty} \qquad (3)$$

where ρ_0 is the density of the uncured formulation and ρ_∞ is the density of the fully cured material obtained at the same conditions than DMTA samples.

Thermogravimetric analysis was carried out with a Mettler-Toledo TGA/SDTA 851e thermobalance. Cured samples with an approximate mass of 5 mg were heated from 30 to 800ºC at a heating rate of 10 ºC/min in a nitrogen atmosphere.

Chemical degradation was carried out in a solution 1M of KOH in ethanol at reflux temperature. Samples after different saponification times were taken and dried and T_gs were measured in a DSC scan from 30 to 200ºC at 20 ºC/min.

Impact tests were performed at room temperature by means of a Zwick 5110 impact tester according to ASTM D 4508-05 using rectangular samples (25 x 12 x 2.5 mm^3). The pendulum employed had a kinetic energy of 1 J. For each material, 9 determinations were made. The impact strength (IS) was calculated from the energy absorbed by the sample upon fracture as:

$$\mathrm{IS} = \frac{E - E_0}{S} \qquad (4)$$

where E and E_0 are the energy loss of the pendulum with and without sample respectively, and S is the cross-section of the samples. The fracture area of impacted samples was metalized with gold and observed with a scanning electron microscope (SEM) Jeol JSM 6400.

Microhardness was measured with a Wilson Wolpert (Micro-Knoop 401MAV) device following the ASTM D1474-98 (2008) standard procedure. For each material 10 determinations were made with a confidence level of 95%. The Knoop microhardness (HKN) was calculated from the following equation:

$$\mathrm{HKN} = \frac{L}{A_P} = \frac{L}{l^2 C_p} \qquad (5)$$

where L is the load applied to the indenter (0.025 kg), A_p is the projected area of indentation in mm^2, l is the measured length of long diagonal of indentation in mm, and Cp is the indenter constant (7.028×10^{-2}) relating l^2 to A_p. The values were obtained from 10 determinations with the calculated precision (95% of confidence level).

6.3. Results and discussion

In a previous study,[20] we modified DGEBA thermosets by adding a multiarm star polymer with a hyperbranched poly(glycidol) core and PCL arms and the results compared with those obtained by addition of a linear PCL modifier. In that study $Yb(OTf)_3$ was used as cationic initiator. It was put into evidence the advantages of the star topology, such as a better processability and a slight retardation of the curing, attributed

to the lower viscosity in comparison to the linear analogue. Moreover, mechanical characteristics were better for star modified materials, while maintaining the homogeneous appearance. However, the T_g of the thermosets was reduced, possibly due to the highly flexible structure of the PGOH-PCL modifier.

These precedents moved us to further investigate the use of similar structures with the aim, not only to increase T_g and mechanical characteristics, but also to improve chemical reworkability, maintaining thermal stability. According to that, aromatic-aliphatic hyperbranched polyester was used as the core and PCL arms were grown from the phenol end groups. The presence of aromatic polyesters in the core allows maintaining the thermal stability, although the saponification with a base is still possible.[21]

6.3.1. Synthesis and characterization of HBPCL

Among the synthetic approaches used in the synthesis of multiarm star polymers the core first strategy was selected using a preformed aliphatic-aromatic hyperbranched polyester, previously described,[24] as the core.

The polymerization of ε-caprolactone catalyzed by $Sn(Oct)_2$ was selected to grow the PCL arms from the hydroxyl phenolic groups. In the case of aliphatic hydroxyl groups this procedure allows the control of the length of the arms by the proper selection of the proportion of the monomer to the OH groups in the core structure by its leaving character. The synthetic pathway is depicted in **Scheme 1**.

The degree of polymerization of the arms was determined by means of ^{1}H NMR spectroscopy. **Figure 1** shows the ^{1}H-NMR spectrum in $CDCl_3$ of HBPCL multiarm star with the corresponding assignments.

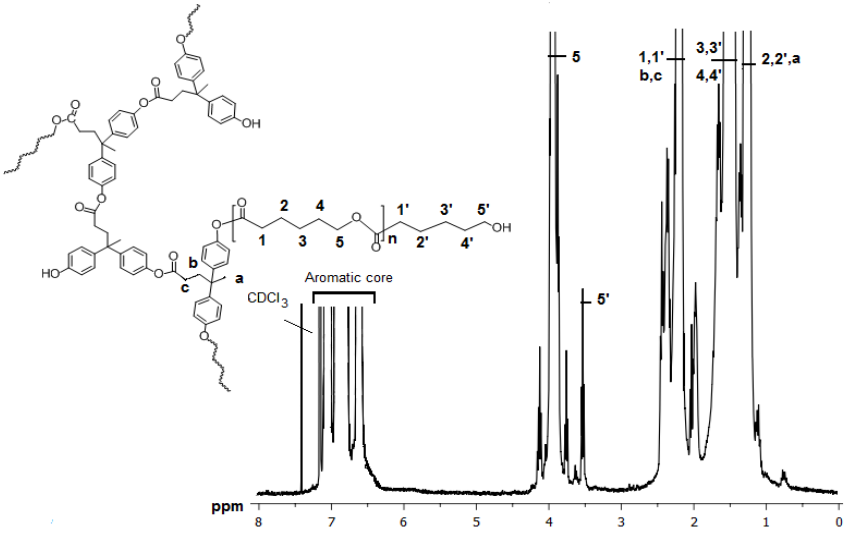

Figure 1. ^{1}H NMR spectrum of HBPCL multiarm star in $CDCl_3$.

The core signals can be appreciated as a broad and complex multiplet in the aromatic zone due to the low mobility of the core that leads to a quick relaxation and the subsequent broadening of the signals. The central methylene protons of the ε-caprolactone unit in the arms appear between 1.4 and 1.7 ppm. The protons directly attached to carbonyl group (1 and 1') appear overlapped at 2.3 ppm. Thus, the only signals that can be used to evaluate the degree of polymerization are the methylene protons 5 and 5', attached to the oxygen of ester in the repeating unit or to hydroxyl terminal group, which appear separately. Thus, the degree of polymerization of PCL arms ($\overline{DP}_{arm}$) was calculated from the integration of these signals by dividing peak 5 by peak 5' and adding a terminal unit, as follows:

$$\overline{DP}_{arm} = \frac{I_5}{I_5'} + 1 \qquad (6)$$

The use of the signals of carbons **5** and **5'** for DP evaluation of the arms is possible due to the absence of PCL homopolymer, which was confirmed by SEC experiments. The SEC curve had a unimodal distribution and without any signals at lower molecular weight, meaning that no detectable PCL homopolymer was formed during the ring-opening polymerization process. By these calculations we obtained a surprisingly high length of the arms, 65 CL units by each arm. If we take into account that the molar proportion of ε-CL monomer to phenol group used in the synthesis was about 7, we get to the conclusion that not all the 46 arms per molecule grow, but only an average of 5.

The growth of PCL from phenolic groups with $SnOct_2$ has not been described up to now in the literature. The lower activity of phenolic in reference to alcoholic groups can explain that once one of the phenol groups has reacted with an ε-CL monomer, the aliphatic OH group formed is able to react much more easily than another phenol group. Therefore, the arms are longer than expected and the final star has fewer arms than the predicted by the number of end groups of the core structure.

6.3.2. Study of the curing of DGEBA-HBPCL mixtures

$Yb(OTf)_3$ has been selected in the present study as the cationic curing agent[28] because, in addition to the ring opening polymerization of epoxides, this initiator promotes the covalent incorporation of alcohols to the epoxy network by the so called monomer activated mechanism (AM).[29] This allows the covalent linkage of hydroxyl terminated star to the epoxy network, which allows reducing the loss of thermomechanical characteristics usually produced in thermoplastic modified thermosets.

Non-isothermal calorimetric analysis was applied to study the curing process and the effect of adding the star modifier in the curing rate. **Figure 2** shows the evolution of the conversion in front of the temperature for the neat formulation and that modified with 5 and 10% of the HBPCL star.

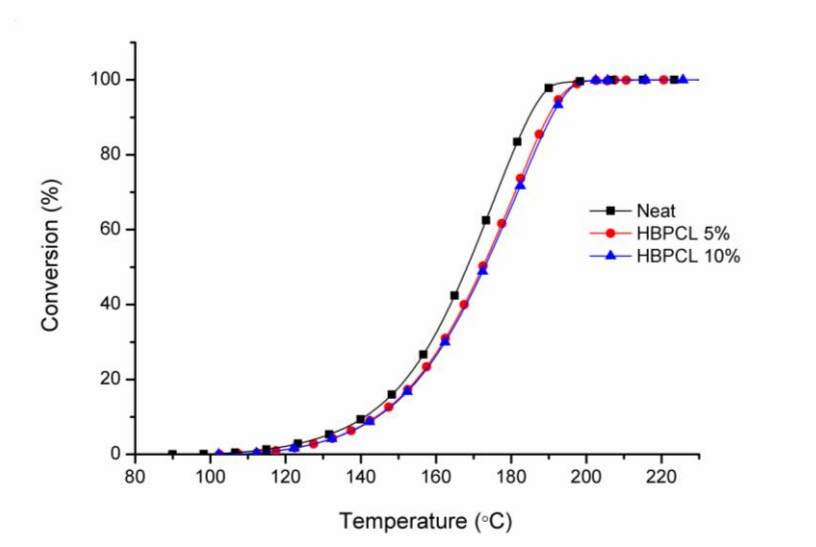

Figure 2. Plot of conversion against temperature obtained by non-isothermal DSC studies.

As we can see, there is a little retarding effect in the curing on adding the modifier to the formulation and this delay slightly increase with the amount of the multiarm star. The retarding effect can be usually related to an increased viscosity of the modified formulations.

To investigate if the viscosity is the responsible of this delay, a rheological study of the formulations was performed. **Figure 3** shows that the mixtures studied have a Newtonian behaviour in the range of frequencies studied and that the higher the proportion of the HBPCL in the formulation the higher the viscosity value. However, the complex viscosity of the formulation is not much increased, even at 40ºC, and therefore the processability remains in the proper values for technological applications. In a previous study, we proved that the viscosity depends on the length of the arms of the multiarm star being lower when the arms were shorter.[30] In the present case, the length of the arms in the structure synthesized is quite long, but even with this structure the viscosity of the formulation is not much increased, especially if we compare it with the increase produced on adding linear PCL to the formulation.[31] Whereas, the progressive addition of 5 or 10% of modifier increases the viscosity less as twice by each the addition of linear PCL increases in much than one order of magnitude for each 5%.

From the rheological study, we can state that the viscosity is not fully related to the retarding effect observed, because in the formulation with a 10% of HBPCL the delay in the curing was practically unappreciable while the viscosity still increases. It should be commented, that the higher amount of phenol and alcohol groups in the formulation, from the added multiarm star, can activate the AM mechanism, which occurs quicker than the alternative chain end mechanism (ACE). Both factors, viscosity and concurrence among mechanisms, influence in a different way the rate of the curing process.

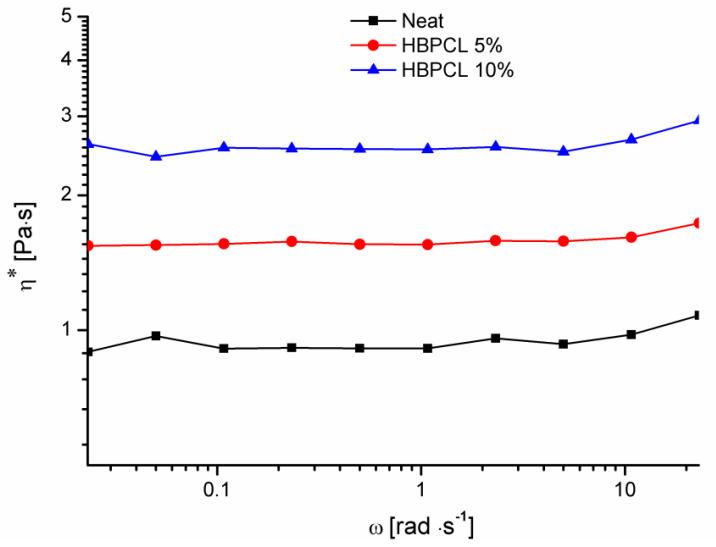

Figure 3. Plot of viscosity against frequency at 40ºC for the formulations studied.

The calorimetric data of the curing process and the calculated kinetic parameters for the formulations studied are collected in **Table 1**. The maximum of the calorimetric peak is shifted to higher temperature on adding the modifier. Both the enthalpy per gram and the enthalpy per epoxy equivalent decrease on adding the star modifier. The lower enthalpy per epoxy equivalent in the modified formulations could be attributed to topological restrictions by the presence of the modifier, which makes it difficult to reach the complete reaction of epoxide groups. It should be said that a value close to 100 kJ/ee which is an acknowledged value for epoxy resin curing was determined.[32]

The presence of HBPCL in the thermoset reduces the glass transition temperature, but this reduction is quite limited. On comparing the values measured with those calculated by the Fox equation,[26] which takes into account the T_g of the HBPCL (-30 ºC), and that of the neat material, it can be observed that both are similar, which indicates a complete miscibility of the star modifier in the epoxy matrix.

From the kinetic studies, we could observe that the activation energy remained quite constant during the curing process, indicating that there is mainly one mechanism governing the process. In the table we can see that the value at a conversion of 0.5 does not show any definite trend on changing the proportion of modifier, similarly to what happens with the pre-exponential factor. However, the calculation of the constant rate, taking as the kinetic model the R_2 and using the Arrhenius equation, provides evidence of the delaying effect of the modifier in the formulation. The calculated values agree with the experimental conversion-temperature curves in **Figure 2**. Although hydroxyl groups promote chain transfer reactions by the AM mechanism, which produce an accelerative effect, its contribution is low, due to their low proportion in the formulation.

Table 1. Calorimetric data and kinetic parameters determined for the curing of the different formulations studied.

Formulation	T_{max} [a] (°C)	Δh [b] (J/g)	Δh [b] (kJ/eq)	T_g [c] (°C)	T_g^{FOX} [d] (°C)	E_a [e] (kJ/mol)	ln$A$ [f] (s^{-1})	$k_{170°C}$ [g] (min^{-1})
Neat	176	537	99	144	-	79.3	19.65	0.151
5% HBPCL	183	497	92	125	129	83.6	20.59	0.122
10% HBPCL	183	477	88	118	116	78.0	18.98	0.112

a. Temperature of the maximum of the curing exotherm
b. Enthalpy of the curing process by gram of mixture or by epoxy equivalent
c. Glass transition temperature determined by DSC in a second scan after a dynamic curing
d. Glass transition temperature predicted by the Fox equation
e. Apparent activation energies determined by isoconversional non-isothermal procedure at a conversion of 0.5
f. Pre-exponential factor at a conversion of 0.5 for the kinetic model R_2
g. Rate constant determined using Arrhenius equation at a conversion of 0.5 for kinetic model R_2 with $g(\alpha)=\left[1-(1-\alpha)^{0.5}\right]$

In the curing process gelation is one of the most determining phenomena in view of the application of the resin as adhesive or coating. At the gelation point the molecular weight tends to infinite at molecular level and after it the material loses its mobility and the formation of internal stresses initiates. Thus, it is important to know the time of gel and the conversion at the gel point and the effect of the modifiers added on them.

The calculation of gel times by rheometry was made by the time corresponding to the point where the phase angle δ or tan δ is independent of frequency.[33] The determination of the gel point for the neat formulation at 100ºC is illustrated in **Figure 4**. It is worth noting that the determination of gelation as the G'-G" crossover gives very similar results to those obtained with the frequency-independent δ crossover.

The values determined by this methodology are collected in **Table 2**. As we can see, the gelation time increases on adding the star modifier, in agreement with the curing kinetics. This result is significant from the point of view of the application, since it indicates a longer pot-life of the modified formulations. The conversion at the gelation obtained by the combination of rheometric and calorimetric measurements is also collected. Conversion at the gel point (α_{gel}) increases only when a proportion of 10% of HBPCL was added.

Another parameter influencing the apparition of stresses is the shrinkage taking place during curing. By measuring the densities of the material before and after curing the global shrinkage can be evaluated. The values obtained are collected in **Table 2**. Ring-opening polymerization usually leads to low shrinkage, which is even reduced by the addition of the star modifier. Probably the decreases of intermolecular and

intramolecular H-bond in HBPCL when the terminal hydroxyl groups react with the epoxy group con justify this behaviour. This should be considered another improved characteristics of the modified thermosets proposed in this study

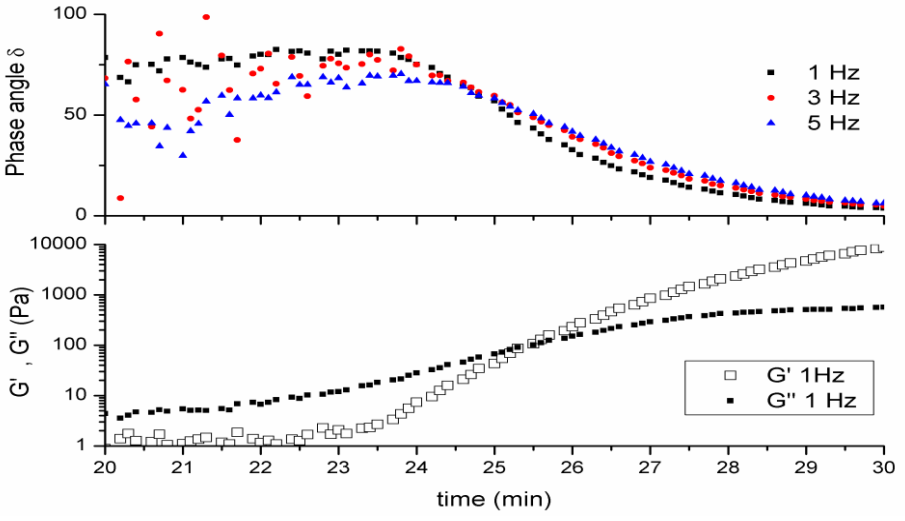

Figure 4. Determination of the gel time for the neat formulation by rheometric experiments performed at 100ºC, as the frequency independent crossover of δ (upper graph) and from the crossover between G' and G'' (lower graph).

Table 2. Gelation data, densities and shrinkage of the systems studied.

Formulation	t_{gel}[a] (min)	α_{gel}[b] (%)	$\rho_{monomer}$ (g/cm^3)	$\rho_{polymer}$ (g/cm^3)	Shrinkage[c] (%)
Neat	24.4	34.2	1.146	1.164	1.55
5% HBPCL	30.8	30.5	1.143	1.151	0.69
10% HBPCL	35.8	38.1	1.144	1.153	0.78

a. Determined by rheometry.
b. Determined as the conversion reached by rheometry and DSC tests at 10 ºC/min.
c. Shrinkage determined as $[(\rho_{polymer} - \rho_{monomer})/\rho_{polymer}]$.

6.3.3. Characterization of the materials by DMTA

Table 3 collects the results of the DMTA analysis of the cured materials. The values of Young modulus slightly decrease on adding the modifier. This is produced by the plasticizing effect of the poly(ε-caprolactone) arms compatible in the network structure. This plasticization can positively affect toughness characteristics.

Table 3. DMTA and TGA data obtained from all the materials prepared.

Formulation	Young Modulus (GPa)	$T_{tan\ \delta}$ [a] (ºC)	E' [b] (MPa)	T_{onset} [c] (ºC)	T_{max} [d] (ºC)	Char Yield [e] (°C)
Neat	2.5	152	38	314	355	15.5
5 % HBPCL	2.4	143	27	318	357	16.1
10 % HBPCL	2.3	127	15	322	360	17.1

a. Temperature of maximum of the tan δ at 1 Hz.
b. Relaxed modulus determined at the $T_{tan\delta}$ + 40 ºC.
c. Temperature of the onset decomposition in the TGA calculated for a 5 % of weight loss.
d. Temperature of the maximum decomposition rate determined by TGA in N_2 at 10 ºC/min
e. Char residue at 800 °C.

Not only the tan δ peak temperature values are important, but also their shape to know about the morphology of the materials. **Figure 5** shows the shape of the tan δ curves for the materials prepared. In agreement with calorimetric measurements, the glass transition temperature shifts to lower temperatures on adding HBPCL, due to the plasticization effect of the PCL arms. It is worth to note that the shape of the curves is similar and typical for a homogeneous material. No new relaxations appeared at lower temperatures in the modified thermosets, confirming the complete compatibility of the modifier in the network structure.

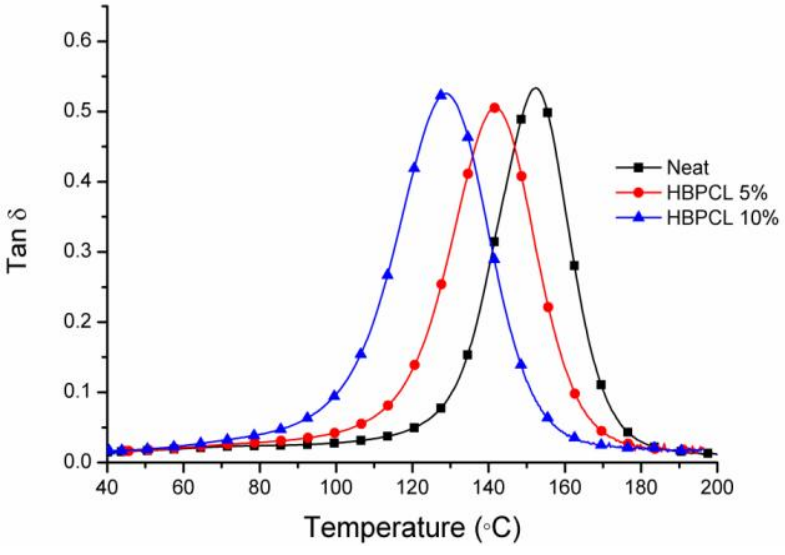

Figure 5. Plots of tan δ curves for the materials prepared.

The values of the modulus after relaxation are an indication of the crosslinking density, since the modulus is related to the molecular weight between crosslinks in the basis of the rubber elasticity theory.[34] It is clear, from the values in **Table 3**, that the crosslinking density is highly reduced by the addition of HBPCL. This is a consequence of the chain transfer reactions produced by the presence of hydroxyl groups at the end of the arms which react through the AM mechanism and the presence of star structure with long PCL arms, which leads to a dilution effect of the crosslinks of the matrix.

6.3.4. Thermal and chemical stability of the thermosets prepared

The thermal stability of the prepared thermosets was studied by TGA. Usually, the presence of ester groups reduces the thermal stability of the structures by the occurrence of β-elimination processes, taking place at temperatures about 250 ºC. The presence of hydrogen atoms in γ-position favours this mechanism and therefore increases the thermal degradability of the cured thermosets. In the structure of the modifier there are primary aliphatic ester groups and aromatic ester groups, with low degradability the former and non-degradable the latter. The initial decomposition temperature shown in **Table 2** is higher than 300 ºC and even increases slightly when HBPLC was in the formulation. Similarly, the temperature of the maximum decomposition rate and the char yield increases slightly with the proportion of star modifier.

In **Figure 6** the TGA curves in N_2 atmosphere are represented. As can be seen, the shape of the curves is similar and it is interesting to note that the curves show an only degradation step, indicating that all the types of covalent bonds break simultaneously.

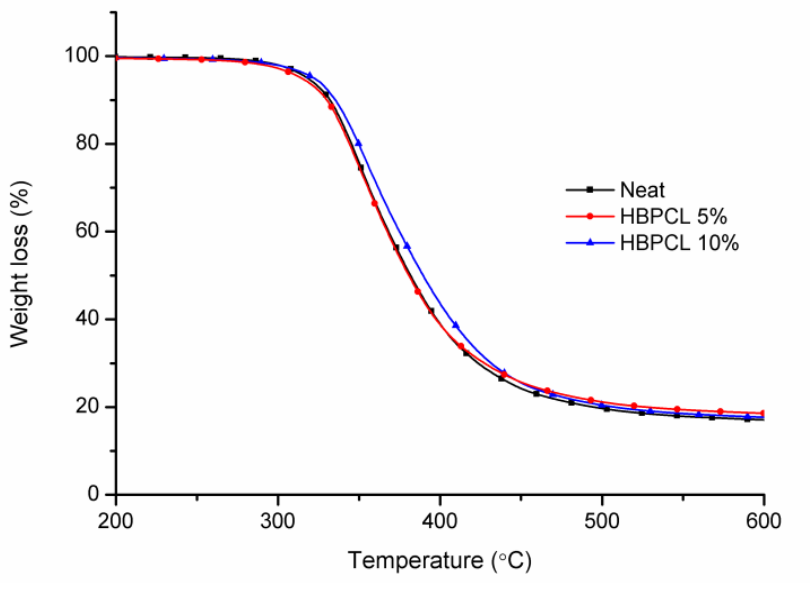

Figure 6. TGA plots in N_2 atmosphere of the cured materials.

The presence of ester groups in the network structure allows the saponification in basic medium. Thus, the chemical degradation has been studied by monitoring the T_g after selected saponification times. The values shown in **Table 4** indicate that chemical degradation occurs and this capability increases with the proportion of modifier.

Table 4. T_g values determined by DSC of the thermosets treated with KOH 1M for several time.

Formulation	**Saponification time (hours)**					
	0	**2**	**4**	**10**	**15**	**24**
Neat	145	145	144	144	142	142
5% HBPCL	133	129	121	114	102	75
10% HBPCL	126	123	119	110	94	68

Taking into account these results we can state that the addition of HBPCL allows the preparation of chemically reworkable thermosets, while maintaining the thermal stability, which can be necessary for several applications. Thus, these materials can stand high temperatures without appreciable degradation but can be removed from the substrate quite easily by saponification and mechanical elimination of the degraded coating.

6.3.5. Mechanical and morphological characterization

Microhardness measurements, which rate the resistance of the materials against penetration by a static load, were performed. These results obtained using a Knoop microindenter are represented in **Figure 7**. As we can see, the addition of HBPCL firstly improves this characteristic and then slightly decreases, when the proportion of modifier is higher. Thus, from the point of view of this property the addition of a 5% of HBPCL gives the best result. On comparing these data with the ones obtained by adding linear poly(ε-caprolactone) or multiarm star with poly(glycidol) as the core and poly(ε-caprolactone) arms (PGOH-PCL) [20] we can conclude that the materials obtained in the present study are much better, since reductions in this parameter of about 30 and 20%, respectively were reported in the previous study. This indicates that not only the structure of the arms but also the structure of the core affects this property.

The results of impact tests are represented in **Figure 8** for the materials prepared. It can be observed that the modification of DGEBA with the HBPCL star improves toughness characteristics in comparison to the neat material. However, the achieved improvement is much lower than the one obtained with a 10% of PGOH-PCL star modifier with a 75% of increase. The differences can be explained by the different plasticization effect caused by the core of both star modifiers, more rigid in HBPCL and

more flexible in PGOH-PCL. Again, the structure of the core seems to play a role in mechanical characteristics. To reach higher improvements in toughness by addition of dendritic structures, micro or nanophase separation is usually required and homogeneous materials leads to discrete increases, as previously reported.[11,22,35]

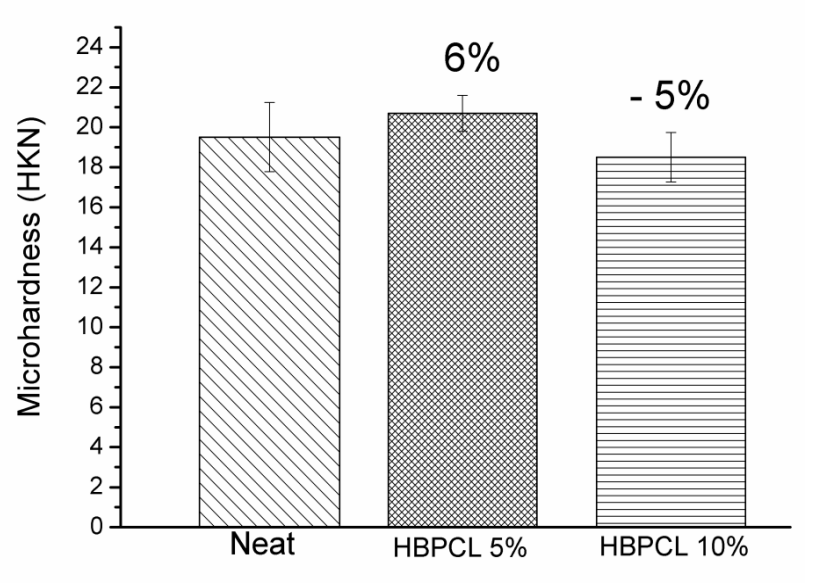

Figure 7. Knoop microhardness for the materials prepared.

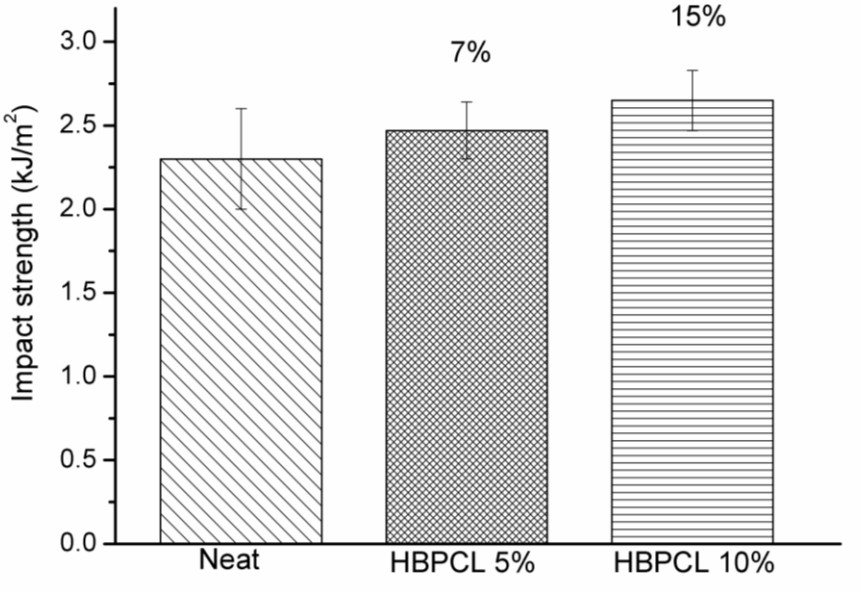

Figure 8. Impact test data for the materials prepared.

The homogeneous characteristics of the materials were proved by inspection of fracture surfaces by SEM. **Figure 9** shows the micrographs for the materials prepared.

The appearance of the surfaces is quite similar but the modified materials seem to have a more plastic fracture, related to ductility, which defines their toughness characteristics.[36] Because of the impact resistance does not show great differences, the type of fracture should be quite similar, as observed.

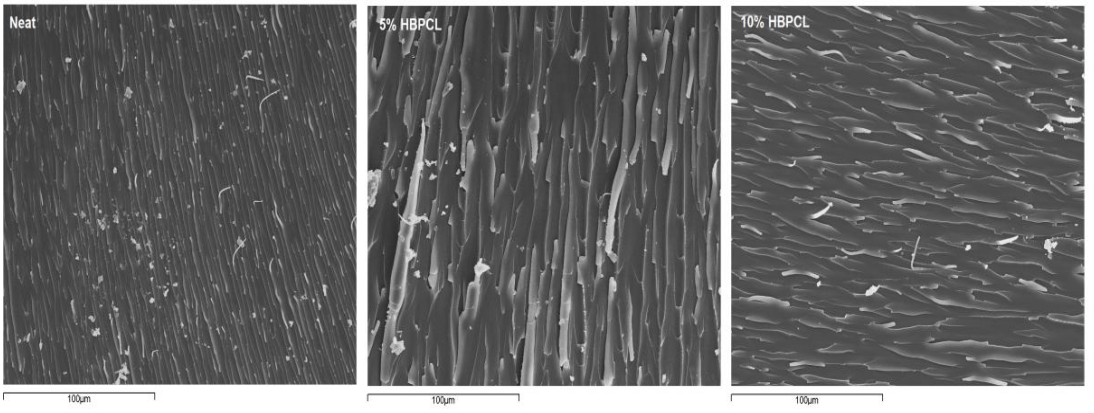

Figure 9. SEM micrographs for the fracture surfaces of the materials prepared.

6.4. Conclusions

A new multiarm star with a hyperbranched aliphatic-aromatic polyester core and an average number of five poly(ε-caprolactone) arms per molecule has been synthesized and characterized and then used as polymeric modifier of DGEBA thermosets cured cationically by $Yb(OTf)_3$. The addition of the modifier slightly delayed the curing process, reduced the shrinkage on curing and increased the pot life.

The materials obtained were homogeneous and the T_g was slightly reduced proportionally to the amount of HBPCL in the material, acting as a plasticizer.

Young modulus slightly decreased by the addition of HBPCL but the impact strength increased whereas the microhardness was not much affected.

The modified materials show good thermal stability and can be saponified. Thus, the modified thermosets can be considered as thermally stable but chemically reworkable coatings, since they can be eliminated from the substrate by basic treatment.

Acknowledgements

The authors would like to thank MINECO (MAT2011-27039-C03-01, MAT2011-27039-C03-02) and Generalitat de Catalunya (2009-SGR-1512) for giving financial support. A.T. acknowledges the grant FI-DGR 2010 given by the Generalitat de Catalunya and X.F. acknowledges the contract JCI-2010-06187 from MINECO.

References

[1] May CA, ed. *Epoxy Resins. Chemistry and Technology*. 2nd ed. Marcel Dekker: New York; 1988.
[2] Petrie EM, *Epoxy Adhesive Formulations*, McGraw-Hill: New York; 2006.
[3] Zheng S, in: Pascault JP, Williams RJJ, eds. *Epoxy Polymers. New Materials and Innovations*, Wiley-VCH; 2010, Chapter 5.
[4] Chen J-S, Ober CK, Poliks MD, *Polymer* **43**: 131-139 (2002).
[5] Chen J-S, Ober CK, Poliks MD, Zhang Y, Wiesner U, Cohen C, *Polymer* **45**: 1939-1950 (2004).
[6] Sastri VR, Tesoro GC, *J Appl Polym Sci* **39**: 1425-1437 (1990), *ibid.* **39**: 1439-1457 (1990).
[7] Wang L, Li H, Wong CP, *IEEE Trans Electron Packag Manuf* **24**: 115-122 (2001).
[8] Giménez R, Fernández-Francos X, Salla JM, Mantecón A, Serra A, Ramis X, *Polymer* **46**: 10637-10647 (2005).
[9] Arasa M, Ramis X, Salla JM, Mantecón A, Serra A, *Polym Degrad Stab* **92**: 2214-2222 (2007).
[10] González L, Ramis X, Salla JM, Mantecón A, Serra A, *Polym Degrad Stab* **92**: 596-604 (2007).
[11] Morell M, Erber M, Ramis X, Ferrando F, Voit B, Serra A, *Eur Polym J* **46**: 1498-1509 (2010).
[12] Bagheri R, Marouf BT, Pearson RA, *Polym Rev* **49**: 201-225 (2009).
[13] Pascault JP, Sauterau H, Verdu J, Williams RJJ, *Thermosetting Polymers*. Marcel Dekker: New York 2002.
[14] Pearson R A, Yee AF, *Polymer* **34**: 3658-3670 (1993).
[15] Boogh L, Pettersson B, Månson JAE, *Polymer* **40**: 2249-2261 (1999).
[16] Mezzenga R, Boogh L, Månson JAE, *Compos Sci Technol* **61**: 787-795 (2001).
[17] Meng Y, Zhang XH, Du BY, Zhou BX, Zhou X, Qi JR, *Polymer* **52**: 391-399 (2011).
[18] Van Benthem RATM, *Prog Org Coat* **40**: 203-214 (2000).
[19] Foix D, Khalyavina A, Morell M, Voit B, Lederer A, Ramis X, Serra A, *Macromol Mater Eng* **297**: 85-94 (2012).
[20] Morell M, Ramis X, Ferrando F, Serra A, *Polymer* **52**: 4694-4702 (2011).
[21] Foix D, Erber M, Voit B, Lederer A, Ramis X, Mantecón A, Serra A, *Polym Degrad Stab* **95**: 445-452 (2010).
[22] Flores M, Fernández-Francos X, Ferrando F, Ramis X, Serra A, *Polymer* **53**: 5232-5241 (2012).
[23] Moore JS, Stupp SI, *Macromolecules* **23**: 65-70 (1990).
[24] Schallausky F, Erber M, Komber H, Lederer A, *Macromol Chem Phys* **209**: 2331-2338 (2008).
[25] Schmaljohann D, Komber H, Voit B, *Acta Polym* **50**: 196-204 (1999).
[26] Brostow W, Chiu R, Kalogeras IM, Vassilikou-Dova A, *Mater Lett* **62**: 3152-3155 (2008).
[27] Ramis X, Salla JM, Mas C, Mantecón A, Serra A, *J Appl Polym Sci* **92**: 381-393 (2004).
[28] Castell P, Galià M, Serra A, Salla JM, Ramis X, *Polymer* **41**: 8465-8474 (2000).
[29] Kubisa P, Penczek S, *Prog Polym Sci* **24**: 1409-1437 (1999).
[30] Morell M, Lederer A, Ramis X, Voit B, Serra A, *J Polym Sci Part A: Polym Chem* **49**: 2395-2406 (2011).
[31] Barone L, Carciotto S, Cicala G, Recca A, *Polym Eng Sci* **46**: 1576-1582 (2006).
[32] Ivin KJ, in: Brandrup J, Immergut EH, eds. *Polymer Handbook*, Wiley: New York; 1975.
[33] Sperling LH, *Introduction to Physical Polymer Science*. Wiley Interscience: Hoboken; 2006**,** p 573.
[34] Nielsen LE, *J Macromol Sci Macromol Chem* **C3(1)**: 69-103 (1969).
[35] Zhang J, Guo Q, Fox B, *J Polym Sci Part B: Polym Phys* **48**: 417-424 (2010).
[36] Levita G, Petris SD, Marchetti A, Lazzeri A, *J Mater Sci* **26**: 2348-2352 (1991).

Chapter 7

Enhanced chemical reworkability of DGEBA thermosets cured with rare earth triflates using aromatic hyperbranched polyesters (HBP) and multiarm star HBP-b-poly(ε-caprolactone) as modifiers

ENHANCED CHEMICAL REWORKABILITY OF DGEBA THERMOSETS CURED WITH RARE EARTH TRIFLATES USING AROMATIC HYPERBRANCHED POLYESTERS (HBP) AND MULTIARM STAR HBP-*b*-POLY(ε-CAPROLACTONE) AS MODIFIERS

Adrian M. Tomuta,[1] Xavier Fernández-Francos,[1] Francesc Ferrando,[2] Xavier Ramis,[3] Àngels Serra[1]

[1] Department of Analytical and Organic Chemistry, Universitat Rovira i Virgili, C/ Marcel·lí Domingo s/n, 43007, Tarragona, Spain.

[2] Department of Mechanical Engineering, Universitat Rovira i Virgili, C/ Països Catalans, 26, 43007, Tarragona, Spain.

[3] Thermodynamics Laboratory, ETSEIB Universitat Politècnica de Catalunya, Av. Diagonal 647, 08028, Barcelona, Spain.

Abstract

A hyperbranched aromatic polyester (HBPOH) has been synthesized and poly(ε-caprolactone) arms have been grown on some of its end hydroxyl groups (HBPCL). These modifiers have been used in cationic DGEBA formulations cured with ytterbium triflate as cationic initiator. The effect of HBPOH and HBPCL on the curing kinetics has been studied using differential scanning calorimetry (DSC). The obtained materials have been characterized by dynamomechanical analysis (DMA), DSC, thermogravimetric analysis (TGA) and mechanical tests. The modifiers are incorporated into the thermosetting network because of the participation of the end hydroxyl groups in the cationic curing of epoxides by the activated monomer mechanism. Homogeneous thermosets have been obtained with a remarkable increase in impact strength without sacrificing elastic modulus or hardness. A compromise between the rigid structure of the aromatic hyperbranched core and the flexibilizing effect of the poly(ε-caprolactone) arms is believed to be responsible for the overall thermal and mechanical properties of the materials. The use of these polymeric modifiers increases the thermal stability of the resulting materials because of the low degradability of the aromatic ester groups in the hyperbranched core and the incorporation of the modifier into the network structure. However, the presence of such ester groups makes them reworkable by hydrolysis or alcoholysis in an alkaline medium, thus opening a way for recovery of valuable substrates.

Keywords: DGEBA, thermoset, hyperbranched polymer, impact strength, reworkability.

7.1. Introduction

Epoxy resins are commonly used as thermosetting materials due to their excellent thermomechanical properties and chemical and environmental stability.[1] They present also good processability before curing. Their broad range of applications can be explained due to the fact that they are probably one of the most versatile thermosets because not only the type of resin and the chemistry of the curing can be varied, but also a huge number of organic and inorganic modifiers and fillers can be added to improve their properties.[2] Among them, hyperbranched polymers (HBPs) are a class of dendritic polymers which are very promising in terms of processability because of the low entanglement that leads to low viscosities in comparison to linear polymers.[3] By partial or complete modification of their numerous hydroxyl terminal groups, it is possible to tune their interaction with the matrix or facilitate their covalent linkage to the epoxy matrix, which can lead to phase separated or homogeneous morphologies. The presence of non-modified reactive groups in the HBP shell can improve the interaction in the interphase between the separated particles and the matrix.

Although rigidity and strength are desired properties in engineering applications, toughness is one of the restrictions in the use of epoxy resins. The low toughness, coming from the high crosslinking density, affects the durability of coatings and places strong constraints on design parameters.[4] Good toughening is achieved in phase-separated morphologies because of the concurrence of different energy absorption mechanisms in phase-separated morphologies.[5-7] To overcome the limitations of rubbers or linear thermoplastics used as tougheners, which leads to a reduction of the thermomechanical characteristics and to an increased viscosity before curing, the use of hyperbranched polymers (HBPs) has been proposed by several authors.[8-12] We have recently reported that significant toughening can take place without sacrificing thermal-mechanical properties by a proper choice of a hyperbranched core and its partial modification with end 10-undecenoyl chains,[13] which leads to phase-separated morphologies but with some compatibility by the partial covalent bonding between the matrix and the particles.

Reworkability of cured thermosets, under controlled thermal or chemical conditions, is also desirable because it allows the recovery of valuable substrates in several applications once the service life of the component is over. The thermal reworkability of epoxy thermosets has been found to depend on the presence of thermally labile groups such as esters of tertiary alkyl moieties in the monomer structure,[14] which can degrade easily upon heating leading to a fast network breakdown with a dramatic loss in thermal and mechanical properties. A different approach consists in the use of comonomers with ester groups which can get incorporated into the network structure, facilitating the thermal degradation of the resulting materials.[15,16] Recently, we have reported that hyperbranched poly(ester-amide)s can be used in epoxy formulations with an enhanced thermal degradability.[17,18] However, using hyperbranched aromatic polyesters as modifiers the opposite effect was obtained but, nevertheless, chemical reworkability of the modified thermosets in a basic hydrolytic medium was still possible.[19]

In the present work we have synthesized poly(ε-caprolactone) stars (HBPCL) using a hyperbranched aromatic polyester (HBPOH) as a core and used both polymers as modifiers in DGEBA formulations cured with ytterbium triflate. In a previous work, we found that the use of a multiarm star with poly(ε-caprolactone) arms and a hyperbranched core was advantageous from the processability point of view in comparison with linear polymers,[20] and because of the superior mechanical properties of the resulting materials. The synthesized dendritic structures have been characterized by GPC, NMR, DSC and rheometric measurements. The curing kinetics has been studied by DSC. The thermal and dynamomechanical properties have been determined using DSC, TGA and DMA. The global shrinkage on curing has been calculated from the densities of the material before and after curing. The chemical reworkability has been studied by treating the materials in a basic medium and determining the evolution of the T_g. Mechanical characteristics such as the Young modulus, microhardness and impact strength have also been evaluated.

7.2. Experimental

7.2.1. Materials

3,5-Dihydroxybenzoic acid, N,N'-dicyclohexylcarbodiimide (DCC), tin 2-ethylhexanoate ($Sn(Oct)_2$) and ytterbium (III) trifluoromethanesulfonate ($Yb(OTf)_3$) were supplied by Sigma-Aldrich and used without further purification. ε-Caprolactone (CL, Sigma-Aldrich) was dried over CaH_2 and subsequently distilled under vacuum. Diglycidyl ether of Bisphenol A (DGEBA) Epikote Resin 828 was provided by Shell Chemicals with an epoxy equivalent of 184 g/eq and was dried in vacuum before use.

All the organic solvents were purchased from Scharlab and purified by standard procedures. 4-(N,N-dimethylamino) pyridinium p-toluenesulfonate (DPTS) was prepared as described in the literature.[21] All the solvents were purchased in Scharlab and were purified by standard procedures.

7.2.2. Synthesis of the aromatic hyperbranched polyester (HBPOH)

HBPOH was synthesized as reported previously by M. Erber et al.[22] In a flask fitted with magnetic stirrer and septum, 3,5-dihydroxybenzoic acid (15 g, 97.2 mmol) and DPTS (4.98 g, 16.8 mmol) were introduced and then it was flushed with argon. 120 mL of dried N,N-dimethylformamide were added via a syringe through the septum and the mixture was stirred until the reagents were dissolved. After cooling in an ice bath, N,N'-dicyclohexylcarbodiimide (DCC) (20 g, 97.2 mmol) was added to the flask and then stirred at room temperature for 48 h. Once the reaction was completed, the formed urea derivative was filtered out and carefully washed with solvent. Subsequently, the polymer solution was precipitated in CH_2Cl_2, then dissolved in THF and precipitated again in an acidic water solution (HCl, 1 %). After filtration, the precipitate was dried at 50°C in vacuum to yield a whitish powder (75 % of conversion). ^{1}H NMR in (400 MHz, DMSO, δ in ppm): 9.75 broad (OH), 8.2-7.7 (m, H_{ar}, dendr.), 7.6-7.4 (m, H_{ar} lineal), 7.2-6.9 (m, H_{ar} lineal, H_{ar} term.), 6.53 (m, $H_{ar,}$term.). $\overline{M_w} = 6100$ g/mol, $\overline{M_n} = 4660$ g/mol and molecular weight dispersity D = 1.31 (by SEC). T_g = 138 ºC (by DSC). The amount of hydroxyl

groups was determined according to ISO 2554-1974 standards. The number of hydroxyl groups per molecule was 34.

7.2.3. Synthesis of the multiarm star HBPCL (Scheme 1)

In a 25 mL round bottomed flask 2 g of HBPOH (6.85 mmol OH) were dissolved in 7.82 g (68.5 mmol) of ε-caprolactone at 130 °C under argon atmosphere, under gentle stirring for 1 hour. Then, 4 drops of tin 2-ethylhexanoate were added to the mixture and the temperature was raised to the 150 °C and kept for 24 hours.

After the reaction, the polymer mixture was dissolved in 50 mL of THF and precipitated twice in 500 mL of cold diethyl ether. After filtration, the polymer was dried at 40 °C overnight in a vacuum oven. Conversion: 96 %. T_g = - 30 ºC and T_m = 62 ºC (by DSC). $\overline{M_n} = 12400$ g/mol , $\overline{M_w} = 20000$ g/mol and molecular weight dispersity 1.7 (by SEC), 7.1 as the number of arms per molecule and 29.3 as the average polymerization degree of the arms, both determined by ^{1}H-NMR analysis.

^{1}H NMR (**Figure 1**) (400 MHz, CDCl3), δ (in ppm): 1.34-1.49 m (-CH_2-); 1.55-1.62 m (-CH_2-); 2.3-2.4 m (-CH_2-); 3.6 m (-CH_2-); 4.0 m (-CH_2-).

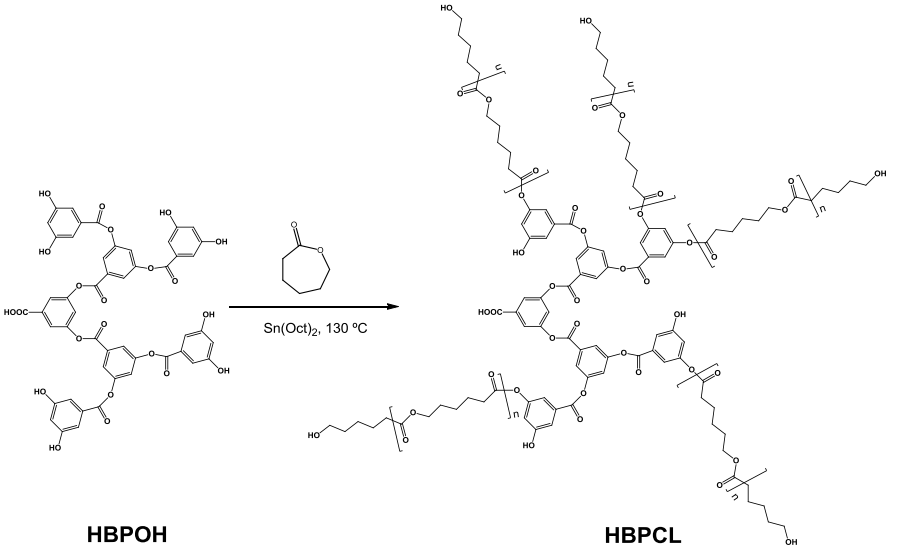

Scheme 1. Chemical structures of HBPOH and HBPCL.

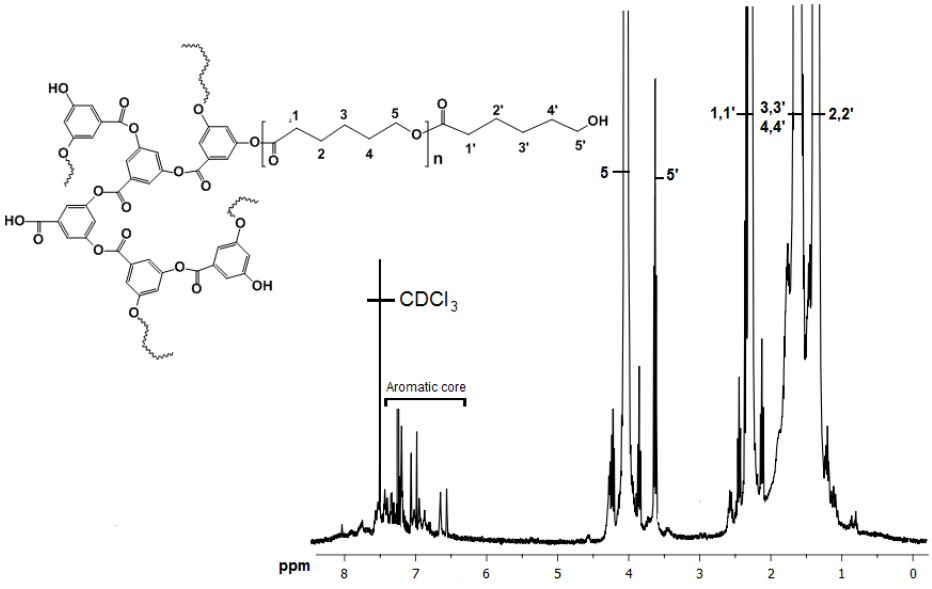

Figure 1. ^{1}H NMR spectrum of the multiarm star synthesized in $CDCl_3$ with the corresponding assignments.

7.2.4. Preparation of the curing mixtures

Mixtures containing DGEBA and the selected proportion of the modified HBP were heated gently using a thermal gun until the modifier was dissolved and the solution became clear. The mixture was then cooled down to room temperature and added to the corresponding amount of initiator previously dissolved in a small amount of acetone. The samples were carefully stirred and were kept under vacuum at 40 ºC for 20 minutes to remove the acetone. The samples were kept at -18 ºC before use to prevent polymerization. The HBP was used at a concentration of 5 or 10 % with respect to the DGEBA. The initiator was used at a concentration of 1 phr with respect to the DGEBA.

Table 1 shows the notation and composition of the different formulations studied. It must be noted that it was not possible to prepare the formulation with 10% HBP-OH because of its poor solubility in DGEBA.

Table 1: Composition of the neat and modified formulations with different amounts of HBPOH or HBPCLin weight percentage (%wt.).

Formulation	DGEBA (wt. %)	Yb (wt. %)	HBP (wt. %)
Neat	99.01	0.99	0
5% HBPOH	94.34	0.94	4.72
5% HBPCL	94.34	0.94	4.72
10% HBPCL	90.09	0.90	9.01

Samples for thermal and mechanical characterization were cured isothermally in a teflon mold at 130 ºC for 2 h and then post-cured for 1.5 h at 170 ºC.

7.2.5. Characterization

The 400 MHz ^{1}H-NMR and 100.6 MHz ^{13}C-NMR spectra were obtained with a Varian Gemini 400 spectrometer with Fourier Transformed. ^{1}H-NMR spectra were acquired in 1 min and 16 scans with a 1.0 s relaxation delay (D1). $DMSO_6$ was used as a solvent and tetramethylsilane (TMS) as internal standard.

Calorimetric analyses were carried out on a Mettler DSC822e thermal analyzer. Samples of ~ 10 mg in weight were placed in aluminum pans under nitrogen atmosphere. The calorimeter was calibrated using an indium standard (heat flow calibration) and an indium-lead-zinc standard (temperature calibration).

Non-isothermal curing experiments were performed from 50 to 250 ºC at heating rates of 2, 5, 10 and 15 ºC/min to determine the reaction heat and the kinetic parameters. In a non-isothermal curing process, the degree of conversion by DSC was calculated as follows

$$\text{Conversion} = \frac{\Delta H_T}{\Delta H_{dyn}} \qquad (1)$$

, where ΔH_T is the heat released up to a temperature T, obtained by integration of the calorimetric signal up to this temperature, and ΔH_{dyn} is the total reaction heat associated with the complete conversion of all reactive groups.

The synthesized polymers were analyzed by DSC on a heating scan at 10ºC/min from -100 to 200 ºC. The glass transition temperature (T_g) was determined as the halfway point in the heat capacity step during the glass transition. The fusion peak temperature (T_m) and the fusion enthalpy (Δh_m) were determined using a straight baseline for the integration. The glass transition temperature (T_g) of cured samples was determined by DSC on a heating scan at 20 ºC/min as the halfway point in the heat capacity step during the glass transition.

The linear integral isoconversional, model-free method of Kissinger-Akahira-Sunose (KAS)[23,24] was used for the determination of the activation energy based on the dynamic curing curves. The kinetic model was determined using the so-called composite integral method.[25,26] A list of available models can be found in the literature.[27-29]

Rheometric measurements were carried out in a parallel plate geometry (disposable aluminium plates 25 mm diameter) mode with an ARG2 rheometer (TA Instruments, UK, equipped with electrical heated plates, EHP). Complex viscosity (η^*) of the pre-cured mixtures was recorded as function of angular frequency (0.05 – 100 rad/s) with a constant deformation of 50 % at 40 ºC.

Thermogravimetric analysis was carried out in a nitrogen atmosphere with a Mettler TGA/SDTA 851e/LF/1100 thermobalance. Samples with an approximate mass of 8 mg were degraded between 30 and 800 ºC at a heating rate of 10 ºC/min in a nitrogen atmosphere (100 cm^3/min measured in normal conditions).

Dynamic mechanical analyses were carried out with a TA Instruments DMA Q800. Single cantilever bending at 1 Hz and 0.05 % strain was performed at 3 ºC/min, from 40 ºC to 200 ºC on prismatic rectangular samples (10 x 9 x 1.5 mm^3).

The Young's modulus was determined using DMA. A three point bending assembly has been used for this test in order to obtain flexural modulus of elasticity in a non-destructive test. The support span of the assembly was 10 mm and a load rate of 3 N/min was used. In this testing configuration, the maximum stress is in the central section of the beam. The modulus of elasticity is calculated, like in previous works,[13] using the slope of the load deflection curve in accordance with Eq. 2

$$E_f = \frac{S^3 m}{4bd^3} \qquad (2)$$

in this formula the following parameters are used:

- E_f = flexural modulus of elasticity (MPa)
- S = support span (mm)
- b = width of test beam (mm)
- d = depth of tested beam (mm)
- m = the gradient (i.e., slope) of the initial straight-line portion of the load deflection curve (P/D) (N/mm)

The impact test was performed at room temperature by means of an Izod 5110 impact tester, according to ASTM D 4508-05 (2008) using rectangular samples (25.4 x 12.7 x 2 mm^3). The pendulum employed had a kinetic energy of 0.5 J. For each material, 9 determinations were made. The impact strength (IS) was calculated from the energy absorbed by the sample upon fracture as

$$\mathrm{IS} = \frac{E - E_0}{S} \qquad (3)$$

, where E and E_0 are the energy loss of the pendulum with and without sample respectively, and S is the cross-section of the samples.

Microhardness was measured with a Wilson Wolpert (Micro- Knoop 401MAV) device following the ASTM D1474-98 (2002) standard procedure. For each material 10 determinations were made with a confidence level of 95 %. The Knoop microhardness (HKN) was calculated from the following equation

$$HKN = \frac{L}{A_p} = \frac{L}{l^2 C_p} \qquad (4)$$

, where L is the load applied to the indenter (0.025 kg), A_p is the projected area of indentation in mm^2, l is the measured length of long diagonal of indentation in mm, C_p is the indenter constant (7.028×10^{-2}) relating l^2 to A_p. The values were obtained from 10 determinations with the calculated precision (95 % of confidence level).

The fracture area of samples were metalized with gold and observed with a scanning electron microscopy (SEM) Jeol JSM 6400. The samples were fractured by impact at room temperature.

Chemical reworkability was studied by saponification in a solution 1M of KOH in ethanol under reflux conditions. Samples were removed at different saponification times and, after drying, their T_g was measured by DSC.

7.3. Results and discussion

7.3.1. Synthesis and characterization of the modified hyperbranched polymers

Multiarm star polymers can be synthesized by the so-called core first strategy using as core a previously synthesized aromatic hyperbranched polyester, HBPOH in the present study. From the terminal OH of the core molecule poly(ε-caprolactone) arms were grown, from the corresponding monomer by a cationic ring opening mechanism catalyzed by $Sn(Oct)_2$. In the case of aliphatic hydroxyl groups this procedure allows the control of the length of the arms by the proper selection of the proportion of the monomer to the OH groups in the core structure by its leaving character. The synthetic pathway is depicted in **Scheme 1**.

^{1}H-NMR spectra allows determining the length of the PCL arms by measuring the areas of the peaks 5 and 5' of the spectrum in **Figure 1**, by the use of the following formula:

$$\overline{DP}_{arm} = \frac{I_5}{I_5'} + 1 \qquad (5)$$

In the spectrum in **Figure 1** the core signals can be appreciated as a complex multiplet in the aromatic zone. The central methylene protons of the ε-caprolactone unit in the arms appear between 1.4 and 1.7 ppm. The protons directly attached to carbonyl group (1 and 1') appear overlapped at 2.3 ppm. The signals of the protons 5 and 5', attached to the oxygen of ester in the repeating unit or to hydroxyl terminal group, which appear separately, are the ones that can be easily integrated. The use of the signals of carbons 5 and 5' for DP evaluation of the arms is possible due to the absence of PCL homopolymer, which was confirmed by SEC analysis. From the calculations we obtained a higher length of the arms than expected, 29 CL units by each arm. If we consider that the molar proportion of ε-CL monomer to phenol group used in the synthesis was about

10, we get to the conclusion that not all the 34 arms per molecule grow, but only an average of 7.1. The growth of PCL from phenolic groups with $Sn(Oct)_2$ has been described recently,[30] but no other references appear in the literature. Thus, it seems that phenol groups are less reactive than alcohols and therefore once the aliphatic OH group is formed in the first attack of the phenol to CL, it is able to react much more easily than another phenol group.

Figure 2 compares the conversion curves obtained from the curing thermograms of the neat formulations and the formulations with 5 % of HBPOH and 5 and 10 % of HPBCL initiated by $Yb(OTf)_3$.

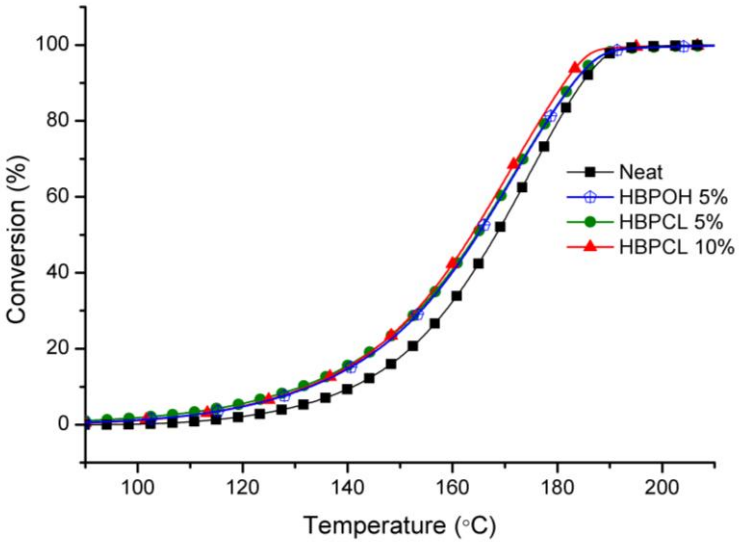

Figure 2. Degree of conversion against temperature of the curing of the neat and the modified formulations at 10ºC/min in nitrogen atmosphere

It is observed a clear decrease in the curing temperature upon addition of both HBPOH and HBPCL with respect to the neat DGEBA formulation. However, there is no relevant difference between any of the modified formulations. As reported previously by Kubisa and Penczek,[31] hydroxylic compounds are known to participate in the cationic curing of epoxides following the so-called activated monomer (AM) mechanism, by which a hydroxylic group attacks a tertiary oxonium ion leading to a chain-transfer of an active proton to an unreacted epoxy group. The secondary oxonium ion formed can then propagate the polymerization by the active chain-end mechanism (ACE), leading to the formation of another hydroxyl chain end and another tertiary oxonium ion. Hydroxyl-terminated HBPs are known to accelerate the cationic curing of epoxides because of their participation in the curing process by the AM mechanism.[11,32] However, their effect is complex and may also depend on the amount of HBP incorporated into the reactive mixture.[33] In fact, the opposite effect was obtained using poly(ε-caprolactone) star polymers with a hyperbranched polyglycidol as the core.[20] The lower mobility of the

species formed by the participation of the HBP in the curing process or the deactivation of the cationic active species by ether groups present in the network structure[34] may offset the acceleration produced by the occurrence of the AM mechanism. In the present case the accelerating effect is remarkable, especially taking into account that, as seen in **Figure 3**, the use of these multiarm stars produces an increase in the viscosity of the mixture, thus decreasing the mobility of the propagating species. However, the complex viscosity of the formulations containing up to a 10 % of HBPCL remains in the adequate values to maintain the processability. In a previous paper on the use of multiarm stars with polyglycidol core and PCL arms it was proved the advantage of star topologies in comparison to linear PCL to maintain a limited viscosity of the formulation.[20]

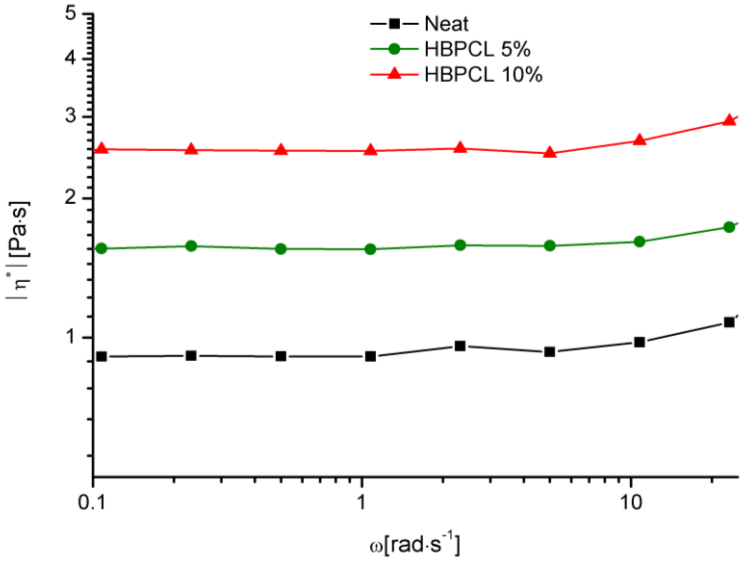

Figure 3. Complex viscosity η* with respect to angular frequency, at 40ºC, of the neat and modified formulations with HBPCL.

Table 2 summarizes relevant data from the curing of the formulations. It is observed that the reaction heat of all formulations is around or slightly below 100 kJ/ee, the theoretical reaction heat for epoxy polymerization.[35] The present results are in good agreement with previously reported data of DGEBA cured with rare earth triflates,[34,36] indicating that the participation of the dendritic modifiers in the curing process did not affect the extent of the reaction of epoxy groups. In Table 2 we also show the values of T_g after the dynamic curing at 10 ºC/min. Both HBPOH and HBPCL reduce the T_g of the materials, apparently because of their participation in the curing process. Their effect on the thermomechanical properties will be discussed in more detail in the following section.

The curing kinetics was analyzed following the methodology described in section 2.5. In **Figure 4** it is observed how the activation energy of the process remains practically constant, with values between 75 and 85 kJ/mol without a well-defined trend

between the different formulations. The model that best described the curing was found to be the R2 model with $f(x)=2\cdot(1-x)^{1/2}$ and $g(x)=1-(1-x)^{1/2}$. Elucidation of the curing mechanism on the basis of fitting of data to simple phenomenological models should be avoided. However, it is possible to use the results as a means of comparison between the different formulations. Using the R2 model, we have detailed in **Table 2** the pre-exponential factor and the kinetic constant at 0.5 conversion calculated at 170 ºC and as can be observed, both modifiers have a similar accelerating effect, in agreement with previous results.[30]

Table 2. Calorimetric data and kinetic parameters obtained from the dynamic curing of the formulations.

Formulations	ΔH (J/g)	ΔH[a] (kJ/ee)	T_{max}[b] (ºC)	T_g[c] (ºC)	E_a[d] (kJ/mol)	ln$A$[e] (s^{-1})	$k_{170°}$[f] (min^{-1})
Neat	537	99	176	144	81.3	20.18	0.153
5% HBPOH	447	87	177	139	78.8	19.70	0.187
5% HBPCL	465	90	171	126	69.8	19.48	0.186
10% HBPCL	479	97	170	110	80.0	20.09	0.198

a. Enthalpies per equivalent of epoxy group.
b. Temperature of the maximum of the curing exotherm at 10 ºC/min.
c. Glass transition temperature after a dynamic curing at 10 ºC/min, determined on a second DSC scan at 20 ºC/min.
d. Apparent activation energy at 50% conversion determined by the isoconversional non-isothermal procedure.
e. Pre-exponential factor calculated for R2 model at 50% conversion.
f. Kinetic constant at 170ºC calculated using the Arrhenius equation at 50% conversion and the R2 model

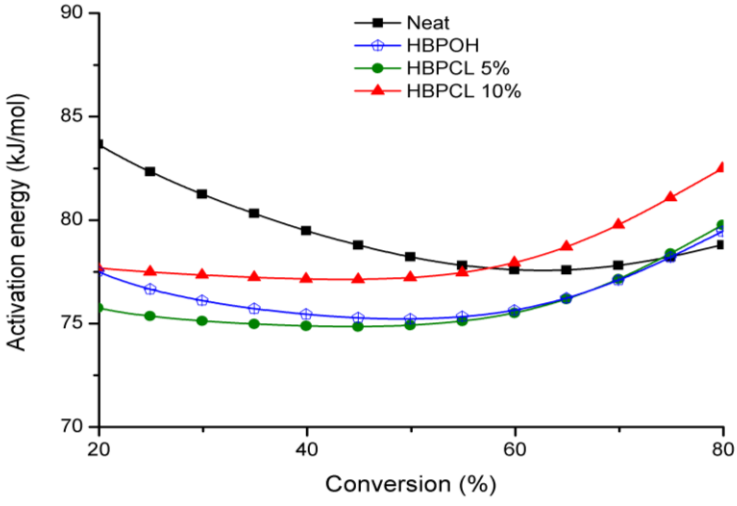

Figure 4. Apparent activation energy during curing of the neat and the modified formulations.

7.3.2. Mechanical and thermo mechanical properties of the thermosets

Table 3 summarizes the results of the dynamomechanical and thermal analysis of the samples prepared following the curing schedule described in section 2.4. **Figure 5** plots the evolution of tan δ with temperature during the DMA analysis of the materials.

Table 3. Relevant DMA and TGA data of the cured neat and modified formulations.

Formulation	DMA			TGA		
	Young Modulus (GPa)	$T_{tan\ \delta}$ [b] (ºC)	E'_r [c] (Mpa)	T_{onset} [d] (ºC)	T_{max} [e] (ºC)	Char Yield[f] (°C)
Neat	2.5	152	38	314	355	15.49
5% HBPOH	3.1	141	25	324	368	16.28
5% HBPCL	2.8	137	27	333	377	13.72
10% HBPCL	2.3	117	15	345	392	14.95

a. % by weight of 140 multiarm star polymer.
b. Temperature of maximum of the tan δ at 1 Hz.
c. Relaxed modulus determined at the $T_{tan\delta}$ + 40 ºC.
d. Temperature of the onset decomposition on the TGA data at 10 ºC/min calculated for a 5 % of weight loss.
e. Temperature of the maximum decomposition rate based on the TGA data at 10 C/min.
f. Solid residue at 800ºC.

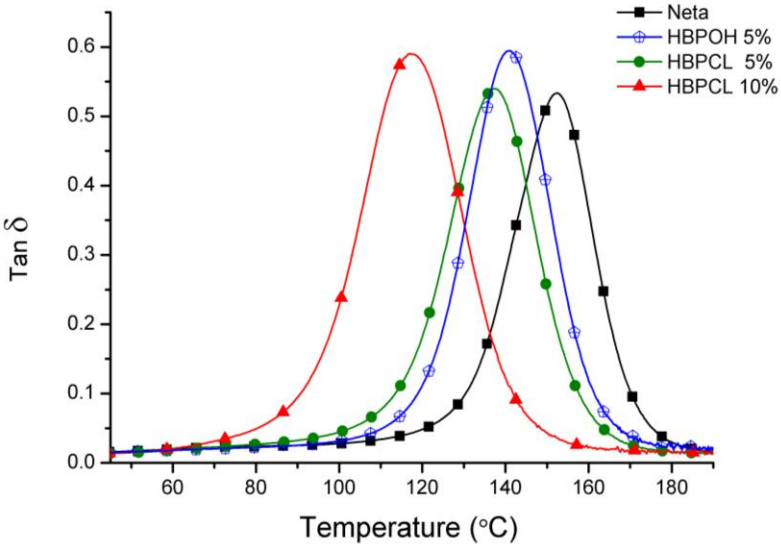

Figure 5. Tan δ against temperature curves of the cured materials.

It can be observed that, upon addition of 5 % of the modifiers to the formulation, the T_g of the resulting material decreases only slightly, but upon further addition up to 10% of HBPCL the effect becomes relevant. The relaxed modulus of the formulation decreases only discretely when 5 % of the modifier is added but the effect becomes more significant

when 10 % of HBPCL is added. Given that the relaxed modulus after the relaxation decreases on adding the modifiers, as seen in **Table 3,** we hypothesize that their presence may reduce the crosslinking density due to their participation in the curing process along with certain plasticizing effect of the long poly(ε-caprolactone) arms.

The use of HBPOH leads to a significant increase in elastic modulus due to its rigid aromatic structure and its incorporation into the network structure. However, the effect of the aromatic core is partially offset by the long poly(ε-caprolactone) arms, which reduce its value because of their plasticizing effect, reaching a value lower than that of the unmodified formulation with 10% of HBPCL. Overall, these results are comparable to those obtained previously in the modification of cationic DGEBA formulations with a multiarm poly(ε-caprolactone) star using polyglycidol as core,[20] in spite of the different core structure, degree of modification and arm length.

The results of the impact strength and the microhardness measurements of the cured materials are shown in **Figure 6** and **Figure 7** respectively. It can be seen that all the modifiers produce an increase in impact strength, which is as high as 45 % when 10 % HBPCL is added to the formulation. Given that the use of these modifiers results in homogeneous materials with a lower crosslinking density and T_g, it is hypothesized this is a consequence of an *in-situ* reinforcement caused by the loosening of the network structure and plasticization of the cured material. The use of 5 % HBPOH results in a significant increase in the microhardness due to the rigid structure of the aromatic hyperbranched, but when HBPCL is used the value of microhardness decreases slightly, because of the loosening and plasticizing effect of the poly(ε-caprolactone) arms. This effect is similar to that on the elastic modulus.

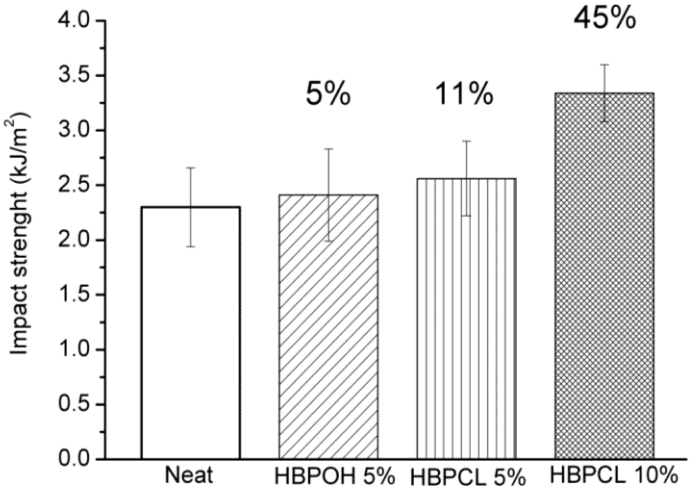

Figure 6. Impact strength of the neat and modified formulations.

In comparison with previous results obtained with multiarm poly(ε-caprolactone) stars using a polyglycidol core,[20] the use of HBPCL seems to be advantageous in that it is achieved a comparable enhancement in impact strength without sacrificing

microhardness or elastic modulus, which can be attributed to the high rigidity of the aromatic hyperbranched core.

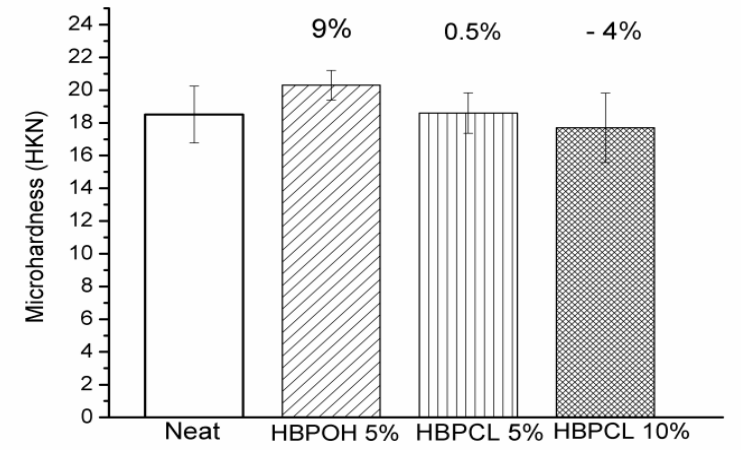

Figure 7. Microhardness of the neat and modified formulations.

Figure 8 shows the SEM micrographs of the fractured surfaces of the materials after the impact strength test. No significant morphological features are present, in agreement with our previous analysis of DMA data, resulting from the incorporation of the polymeric modifier into the network structure. All the pictures show features which are typical of a brittle fracture, especially for neat DGEBA. Only for the formulation with 10 % HBPCL a somewhat higher concentration of shear bands are observed, resulting from plastic deformation upon fracture, in agreement with the higher impact strength shown in **Figure 6**.

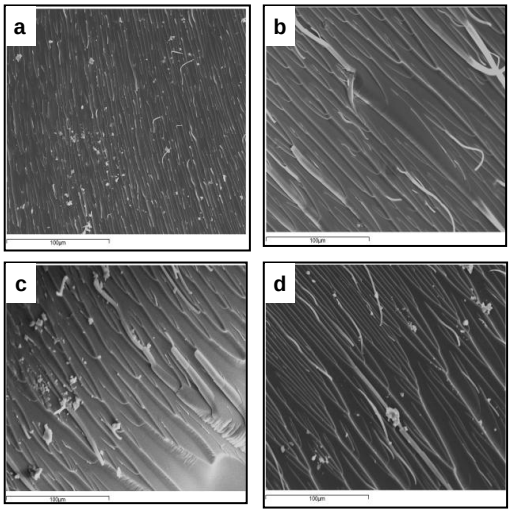

Figure 8. SEM micrographs of the fractured surface of the cured formulations (a) neat, (b) 5% HBPOH, (c) 5% HBPCL and (d) 10% HBPCL.

7.3.3. Thermal and chemical degradability

Figure 9 shows the thermal degradation curves of the cured materials. It can be seen that the degradation process takes place in one single step between 300 and 450 ºC for all the cured materials. In spite of the presence of a higher proportion of ester groups in the thermoset with the incorporation of HBPOH and HBPCL into the DGEBA formulations, no decrease in the thermal stability was observed but just the contrary behaviour, especially in the initial degradation temperature, as collected in **Table 3** and as illustrated in **Figure 9**. This is a feature previously observed when aromatic-aliphatic hyperbranched polyesters were used as modifiers in DGEBA formulations.[19] We can attribute this to the higher thermal stability of the aromatic hyperbranched core and the fact that aromatic and primary aliphatic esters are not easily degradable in comparison with labile aliphatic tertiary esters.[14] However, ester groups can be readily degraded by basic hydrolysis, thus opening a way for chemical reworkability, as previously reported.[19]

Table 4 shows how, upon saponification in KOH/ethanol in reflux conditions, the T_g of the materials modified with HBPOH and HBPCL decreases significantly, in contrast with the neat formulation, which can be explained by the fact that the network structure is modified by the incorporation of the dendritic structures containing chemically labile groups.

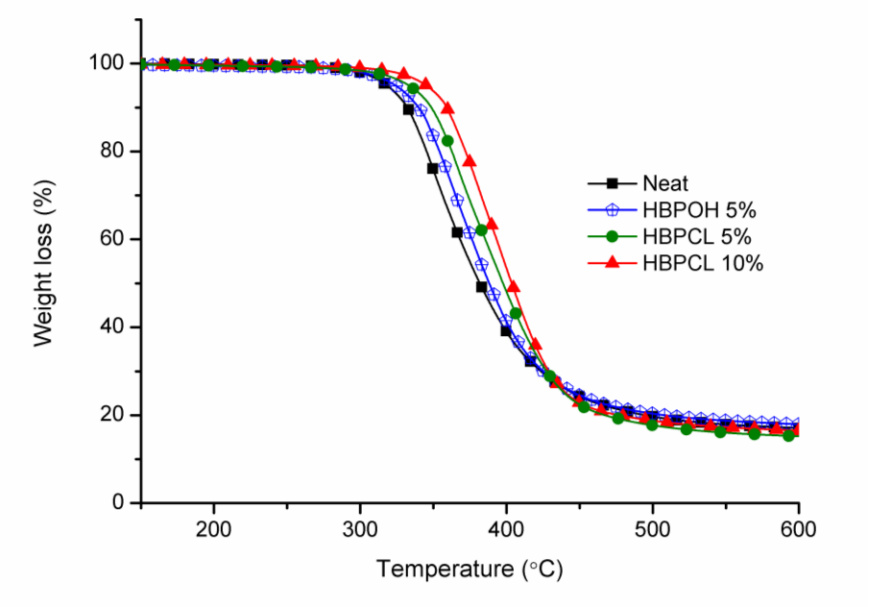

Figure 9. TGA mass loss curves of the cured formulations at 10ºC/min in nitrogen atmosphere.

Table 4. T_g (in ºC) determined on a dynamic DSC scan at 20ºC/min after saponification in KOH/EtOH solution at different times.

Formulation	Saponification time (hours)					
	0	**2**	**4**	**10**	**15**	**24**
Neat	145	145	144	142	142	140
5% HBPOH	139	135	131	123	116	88
5% HBPCL	129	125	118	108	97	78
10% HBPCL	122	116	112	101	91	63

7.4. Conclusions

A core-first strategy has been followed to synthesize a multiarm star with an aromatic hyperbranched core and poly(ε-caprolactone) arms. Previously, an aromatic hyperbranched polyester with final OH groups (HBPOH) has been synthesized following an AB_2 polycondensation procedure. Poly(ε-caprolactone) arms have been grown on some of the final OH groups of HBPOH, Both polymers have been used as modifiers in DGEBA formulations cured with ytterbium triflate as cationic initiator.

The use HBPOH and HBPCL accelerates the curing process because of the participation of the end OH groups of the poly(ε-caprolactone) arms and end phenol groups in the activated monomer mechanism (AM) occurring during cationic curing of epoxides. Because of that, both modifiers can get incorporated into the network structure. This effect is significant enough to offset the discrete increase in the viscosity of the formulations.

A significant increase in Young modulus has been obtained with HBPOH because of its rigid aromatic structure but with little effect on the impact strength. The use of HBPCL may result in a significant enhancement of impact strength but a somewhat negative effect in the elastic modulus and microhardness, because of the plasticizing effect of the poly(ε-caprolactone) arms. In all cases, a reduction in T_g was observed, because the participation of the modifiers in the curing process leads to the loosening of the network structure and because of the plasticizing effect of the poly (ε-caprolactone) arms.

The modified materials have a higher thermal stability than the neat DGEBA thermoset but chemical reworkability of the materials is still possible because of the significant amount of ester groups introduced into the network structure.

Acknowledgements

The authors would like to thank MINECO (MAT2011-27039-C03-01, MAT2011-27039-C03-02) and Generalitat de Catalunya (2009-SGR-1512) for giving financial support. X.F-F. acknowledges the contract JCI-2010-06187 granted by MINECO and A.T. the grant FI-DGR 2010 given by the Generalitat de Catalunya.

References

[1] May CA, ed. *Epoxy Resins: Chemistry and Technology*. 2nd ed.Marcel Dekker: New York; 1988.
[2] Petrie EM, *Epoxy adhesive formulations*. McGraw-Hill: New York; 2006.
[3] Voit B, Lederer A, *Chem Rev* **109**: 5924-5973 (2009).
[4] Bagheri R, Marouf BT, Pearson RA, *Polym Rev* **49**: 201-225 (2009).
[5] Brooker R.D, Kinloch AJ, Taylor AC, *J Adhesion* **86**: 726-741 (2010).
[6] Qian JY, Pearson RA, Dimonie VL, Shaffer OL, El-Aasser MS, *Polymer* **38**: 21-30 **(**1997).
[7] Ruiz-Pérez L, Royston GJ, Fairclough JPA, Ryan AJ, *Polymer* **49**: 4475-4488 (2008).
[8] Boogh L, Pettersson B, Manson J-AE, *Polymer* **40**: 2249-2261 (1999).
[9] Ratna D. Simon G.P, *Polymer* **42**: 8833-8839 (2001).
[10] Ratna D, Varley Rm Simon GP, *J Appl Polym Sci* **89**: 2339-2345 (2003).
[11] Sangermano M, Malucelli G, Bongiovanni R, Priola A, Harden A, *Polym Int* **54**: 917-921 (2005).
[12] Zhang D, Jia D, *J Appl Polym Sci* **101**: 2504-2511 (2006).
[13] Flores M, Fernández-Francos X, Ferrando F, Ramis X, Serra A, *Polymer* **53**: 5232-5241 (2012).
[14] Chen JS, Ober CK, Poliks MD, *Polymer* **43**: 131-139 (2002).
[15] González L, Ramis X. Salla JM, Mantecón A, Serra A, *Polym Degrad Stabil* **92**: 596-604 **(2007)**.
[16] Gimenez R, Fernandez-Francos X, Salla JM, Serra A, Mantecon A, Ramis X, *Polymer* **46**: 10637-10647 (2005).
[17] Morell M, Ramis X, Ferrando F, Yu Y, Serra A, *Polymer* **50**: 5374-5383 (2009).
[18] Fernandez-Francos X, Rybak A, Sekula R, Ramis X, Ferrando F, Okrasa L, Serra A, *J Appl Polym Sci* **128**: 4001-4013 (2012).
[19] Foix D, Erber M, Voit B, Lederer A, Ramis X, Mantecón A, Serra A, *Polym Degrad Stabil* **95**: 445-452 (2010).
[20] Morell M, Ramis X, Ferrando F, Serra A, *Polymer* **52**: 4694-4702 (2011).
[21] Moore JS, Stupp SI, *Macromolecules* **23**: 65-70 (1990).
[22] Erber M, Boye S, Hartmann T, Voit BI, Lederer A, *J Polym Sci Part A: Polym Chem* **47**: 5158-5168 (2009).
[23] Starink MJ, *Thermochim Acta* **404**: 163-176 (2003).
[24] Gonzalez S, Fernandez-Francos X, Salla JM, Serra A, Mantecon A, Ramis X, *J Appl Polym Sci* **104**: 3407-3416 (2007).
[25] Diefallah E-HM, *Thermochim Acta* **202**: 1-16 (1992).
[26] Budrugeac P, Segal E, *J Therm Anal Calorim* **82**: 677-680 (2005).
[27] Ramis X, Salla JM, Cadenato A, Morancho J, *J Therm Anal Calorim* **72**: 707-718 (2003).
[28] X. Ramis, J. M. Salla, C. Mas, A. Mantecon and A. Serra, *Journal of Applied Polymer Science* **92**: 381-393 (2004).
[29] Vyazovkin S, Wight CA, *Thermochi Acta* **340-341**: 53-68 (1999).
[30] Tomuta AM, Ramis X, Fernández-Francos X, Ferrando F, Serra A, *Express Polym Lett* **7**: 595-606 (2013).
[31] Kubisa P, Penczek S, *Prog Poly Sci* **24**: 1409-1437 (1999).
[32] Sangermano M, Priola A, Malucelli G, Bongiovanni R, Quaglia A, Voit B, Ziemer A, *Macromol Mat Eng* **289**: 442-446 (2004).

[33] Fernández-Francos X, Foix D, Serra A, Salla JM, Ramis X, *React Funct Polym* **70**: 798-806 (2010).
[34] Santiago D, Morell M, Fernández-Francos X, Serra A, Salla JM, Ramis X, *React Funct Polym* **71**: 380-389 (2011).
[35] Ivin KJ, in: Brandrup J, Immergut EH, eds. *Polymer Handbook*, Wiley: New York; 1975.
[36] González S, Fernández-Francos X, Salla JM, Serra A, Mantecon A, Ramis X, *J Polym Sci Part A: Polym Chem* **45**: 1968-1979 (2007).

Chapter 8

New epoxy-anhydride thermosets modified with multiarm stars with hyperbranched polyester cores and poly(ε-caprolactone) arms

NEW EPOXY-ANHYDRIDE THERMOSETS MODIFIED WITH MULTIARM STARS WITH HYPERBRANCHED POLYESTER CORES AND POLY(ε-CAPROLACTONE) ARMS

Adrian M. Tomuta,[1] Xavier Fernández-Francos,[1] Francesc Ferrando,[2] Àngels Serra,[1] Xavier Ramis[3]

[1] Department of Analytical and Organic Chemistry, Universitat Rovira i Virgili, C/ Marcel·lí Domingo s/n, 43007, Tarragona, Spain.

[2] Department of Mechanical Engineering, Universitat Rovira i Virgili, C/ Països Catalans, 26, 43007, Tarragona, Spain.

[3] Thermodynamics Laboratory, ETSEIB Universitat Politècnica de Catalunya, Av. Diagonal 647, 08028, Barcelona, Spain.

Abstract

Multiarm star polymers with hyperbranched aromatic or aromatic-aliphatic cores and poly(ε-caprolactone) arms have been used as toughness modifiers in epoxy-anhydride formulations catalyzed by benzyldimethylamine. The curing process has been studied by dynamic scanning calorimetry, demonstrating the slight influence of the mobility of the reactive species and the hydroxyl content on the kinetics of this process. The obtained materials have been characterized by thermal and mechanical tests and the microstructure by electron microscopy. Homogeneous thermosets have been obtained with a remarkable increase in impact strength without compromising glass transition temperature, thermal stability or hardness.

Keywords: Hyperbranched, epoxy resin, multiarm star, toughness.

8.1. Introduction

Epoxy resins are a class of high-performance thermosetting polymers, which display a unique combination of properties: high strength and stiffness, low creep, excellent corrosion resistance and appropriate electrical properties. However, in terms of structural applications, epoxy resins are in general brittle and notch sensitive.[1] As a result, a considerable effort has been made during the past years to improve the toughness of epoxy thermosets.[2] The most successful strategy for improving toughness is the incorporation of a second dispersed phase within the epoxy matrix that allows a better dissipation of impact energy.[3] In the last years hyperbranched polymers (HBPs)[4,5,6] and more recently star polymers (SPs)[7,8] have demonstrated to be very interesting epoxy toughenners. They are able to enhance the flexibility of the network and increase toughness without compromising other properties, such as hardness, modulus or glass transition temperature.[9] The improvement in toughness in the case of HBPs and SPs is attributed either to the flexibilizing effect induced by the homogeneous incorporation of

the dendritic polymer, to local inhomogeneities created in the crosslinked network by the different degree of local curing reached or by the formation of phase separated nano- and micro-particles with good interfacial adhesion between phases.[10] Enhancement of interfacial adhesion can be reached via chemical incorporation of the modifier into epoxy matrix or by establishment of effective physical interactions.

In a previous work it was shown that partial modification of hydroxy terminal groups of Boltorn H30 with unpolar 10-undecenoyl moieties made it possible to tune the interaction between this modifier and the epoxy-anhydride matrix, leading to phase separated or homogeneous morphologies. The presence of non-modified reactive groups in the HBP shell can improve the interaction at the interphase between the separated particles and the matrix. Concretely, when the degree of modification of hydroxyl groups with 10-undecenoyl moieties was a 76%, a phase separated material was obtained and more than a 4-fold increase in impact resistance was achieved.[11]

Multiarm stars with poly(ε-caprolactone) arms and hyperbranched aromatic polyester core (Ar-PCL) or aliphatic-aromatic polyester core (Alar-PCL) were synthesized and used as modifiers in DGEBA formulations cured with ytterbium triflate as cationic initiator.[12,13] In both studies the materials obtained were homogeneous, the glass transition temperatures of the final materials decreased only slightly and toughness was improved, but a somewhat negative effect in the elastic modulus and microhardness, because of the plasticizing effect of the poly(ε-caprolactone) arms, was observed. In a different study, aliphatic-aromatic hyperbranched polyesters ended in long or short unreactive vinylic chains were used as toughness modifiers of epoxy-anhydride formulations.[14] An enhancement in impact strength without compromising the glass transition temperature and thermal stability was observed, but this improvement was only limited due to the absence of reactive terminal groups, which did not promote a good interfacial adhesion between matrix and modifier.

Taking into account the above results, the aim of the present work is to improve the toughness of epoxy-anhydride thermosets by the addition of Ar-PCL and Alar-PCL multiarm stars. The structures of the materials used are represented in **Scheme 1**.

Epoxy-anhydride polycondensation can be initiated by hydroxyl terminal groups of Ar-PCL and Alar-PCL, since hydroxyl groups can react with anhydrides giving rise to monocarboxylic esters and carboxyl acid groups, which in turn can react with epoxides to produce a hydroxyester or can protonate the epoxy group giving rise to an activated monomer that leads to polyetherification.[15] In both cases, multiarm stars can become covalently incorporated to the matrix or enhance the interfacial adhesion between phases, if present. The different degree of polymerization, length and amount of arms and core structures, aromatic or aromatic-aliphatic, of the multiarm stars used as modifiers, will tailor the final material properties.

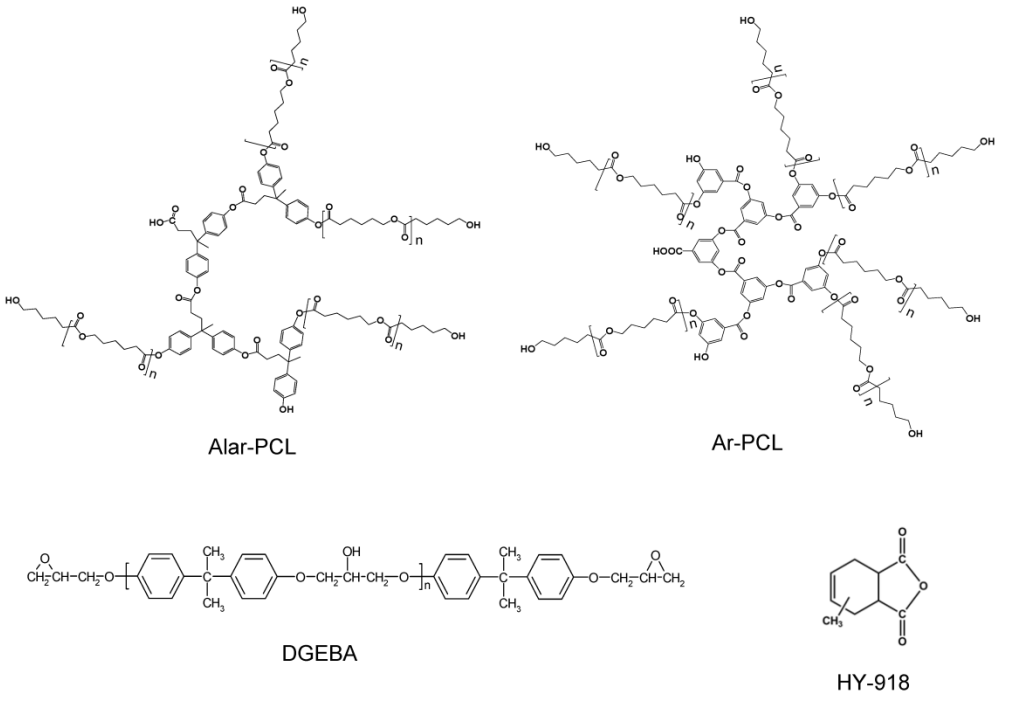

Scheme 1. Structure of the multiarm stars, resin and curing agent used.

8.2. Experimental

8.2.1. Materials

Diglycidylether of Bisphenol A (DGEBA), Epikote Resin 828 from Hexion Specialty Chemicals (epoxy equivalent = 187 g/eq) was used after drying under vacuum. Methyltetrahydrophatalic anhydride (MTHPA), Aradur HY-918 (166 g/mol) and benzyldimethylamine initiator (BDMA), DY 062, from Huntsman were used as received.

Two multiarm stars with poly(ε-caprolactone) arms and hyperbranched aromatic (Ar-PCL) or aliphatic-aromatic (Alar-PCL) core were previously synthesized by us[12,13] by cationic ring opening polymerization of ε-caprolactone from an aromatic or aliphatic-aromatic hyperbranched polyester synthesized following two previously reported procedures.[16,17] The relevant structural parameters and properties of these star polymers are the following:

Alar-PCL: T_g = -22 ºC and T_m = 53 ºC (by DSC). $\overline{M_n}$ = 39,500 g/mol, $\overline{M_w}$ = 88,100 g/mol and molecular weight dispersity 2.2 (by SEC), 5 as the number of arms per molecule and 65 as the average polymerization degree of the arms, both determined by ^{1}H-NMR analysis.

Ar-PCL: T_g = -38 ºC and T_m = 53 ºC (by DSC). $\overline{M_n}$ = 12,400 g/mol, $\overline{M_w}$ = 20,000 g/mol and molecular weight dispersity 1.7 (by SEC), 7.1 as the number of arms per

molecule and 29.3 as the average polymerization degree of the arms, both determined by ^{1}H-NMR analysis.

8.2.2. Preparation of the curing mixtures

DGEBA/MTHPA formulations were prepared by adding the appropriate amounts of each reactant and catalyst to a vial and homogenizing them by mechanical stirring. For the preparation of the formulations with Ar-PCL and Alar-PCL appropriate amounts of DGEBA and HBP were heated up to 150 ºC with a thermal gun and the mixture was homogenized by mechanical stirring; after cooling down, anhydride was added and the resulting mixture was homogenized. Finally, the adequate proportion of catalyst was added and the mixture was homogenized again. Samples were kept at -20 ºC before use to prevent polymerization. For all formulations, the amount of catalyst was 1 phr (parts per hundred grams) with respect to the anhydride. The amount of both modifiers was 5% or 10% with respect to the DGEBA/MTHPA mixture. **Table 1** shows the notation and composition of the different formulations studied.

Table 1. Composition of the formulations studied in this work with different weight percentage of star polymer (indicated in the first column) in percentage by total weight (wt.%) of the mixture and in equivalent ratio, (Xeq).

Formulation	DGEBA		MTHPA		BDMA	
	Xeq	wt.%	Xeq	wt.%	Xeq	wt.%
Neat	1	52.0	1	48.0	0.0065	0.52
Ar-PCL-5%	0.93	48.1	1.07	46.9	0.0061	0.50
Ar-PCL-10%	0.88	44.2	1.14	45.8	0.0061	0.50
Alar-PCL-5%	0.93	48.3	1.07	46.9	0.0061	0.50
Alar-PCL-10%	0.88	44.2	1.14	45.8	0.0061	0.50

Samples for DMTA and thermogravimetric analysis, mechanical tests and electron microscopy were cured isothermally in a mould at 140ºC for 1 h and then post-cured for 1 h at 170ºC.

8.2.3. Characterization techniques

Calorimetric measurements (DSC)

Calorimetric analyses were carried out on a Mettler DSC-822e thermal analyzer. Samples of approximately 10 mg were placed in aluminum pans under nitrogen atmosphere. The calorimeter was calibrated using an indium standard (heat flow calibration) and an indium-lead-zinc standard (temperature calibration).

Non-isothermal curing was performed from 0 to 300ºC at heating rates of 2, 5, 10 and 20 ºC/min to determine the reaction heat associated with the complete conversion of all reactive groups and study the curing kinetics. In a non-isothermal curing process, the degree of conversion by DSC is calculated as follows:

$$\alpha = \frac{\Delta h_T}{\Delta h_{dyn}} \qquad (1)$$

where Δh_T is the heat released up to a temperature T, obtained by integration of the calorimetric signal up to this temperature, and Δh_{dyn} is the total reaction heat associated with the complete conversion of all reactive groups.The linear integral isoconversional, model-free method of Kissinger-Akahira-Sunose (KAS) was used for the determination of the activation energy based on the non-isothermal curing curves.[18,19]

$$\ln\left(\frac{\beta}{T^2}\right) = \ln\left(\frac{A\,R}{g(\alpha)E}\right) - \frac{E}{RT} \qquad (2)$$

β is the heating rate, T the temperature, E the activation energy, A the pre-exponential factor, R the gas constant, and $g(\alpha)$ the integral conversion function. For each conversion degree, the representation of $\ln(\beta/T^2)$ versus $1/T$ produces a straight line and makes it possible to determine E and $\ln[AR/g(\alpha)E]$ from the slope and the intercept without knowing the kinetic model.

The glass transition temperatures ($T_{g\infty}$s) of the obtained thermosets were determined after non-isothermal curing at 10 ºC/min by means of a second scan at 10 ºC/min, as the temperature of the half-way point of the jump in the heat capacity when the material changed from glassy to the rubbery state under N_2 atmosphere and the error is estimated to be approximately ± 1°C. No residual curing exotherm was detected.

Gelation

Rheometric measurements were carried out in the parallel plates (geometry of 25 mm) mode with an ARG2 rheometer (TA Instruments, UK, equipped with electrical heated plates, EHP). The curing was monitored at 100ºC in order to determine the gel point and the conversion at gelation.

Because the visco-elastic properties change dramatically during the curing process a control program was used in which the oscillation amplitude decreases and the applied stress increases as the elastic modulus G' or the viscous modulus G" increase. Gel time was taken as the point where tan δ is independent of frequency.[20] The conversion at the gelation (α_{gel}) was determined by stopping the rheology experiment at gelation and performing a subsequent dynamic DSC scan at 10 ºC/min of the gelled sample.

Dynamomechanical analysis (DMTA)

DMTA was carried out with a TA Instruments DMA Q800. Single cantilever bending at 1 Hz and 0.05 % strain was performed at 3 ºC/min from 30 to 200 ºC on prismatic rectangular samples (ca. 0.5 x 12 x 25 mm^3).

The Young's modulus was determined using DMTA. A three point bending assembly has been used for this test in order to obtain flexural modulus of elasticity in a non-destructive test. The support span of the assembly was 10 mm and a load rate of 3 N/min was used. In this testing configuration, the maximum stress is in the central section of the beam. The modulus of elasticity is calculated using the slope of the load deflection curve in accordance with the following equation:

$$E_f = \frac{L^3 m}{4bd^3} \qquad (3)$$

E_f is the flexural modulus of elasticity (MPa), L the support span (mm), b the width of test beam (mm), d the depth of tested beam (mm) and m the gradient (i.e., slope) of the initial straight-line portion of the load deflection curve (P/D) (N/mm).

Thermogravimetric analysis (TGA)

Thermogravimetric analysis was carried out in a nitrogen atmosphere with a Mettler TGA/SDTA 851e/LF/1100 thermobalance. Samples with an approximate mass of 8 mg were degraded between 30 and 800ºC at a heating rate of 10 ºC/min in a nitrogen atmosphere (100 cm^3/min measured in normal conditions).

Impact resistance

The impact test was performed at room temperature by means of an Izod 5110 impact tester, according to ASTM D 4508-10 (2010) using rectangular samples (25.4 x 12.7 x 2 mm^3). The pendulum employed had a kinetic energy of 0.5 J. For each material, 9 determinations were made. The impact strength (IS) was calculated from the energy absorbed by the sample upon fracture as

$$\mathrm{IS} = \frac{E - E_0}{S} \qquad (4)$$

where E and E_0 are the energy loss of the pendulum with and without sample respectively, and S is the cross-section of the samples.

Microhardness

Microhardness was measured with a Wilson Wolpert (Micro- Knoop 401MAV) device following the ASTM D1474-98 (2008) standard procedure. For each material 10 determinations were made with a confidence level of 95 %. The Knoop microhardness (HKN) was calculated from the following equation:

$$\mathrm{HKN} = \frac{L}{A_p} = \frac{L}{l^2 C_p} \qquad (5)$$

where L is the load applied to the indenter (0.025 kg), A_p is the projected area of indentation in mm^2, l is the measured length of long diagonal of indentation in mm, C_p is the indenter constant (7.028×10^{-2}) relating l^2 to A_p.

Electron microscopy analysis (SEM)

The fracture area of samples were metalized with gold and observed with a scanning electron microscopy (SEM) Jeol JSM 6400 with a resolution of 3.5 nm. The samples examined were previously fractured by impact at room temperature.

8.3. Results and discussion

8.3.1. Curing of DGEBA/MTHPA with different proportions of Ar-PCL and Alar-PCL

The presence of hydroxyl in epoxy-anhydride formulations, coming from the oligomeric DGEBA and both Ar-PCL an Alar-PCL, leads to a complex curing mechanism consisting of polycondensation (initiated by hydroxyl group) and ring-opening polymerization (initiated by tertiary amine),[15,21] the balance between them depending on the relative proportion of epoxy/hydroxyl groups.

Figure 1 shows the plots of degrees of conversion against temperature recorded at 10 ºC/min of neat DGEBA/MTHPA and Ar-PCL and Alar-PCL modified formulations. Calorimetric curves for all formulations showed a unimodal shape, which indicates that the different curing mechanisms occur quasi simultaneously. Although the presence of the multiarm stars does not have a strong influence on the curing, a slight acceleration is observed regardless of the amount and type of modifier. The existence of higher content of hydroxyl groups in formulations containing modifier than in neat formulation, can increase the curing rate via polycondensation mechanism initiated by hydroxyl terminal group of Ar-PCL or Alar-PCL. The slight retarding effect observed in formulations containing 10% of Alar-PCL can be attributed to the participation of less mobile species such as monocarboxylic ester formed between Alar-PCL and anhydride. The overall curing rate is therefore a compromise between different factors such as: hydroxyl group content and mobility of active species.

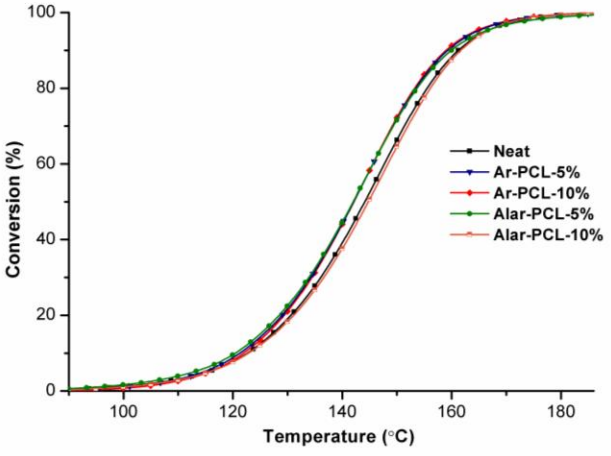

Figure 1. Conversion degrees against temperature of all the formulations studied at a heating rate of 10 ºC/min.

All formulations were cured at several heating rates by DSC. **Table 2** shows the experimental heats of polymerization, Δh, calculated as the average heat of the experiments at different heating rates.

By increasing the proportion of modifier, Δh (J/g) decreases, due to the lower content of reactive epoxy and anhydride groups, whereas Δh (kJ/ee) remains almost constant and similar to the values reported in the literature.[15,22,23,24] FTIR spectra of cured samples showed that the absorbance bands at 913 cm^{-1} and at 1860-1780 cm^{-1}, attributed to the oxirane and anhydride groups respectively, disappeared completely. Moreover, no residual heat was observed after a second dynamic scan made up to 250 ºC to determine T_g. All these results indicate that epoxides/anhydrides have reacted almost completely.

Table 2. Average heat evolved during non-isothermal curing of all formulations Δh in J/g and kJ/ee (kJ/epoxy equivalent). Glass transition temperature of the samples cured at 10ºC/min T_g, calculated glass transition temperature, using DSC data and Fox equation $T_{g,Fox}$, and conversion at the gel point α_{gel} and gelation time t_{gel}.

Formulation	Δh (J/g)	Δh (kJ/ee)	T_g (ºC)	$T_{g,Fox}$ (ºC)	α_{gel}	t_{gel} (min)
Neat	321	114	123	123	0.38	29.7
Ar-PCL-5%	281	107	112	110	0.40	23.4
Ar-PCL-10%	263	109	109	98	0.35	21.6
Alar-PCL-5%	275	105	113	112	0.41	28.1
Alar-PCL-10%	268	111	105	101	0.36	26.9

Figure 2 shows that activation energy remains almost constant during curing of the neat and modified formulations, which indicates that the different mechanisms take place at the same time and in a similar way in the whole range of conversion. Neat and Alar-PCL-10% formulations have higher activation energy, in agreement with their lower curing rate (**Figure 1**). The slightly lower activation energy of Alar-PCL-5% formulation, in comparison with those containing Ar-PCL, with similar curing rates, can be explained by the compensation effect between the activation energy and the pre-exponential factor.[25]

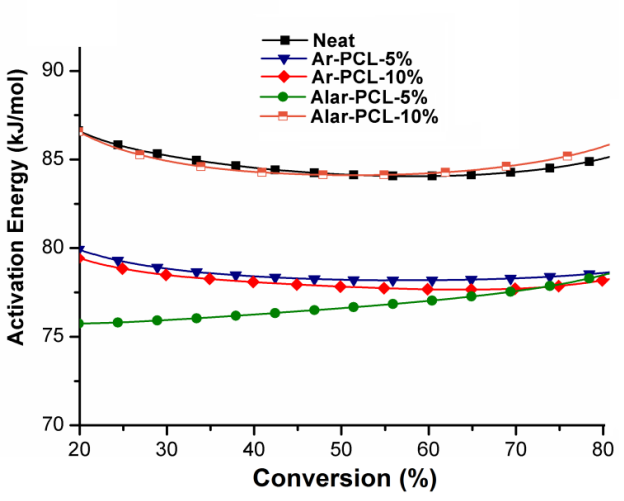

Figure 2. Apparent activation energy during curing of all formulations studied obtained by using the Kissinger-Akahira-Sunose method.

As observed in the table, on increasing the proportion of multiarm star in the formulation the T_g of the material decreases, but this decrease is not much affected by the type of modifier. In order to verify the effect of Ar-PCL and Alar-PCL on the matrix, the Fox equation was used to predict the T_g of the cured materials.[26,27] **Table 2** shows that the calculated values for both modifiers are only slightly lower than the experimental ones. Although this result may suggest that a small part of modifier forms a separate phase, electron microscopy did not show evidence of a second phase observable at the resolution of the SEM device. It can be hypothesized that a strong chemical or physical interaction between modifier and matrix, or even the presence of physical entanglements, which may limit network mobility and therefore increase the T_g, can explain this behavior. Covalent bonds formed by reaction between terminal hydroxyl groups of multiarm star and anhydride and hydrogen bonding between modifier and matrix are the largest interactions expected.

The results of the gelation tests are summarized in **Table 2**. The gelation time slightly decreases with the proportion of modifier. Conversion at the gel point slightly decreases also with the multiarm star content. This result suggests that the network formation process is not strongly affected by the addition of Ar-PCL or Alar-PCL and therefore similar crosslinked densities are expected in the modified materials.

8.3.2. Characterization of the thermosets

Table 3 summarizes the results of the dynamomechanical and thermogravimetric analysis of the samples prepared following the isothermal curing schedule described in the experimental section. **Figure 3** and **4** plots the evolution of tan δ and storage modulus with temperature during the DMTA analysis of the materials, respectively.

Table 3. Relevant DMTA and TGA data of the cured neat and modified materials.

Formulation	DMTA			TGA		
	Young modulus (GPa)	$T_{\tan\delta}$ [a] (ºC)	E' [b] (MPa)	T_{onset} [c] (ºC)	T_{max} [d] (ºC)	Char Yield [e] (°C)
Neat	3.6	135	19	340	398	5.74
Ar-PCL-5%	3.9	130	15	316	405	6.74
Ar-PCL-10%	3.7	123	16	317	404	7.77
Alar-PCL-5%	3.8	135	12	324	401	6.25
Alar-PCL-10%	3.6	126	14	337	409	7.73

a. Temperature of maximum of the tan δ at 1 Hz.
b. Modulus in the rubbery state determined at temperature of maximum tan δ + 50ºC.
c. Temperature of the onset decomposition determined by TGA in nitrogen atmosphere at 10 ºC/min calculated for a 5 % of weight loss.
d. Temperature of the maximum decomposition rate determined by TGA in nitrogen atmosphere at 10 ºC/min.
e. Char residue at 800 °C determined by TGA in nitrogen atmosphere at 10 ºC/min.

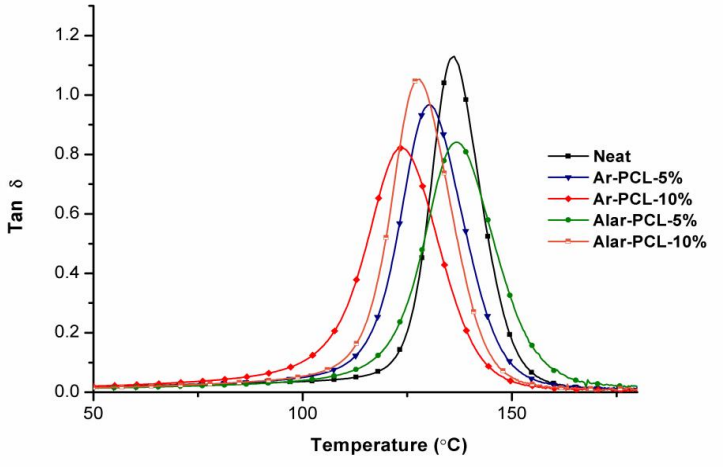

Figure 3. Tan δ versus temperature at 1 Hz of neat DGEBA/MTHPA and thermosets with Ar-PCL and Alar-PCL.

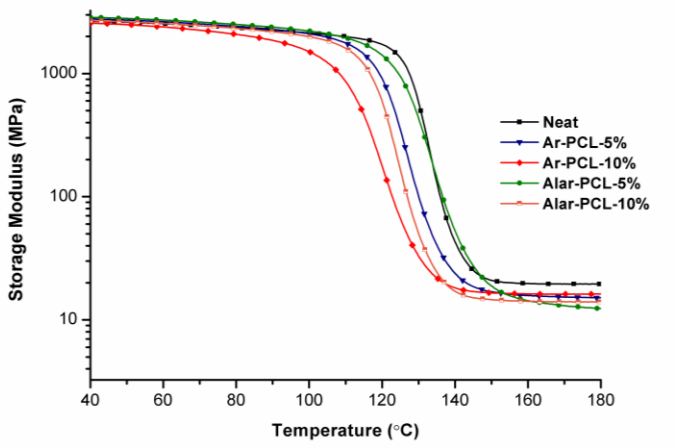

Figure 4. Storage modulus versus temperature at 1 Hz of neat DGEBA/MTHPA and thermosets with Ar-PCL and Alar-PCL.

DMTA curves show a single and unimodal α relaxation, which is typical of single-phase materials, as will be further demonstrated by electronic microscopy. It can be observed that, upon addition of 5 % of the modifiers to the formulation, the maximum of tan δ (T_g) of the resulting material barely decreases and even the formulation containing Alar-PCL the T_g remains unaltered. Upon further addition up to 10% of multiarm stars the decrease becomes more relevant but it is nevertheless low.

The rubbery modulus decreases upon addition of Alar-PCL or Ar-PCL which, according to the rubber elasticity theory,[28] indicates an increase of the molecular weight between crosslinks, resulting from a certain loosening of the network structure by the incorporation of both Ar-PCL and Alar-PCL into the network structure. It is interesting to note the modest *flexibilizing effect* exerted by these modifiers with poly(ε-caprolactone) arms, much less than the ones observed for the modification of DGEBA cured by ytterbium triflate, with linear poly(ε-caprolactone) or stars with poly(glycidol) core.[8] It seems that the more efficient incorporation of hydroxylic stars to the epoxy-anhydride network, coupled with the rigidity of the core, can explain these differences.

Although both modifiers show similar trends, some differences can be detected. Thermosets containing Alar-PCL have larger molecular weight between crosslinks (or lower crosslinking density) but higher T_gs than Ar-PCL materials. Probably, when Ar-PCL is used as modifier, the lower entanglement of its shorter arms compensates for the higher stiffness of its aromatic core leading to materials with lower T_gs. In our previous reports on the modification of DGEBA formulations cured with ytterbium triflate it was observed that higher T_gs were obtained when Alar-PCL was used.[12, 13]

The T_gs obtained by DSC (non-isothermal curing) decrease more than those obtained by DMTA (isothermal curing). This difference should be attributed to the different curing schedule. During non-isothermal curing in DSC, the temperature changes and the balance between de different reactive processes can be significantly altered in

reference to the isothermal curing. Moreover, the higher temperatures reached in DSC can promote the appearance of thermal rearrangements and degradation.

The use of Alar-PCL or Ar-PCL leads to a modest increase in Young moduli due to their rigid structures and their incorporation into the network matrix. Again, the expected flexiblizing effect of poly(ε-caprolactone) arms is hardly observed. Probably, the high degree of entanglement of these chains due to the existence of large number of intermolecular and intramolecular hidrogen bonding can justify this behaviour. This behaviour contrasts with the observed for classical toughness modifiers, which usually reduce Young modulus.[29]

Figure 5 shows that both Alar-PCL and Ar-PCL produce an increase in the impact strength of the cured materials. Taking into account that the use of these modifiers results in homogeneous materials with a slightly lower crosslinking density, it is hypothesized this is a consequence of an *in-situ* reinforcement caused by the loosening of the network structure.[30] The higher impact strength was obtained with 5% of Alar-PCL, in accordance to the lower crosslinking density (**Table 3**), which increases the network mobility and facilitates the dissipation of mechanical energy. However, on comparing both modifiers it is possibly to suspect that other factors such as physical entanglement, matrix-multiarm star interactions and the limited plasticizing effect of poly(ε-caprolactone) arms can also influence the toughness of the studied materials and therefore no general rules can be established for this type of multiarm star modifiers.

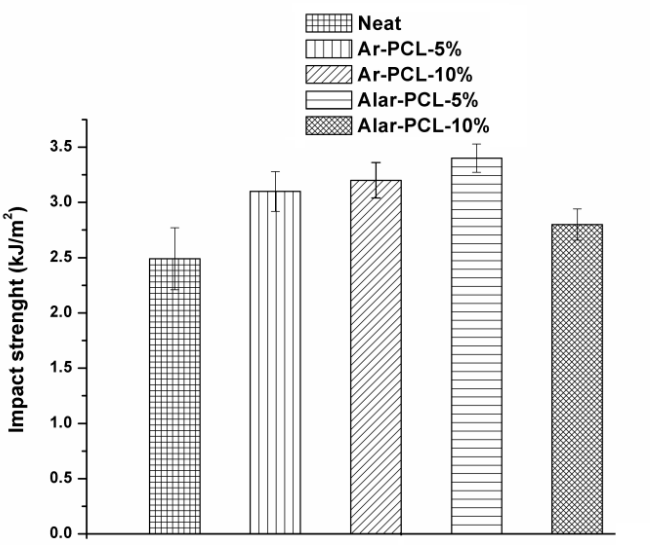

Figure 5. Impact strength of neat DGEBA/MTHPA and thermosets with Ar-PCL and Alar-PCL.

The microhardness measurements have proven to be useful in rating coatings on rigid substrates to know on the resistance that one body offers against penetration to another under static loads**. Figure 6** shows microhardness data for all the materials prepared. In general, the values are not much affected and there is not a systematic trend depending on the type or content of the modifier. Probably, the high rigidity of the aromatic cores in conjunction with the relative high degree of crosslinking and entanglement of the arms of the modified formulations justify the values of microhardness.

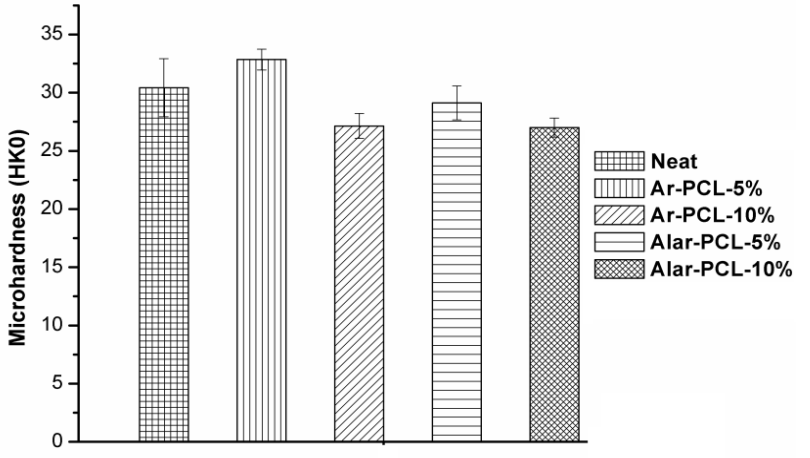

Figure 6. Microhardness of neat DGEBA/MTHPA and thermosets with Ar-PCL and Alar-PCL.

In general the use of Ar-PCL and Alar-PCL seems to be advantageous because it makes it possible to enhance the impact strength without sacrificing microhardness, Young modulus or even glass transition temperature. From the point of view of microhardness, the addition of a 5% of Ar-PCL gives the best result but the addition of a 5% of Alar-PCL leads to the highest improvement in toughness without a significant reduction of the glass transition temperature (**Table 3**) and having virtually the same microhardness as the unmodified material.

Figure 7 shows the SEM micrographs of the fractured surfaces of the materials after the impact strength test. No significant morphological features can be observed, resulting from the incorporation of the polymeric modifier into the network structure and the formation of a homogeneous material. However, under SEM observation particles smaller than 10-20 nm cannot be observed and therefore nanophase separation cannot be discarded. All micrographs show features which are typical of a relatively brittle fracture, especially for neat formulation, with smooth and glassy surface. The fracture surfaces for modified formulations were slightly different from those of the neat DGEBA/MTHPA. These formulations show relatively rough and irregular appearance with filar strips characteristics of more plastic deformation[27,31] in agreement with the

higher impact strength shown in **Figure 5**. A higher concentration of shear bands with stress-whitened zones around the crack, characteristics of toughness enhancement, are observed for the thermoset with 5% of Ar-PCL.

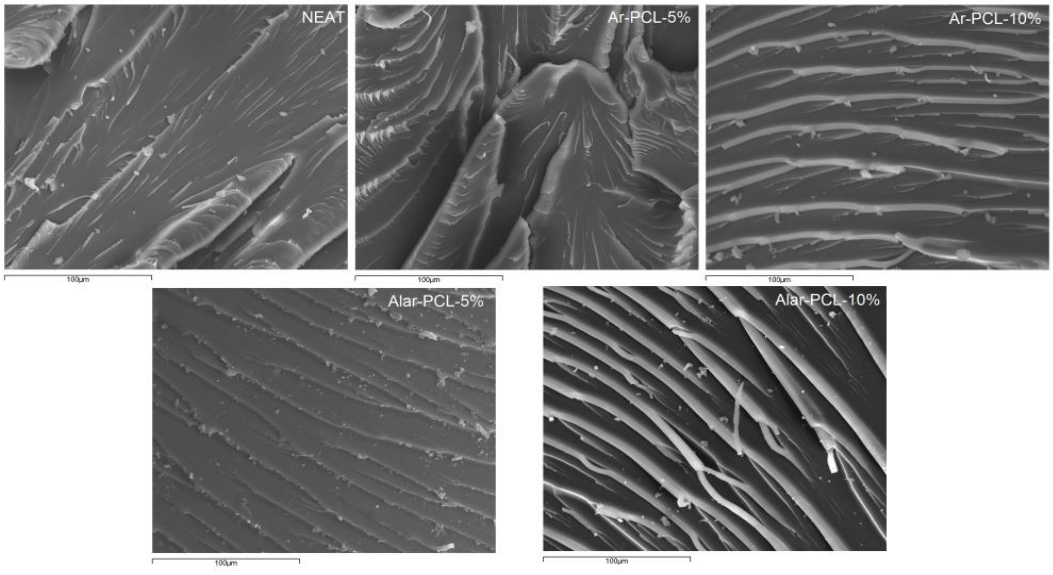

Figure 7. SEM micrographs of the fractured surface of the impacted thermosets.

Figure 8 shows the results of the thermogravimetric analysis in nitrogen atmosphere. Upon addition of Ar-PCL and Alar-PCL the temperature of the maximum degradation rate increases and the onset temperature decreases only slightly, in spite of the presence of a higher proportion of ester groups in the thermoset with the incorporation of Ar-PCL and Alar-PCL into the DGEBA/MTHPA matrix. We can attribute this behaviour to the higher thermal stability of the aromatic and aliphatic-aromatic hyperbranched cores. This higher stability is due to the aromatic character of the esters in both core molecules.

Since the thermal degradability of polyester moieties involves a β-elimination process, which implies a pericyclic reaction involving a six-membered ring in which a proton in γ-position participates,[32,33] the absence of protons in this position prevents the thermal degradation to occur. Ester linkages between core and arms and benzoic esters into the core cannot degrade via β-elimination process and this process can only take place in the poly(ε-caprolactone) arms. **Table 3** shows also the values of char yield at 800ºC. As it can be seen, the presence of these modifiers in the material leads to an increase of this value which is proportional to the amount added to the formulation.

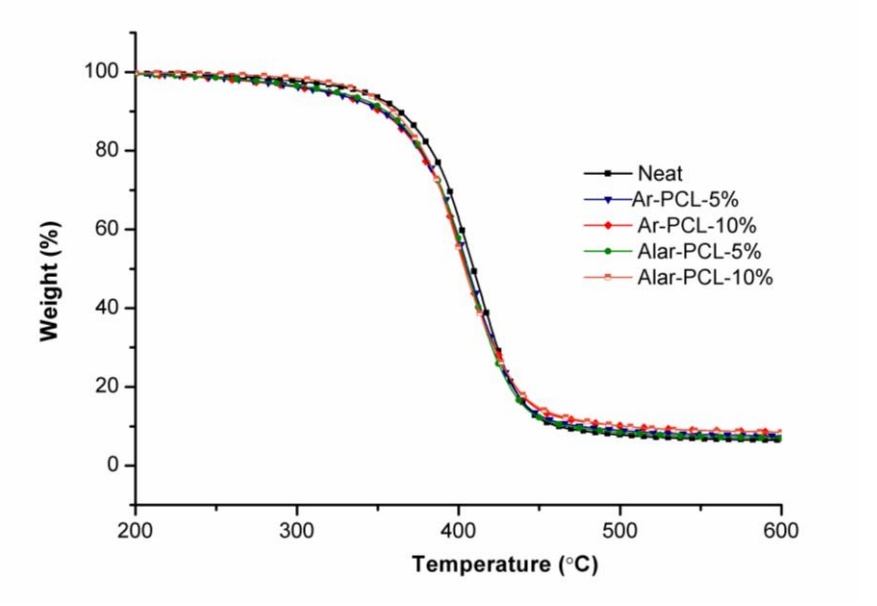

Figure 8. TGA mass loss curves of the cured materials at 10ºC/min in nitrogen atmosphere.

8.4. Conclusions

The use of two multiarm stars polymers, Ar-PCL and Alar-PCL, as modifiers in epoxy-anhydride formulations catalyzed by benzyldimethylamine has been studied. The influence of the mobility of the reactive species and the hydroxyl content on the curing kinetics has been put into evidence.

New epoxy thermosetting materials with improved toughness and Young modulus were obtained with hardly compromise the glass transition temperature, thermal stability and hardness. The new thermosets obtained were homogeneous without any sign of phase separation and the best improvement in impact resistance was obtained with the addition of a 5% of Alar-PCL, which also had the highest glass transition temperature.

The structure and the properties of the resulting thermosets are controlled by the rigidity of the hyperbranched core, the crosslinking density and the amount, length and entanglement of the poly(ε-caprolactone) arms. The compatibility between matrix and modifier through covalent linkages is another factor that controls the toughness improvement.

Acknowledgements

The authors would like to thank MICINN (Ministerio de Ciencia e Innovación) and FEDER (Fondo Europeo de Desarrollo Regional) (MAT2011-27039-C03-01 and MAT2011-27039-C03-02) and to the Comissionat per a Universitats i Recerca del DIUE

de la Generalitat de Catalunya (2009-SGR-1512). A.T. acknowledges the grant FI-DGR 2010 from the Catalonian Government. Huntsman is also acknowledged for giving us products.

References

[1] May CA, ed. E*poxy resins. Chemistry and Technology*. 2nd ed. Marcel Dekker: New York; 1988.
[2] Arends CB, ed. *Polymer Toughening*, Marcel Dekker: New York; 1996.
[3] Bagheri R, Marouf BT, Pearson RA, *J Macromol Sci Part C: Polym Rev* **49**: 201-225 (2009).
[4] Ratna D, Varley R, Simon GP, *J Appl Polym Sci* **89**: 2339-2345 (2003).
[5] Boogh L, Petterson B, Månson JAE, *Polymer* **40**: 2249-2261 (1999).
[6] Zhang D, Jia D, *Polym-Plast Technol* **45**: 1005-1011 (2006).
[7] Meng Y, Zhang XH, Du BY, Zhou BX, Zhou X, Qi JR, *Polymer* **52**: 391-399 (2011).
[8] Morell M, Ramis X, Ferrando F, Serra A. *Polymer*, **52:** 4694-4702 (2011).
[9] Fum J-F, Shi L-Y, Yuan S, Zhang Q-D, Chen Y, Wu J, *Polym Adv Technol* **19**: 15971607 (2008).
[10] Karger-Kocsis J, Fröhlich J, Gryshchuk O, Kautz H, Frey H, Mülhaupt R, *Polymer* **45**: 1185-1195 (2004).
[11] Flores M, Fernández-Francos X, Ferrando F, Ramis X, Serra A, *Polymer* **53**: 5232-5241 (2012).
[12] Tomuta AM, Ramis X, Fernández-Francos X, Ferrando F, Serra A, *Prog Org Coat,* 76:1616-1624 (2013).
[13] Tomuta AM, Fernández-Francos X, Ferrando F, Ramis X, Serra A *Polym Adv Tech,* in press (2013).
[14] Tomuta A, Ferrando F, Serra A, Ramis X *React Funct Polym* **72**: 556-563 (2012).
[15] Fernández-Francos X, Rybak A, Sekula R, Ramis X, Serra A, *Polym Int,* **61**: 1710-1725 (2012).
[16] Erber M, Boye S, Hartmann T, Voit BI, Lederer A, *J Polym Sci Part A: Polym Chem* **47**: 5158-5168 (2009).
[17] Schallausky F, Erber M, Komber H, Lederer A, *Macromol Chem Phys* **209**: 2331-2338 (2008).
[18] Gonzalez S, Fernandez-Francos X, Salla JM, Serra A, Mantecon A, Ramis X, *J Appl Polym Sci* **104**: 3407-3416 (2007).
[19] Vyazovkin S, Burnham AK, Criado JM, Pérez-Maqueda LA, Popesco C, Sbirrazzuoli N, *Thermochim Acta* **520**: 1-19 (2011).
[20] Pascault JP, Saurereau H, Verdu J, Williams RJJ, *Thermosetting Polymers*, Marcel Dekker: New York; 2002.
[21] Morell M, Ramis X, Ferrando F, Yu Y, Serra A. *Polymer* **50:** 5374-5383 (2009).
[22] Xu J, Holst M, Wenzel M, Alig I, *J Polym Sci Part A: Polym Chem* **46**: 2155-2165 (2008).
[23] Montserrrat S, Andreu G. Cortes P, Calventus Y. Colomer P. Hutchinson JM, Malek J, *J Appl Polym Sci* **61**: 1663-1674 (1996).
[24] Montero B, Serra A, Ramirez C, Ramis X, *Polym Comp* **34**: 96-108 (2013).
[25] Vyazovkin S, Wight CA, *Annu Rev Phys Chem* **48**: 125-149 (1997).
[26] Mezzenga R, Månson JAE, *J Mater Sci* **36**: 4883-4891 (2001).
[27] Fox TG. *Bull Am Phys Soc* **1**:123-125 (1956).
[28] Nielsen LE, *J Macromol Sci Macromol Chem* **C3(1)**: 69-103 (1969).
[29] Xiao KQ, Ye L, *Polym Eng Sci* **40**: 2288-2298 (2000).
[30] Zhang D, Jia D, *J Appl Polym Sci* **101**: 2504-2511 (2006).
[31] Yang J-P, Chen Z-K, Yang G, Fu S-Y, Ye L, *Polymer* **49**: 3168-3175 (2008).
[32] Chen J S, Ober C.K, Poliks MD, *Polymer* **43**: 131-139 (2002).
[33] Foix D, Khalyavina A, Morell M, Voit B, Lederer A, Ramis X, Serra A, *Macromol Mat Eng* **297**: 85-94 (2012).

Chapter 9

Global Conclusions

1. A series of dihydrazides, synthesized by reaction of dicarboxylic diester with hydrazine hydrate in ethanol, were used as curing agents for DGEBA epoxy resin and their latent characteristic demonstrated. The temperatures of activation of the curing are dependent on the melting point of crystalline dihydrazides. The addition of a base or a Lewis acid as catalyst accelerates the curing but the latent character is lost. On comparing with DGEBA and DGEBA/anhydride thermosets, much better impact resistance is obtained when dihydrazides are used as curing agent. The flexibility introduced by the dihydrazide structure is the responsible of this behaviour.

2. Novel modified aliphatic-aromatic hyperbranched polyester with vinylic chains of different lengths have been synthesized and used as non-reactive toughening modifier of epoxy/anhydride systems in the presence of a tertiary amine as catalyst. The addition of these modifiers increases significantly the curing rate and the toughness with hardly compromise the thermal stability and the glass transition temperature. The new thermosets obtained are homogenous without any phase separation, but their fracture surface suggests a significant increase in matrix yielding, due to the flexibility introduced by the branched structures.

3. Aliphatic-aromatic hyperbranched polyesters with hydroxyl, undecenoyl or allyl as chain ends were synthesized and used as modifiers in DGEBA/adipic dihydrazides formulations. The addition of these hyperbranched polymers helped to disperse and to compatibilize the crystalline dihydrazide in the reactive mixture. Consequently, the latency of the adipic dihydrazide as epoxy curing agent is reduced, being more noticeable this effect on adding hydroxyl terminated HBPs, which catalyzes the first stages of the curing process. The thermosets obtained show an improvement in microhardness and impact strength without any reduction of the glass transition temperature and even the thermal stability is enhanced. The morphologies of the epoxy thermosets prepared are controlled by the type of terminal groups. Whereas formulations containing HBPs with unreactive vinyl terminal groups show nano or microphase separation, HBPs with reactive hydroxyl groups lead to homogeneous morphologies.

4. Following a core-first strategy, multiarm star polyesters with different structure were obtained. These multiarm star polymers and with an aromatic hyperbranched core and hydroxyl final groups were added as modifier in DGEBA formulations cured with ytterbium triflate as cationic initiator or in DGEBA/anhydride formulations catalyzed by benzyldimethylamine.

5. The addition of a multiarm star with a hyperbranched aliphatic-aromatic polyester core and poly(ε-caprolactone) arms to DGEBA/ytterbium triflate formulations, slightly delays the curing process, reduces the shrinkage on curing and increases the pot life. The homogeneous thermosets obtained show an improvement in impact strength with a discrete reduction of the glass transition temperature proportionally to the amount of modifier. The presence of aromatic and primary aliphatic ester groups in the network structure increases the reworkability in alkaline solutions with the maintenance of thermal stability.

6. In the curing of DGEBA initiated by ytterbium triflate, the addition of a multiarm star with a hyperbranched aromatic polyester core and poly(ε-caprolactone) arms accelerates the curing process because the participation of the end hydroxyl groups in the activated monomer mechanism occurring during cationic curing of epoxides. The thermosets prepared are homogeneous with a remarkable enhancement in impact strength without sacrificing modulus or hardness, but with a reduction in glass transition temperature. A compromise between the rigid structure of the aromatic hyperbranched core and the flexilizing effect of the poly(ε-caprolactone) arms is the responsible of the thermal and mechanical properties of the materials. Chemical reworkability and thermal stability of the thermosets are also improved with both modifiers.

7. The kinetic of curing of DGEBA/anhydride formulations modified by multiarm star polymers with hyperbranched aromatic or aliphatic-aromatic polyester cores and poly(ε-caprolactone) arms, is controlled by the mobility of the reactive species and the hydroxyl content. The thermosets obtained are homogeneous with a remarkable increase in impact strength without compromising glass transition temperature, thermal stability or hardness. The structure and the properties of the resulting materials are controlled by the rigidity of the hyperbranched core, the crosslinking density, the compatibility between matrix and modifier and the amount, length and entanglement of the poly(ε-caprolactone) arms.

Chapter 10

APPENDICES

APPENDIX A: List of acronyms and symbols

α_{gel}	Conversion at gelation
A	Pre-exponential factor
AH	Adipic dihydrazide
Ar-PCL	Aromatic core ε-caprolactone star polymer
Alar-PCL	Aliphatic-aromatic ε-caprolactone polymer
BDMA	N, N, N-benzyldimethylamine
CE	3,4-epoxycyclohexylmethyl-3',4'-epoxycyclohexyl carboxylate
CHH	1,4-Cyclohexyl dihydrazide
Δh_t	Heat released
DB	Degree of branching
DCC	N,N'-Dicyclohexylcarbodiimide
DDH	Dodecanoic dihydrazide
DGEBA	Diglycidyl ether of bisphenol A
$Đ_M$	Molecular weight dispersity
DMF	N, N-dimethylformamide
DMTA	Dynamic mechanical thermal analysis
$\overline{DP}$	Degree of polymerization
DPTS	4-(N,N-dimethylamino)pyridinium p-toluene sulfonate
DSC	Differential scanning calorimetry
E'	Storage modulus
E"	Loss modulus
E_a	Apparent activation energy
ee	Epoxy equivalent
FTIR	Fourier-transformed infrared spectroscopy
ε-CL	*ε*-caprolactone
HBP	Hyperbranched polymer

HBPOH	Aliphatic-aromatic hyperbranched polyester
HKN	Hardness Knoop Number
IPH	Isophtalic dihydrazide
k	Rate constant
MI	1-Methyl imidazole
$\bar{M}_n$	Number average molecular weight
$\bar{M}_w$	Weight average molecular weight
Iη*I	Complex viscosity
NMR	Nuclear magnetic resonance spectroscopy
phr	Parts per hundred of resin
PEDPH	4,4'-(propane-1,3-diylbisoxy) dibenzoic dihydrazide
SEC	Size exclusion chromatography
SEM	Scanning electron microscopy
SP	Star polymer
$Sn(Oct)_2$	Tin(II) 2-ethylhexanoate
tan δ	Loss factor
TEC	Thermal expansion coefficient
T_g	Glass transition temperature
TGA	Thermogravimetric analysis
THF	Tetrahydrofurane
MTHPA	Methyl 1,2,3,6-Tetrahydrophthalic anhydride
TMA	Thermal mechanical analysis
T_{max}	Temperature of the maximum degradation rate
TMS	Tetramethyl silane
T_p	Temperature of the peak of the curing exotherm
$Yb(OTf)_3$	Ytterbium trifluoromethanesulfonate
$T_{x\%}$	Temperature of the lost of x% of weight
wt. %	Weight percentage

APPENDIX B: Publications and Communications

PUBLICATIONS INCLUDED IN THE THESIS

Adrian M. Tomuta, Xavier Ramis, Francesc Ferrando, Angels Serra
The use of dihydrazides as latent curing agents for DGEBA coatings
Progress in Organic Coatings 74 ***(2012)*** *59-66.*

Adrian Tomuta, Francesc Ferrando, Àngels Serra, Xavier Ramis
New aromatic-aliphatic hyperbranched polyesters with vinylic end groups of different length as modifiers of epoxy/anhydride thermosets.
Reactive & Functional Polymers 72 ***(2012)*** *556-563.*

A.M. Tomuta, X. Ramis, S. de la Flor, A. Serra
Influence of end groups in hyperbranched polyesters used as modifiers in the characteristics of epoxy thermosets cured by adipic dihydrazide.
Express Polymer Letters 7 ***(2013)*** *595-606.*

Adrian M. Tomuta, Xavier Ramis, Xavier Fernández-Francos, Francesc Ferrando, Angels Serra
New chemically reworkable epoxy coatings obtained by the addition of polyesters with star topologies to diglycidyl ether of bisphenol A resins.
Progress in Organic Coatings 76 ***(2013)*** *1616-1624.*

Adrian M. Tomuta, Xavier Fernández-Francos, Francesc Ferrando, Xavier Ramis, Àngels Serra
Enhanced chemical reworkability of DGEBA thermosets cured with rare earth triflates using aromatic hyperbranched polyesters (HBP) and multiarm star HBP-*b*-poly(ε-caprolactone) as modifiers;
Polymer for Advanced Technologies (In press).

Adrian M. Tomuta, Xavier Fernández-Francos, Francesc Ferrando, Àngels Serra, Xavier Ramis
New epoxy-anhydride thermosets modified with multiarm stars with hyperbranched polyester cores and poly(ε-caprolactone) arms; *Polymer-Plastics Technology and Engineering* (under revision).

OTHER PUBLICATIONS

Marjorie Flores, Adrian M. Tomuta, Xavier Fernández-Francos, Xavier Ramis, Marco Sangermano, Angels Serra
A new two-stage curing system: thiol-ene/epoxy homopolymerization using an allyl terminated hyperbranched polyester as reactive modifier.
Polymer 54 ***(2013)*** *5473–5481*.

COMMUNICATIONS TO CONGRESSES

Adrian Tomuta, Angels Serra, Xavier Ramis, Ana Mantecón
Study on novel latent curing agents for epoxy resins based on dihydrazides.
43rd IUPAC World Polymer Congress; Glasgow (UK) July 2010; Poster Presentation

Adrian Tomuta, Angels Serra, Xavier Ramis, Francesc Ferrando
New epoxy thermosets obtained from DGEBA and hyperbranched polyesters having unreactive chain ends using adipic dihydrazide as latent curing agent.
European Polymer Congress. Granada (Spain) June-July 2011; Poster Presentation.

Adrian M. Tomuta, Xavier Fernández-Francos, Francesc Ferrando, Angels Serra, Xavier Ramis
New multiarm star based on aromatic hyperbranched polyester core and poly(ε-caprolactone) arms as toughness modifiers of epoxy thermosets.
3rd International Symposium. Frontiers in Polymer Science Sitges (Spain) Mai 2013; Poster Presentation

APPENDIX C: Stages abroad

Organization: Leibniz-Insitute für Polymerforschung
Department: Institute of Macromolecular Chemistry (Prof. Voit)
City: Dresden **Country:** Germany
Duration: 3 months **Year:** 2012